Affine Arithmetic for Power and Optimal Power Flow Analyses in the Presence of Uncertainties

by

Alfredo Vaccaro

A thesis
presented to the University of Waterloo
in fulfillment of the
thesis requirement for the degree of
Doctor of Philosophy
in
Electrical and Computer Engineering

Waterloo, Ontario, Canada, 2015

Author's Declaration

I hereby declare that I am the sole author of this thesis. This is a true copy of the thesis, including any required final revisions, as accepted by my examiners.

I understand that my thesis may be made electronically available to the public.

Abstract

Optimal power system operation requires intensive numerical analyses to study and improve system security and reliability. To address this issue, Power Flow (PF) and Optimal Power Flow (OPF) analyses are important tools, since they are the foundation of many power engineering applications. For the most common formalization of these problems, the input data are specified using deterministic variables resulting either from a snapshot of the system or defined by the analyst based on several assumptions about the system under study. This approach provides problem solutions for a single system state, which is deemed representative of the limited set of system conditions corresponding to the data assumptions. Thus, when the input conditions are uncertain, numerous scenarios need to be evaluated.

To address the aforementioned problem, this thesis proposes solution methodologies based on the use of Affine Arithmetic (AA), which is an enhanced model for self-validated numerical analysis in which the quantities of interest are represented as affine combinations of certain primitive variables representing the sources of uncertainty in the data or approximations made during computations. In particular, AA-based techniques are proposed to solve uncertain PF and OPF problems. The adoption of these approaches allows to express the uncertain power system equations in a more convenient formalism compared to the traditional and widely used linearization frequently adopted in interval Newton methods. The proposed techniques allow to reliably estimate the PF and OPF solution hull by taking into account the parameter uncertainty inter-dependencies, as well as the diversity of uncertainty sources.

A novel AA-based computing paradigm aimed at achieving more efficient computational processes and better enclosures of PF and OPF solution sets is conceptualized. The main idea is to formulate a generic mathematical programming problem under uncertainty by means of equivalent deterministic problems, defining a coherent set of minimization, equality and inequality operators. Compared to existing solution paradigms, this formulation presents greater flexibility, as it allows to find partial solutions and inclusion of multiple equality and inequality constraints, and reduce the approximation errors to obtain better PF and OPF solution enclosures.

Finally, formal methods for knowledge discovery from large quantity of data as an enabling methodology for reducing the complexity of the PF and OPF problem, and for the optimal identification of the affine forms describing their uncertain parameters are proposed. In particular, a knowledge-based paradigm for PF and OPF analysis is used to extract from operation data-sets complex features, hidden relationships and useful hypotheses potentially describing regularities in the problem solutions. This is realized by designing a knowledge-extraction process based on Principal Components Analysis (PCA). The structural knowledge extracted by this process is then used to define a mathematical kernel, which transforms the PF and OPF equations into a domain in which these equations can be solved more effectively. In this new domain, the cardinality of the PF and OPF problem is sensibly reduced and, consequently, a more efficient algorithm can be used to obtain PF and OPF solutions: also it is possible to define a formal connection between the principal components and the noise symbols of the uncertain variables, which furnish an effective method for the optimal identification of the affine forms.

Detailed numerical results are presented and discussed using a variety of test systems, demonstrating the effectiveness of the proposed methodologies and comparing it to existing techniques for uncertain PF and OPF analysis.

Acknowledgements

I would like to thank prof. Claudio A. Canizares who made this research work possible.

Dedication

This research work is dedicated to the memory of Angelo Terlizzi.

Table of Contents

List of Figures

Nomenclature

Parameters

(a_i, b_i, c_i)	Cost coefficients of the i^{th} generator
α	First parameter of the Chebyshev approximation function
β	Second parameter of the Chebyshev approximation function
$\overline{T}$	Integer time window of available historical data
ξ	Third parameter of the Chebyshev approximation function
B_i	Loss coefficient of the i^{th} generator
m	Number of inequality constraints
N	Total number of buses
n	Number of equality constraints
N_N	Number of noise symbols
N_Q	Number of PQ buses
N_u	Number of control/decision variables
N_x	Number of dependent variables
N_{GA}	Total number of dispatchable generators

N_G	Total number of generators
N_{PC}	Number of principal components
N_{PV}	Number of PV buses
N_P	Number of buses in which the active power is specified
N_x	Number of state variables
p	Number of endogenous uncertainty sources
P_D	Power demand
$P_{G_i,max}$	Maximum generation limits for the i^{th} generator
$P_{G_i,min}$	Minimum generation limits for the i^{th} generator
p_{na}	Number of uncertainties generated by AA approximations
q	Number of scalar objective functions
$Q_{i,max}$	Maximum allowable limit for the reactive power generated at the i^{th} bus
$Q_{i,min}$	Minimum allowable limit for the reactive power generated at the i^{th} bus
$V_{i,max}$	Maximum allowable voltage magnitude for the i^{th} bus
$V_{i,min}$	Minimum allowable voltage magnitude for the i^{th} bus
$Y_{ij}\angle\theta_{ij}$	ij^{th} element of the bus admittance matrix
ω_i	Weight of the i^{th} objective function
ζ_{p+1}	Upper bound of the approximation error of the Chebyshev approximation function
P_i^{SP}	Real power injection specified at i^{th} bus
$P_{i,max}^{SP}$	Maximum value of the active power specified at the i^{th} bus

$P_{i,min}^{SP}$ Minimum value of the active power specified at the i^{th} bus

$Q_{i,max}^{SP}$ Maximum value of the reactive power specified at the i^{th} bus

$Q_{i,min}^{SP}$ Minimum value of the reactive power specified at the i^{th} bus

Q_{j}^{SP} Reactive power injection specified at j^{th} bus

$u_{max,i}$ Maximum allowable limit for i^{th} control/decision variable

$u_{min,i}$ Minimum allowable limit for i^{th} control/decision variable

$x_{max,i}$ Maximum allowable limit for i^{th} dependent variable

$x_{min,i}$ Minimum allowable limit for i^{th} dependent variable

$\mathbf{F}^{SP}$ Interval vector defining the specified range of the active and reactive powers

$\mathbf{x}(K)$ Vector of the state variables observed at the integer time K

Sets

$\mathcal{N}_{\mathcal{P}}$ Set of the buses in which the active power is specified

$\mathcal{N}_{\mathcal{Q}}$ Set of the buses in which the reactive power is specified

$\mathcal{N}_{\mathcal{PV}}$ Set of voltage controlled buses

$\mathcal{F}$ Set of the power flow equations

Variables

$\bar{\nabla}(\hat{\chi})$ Upper bound of the affine form $\hat{\chi}$

χ_0 Central value of the affine form $\hat{\chi}$

χ_k k^{th} partial deviation of the affine form $\hat{\chi}$

$\hat{\delta}_i$ Affine form of the i^{th} bus voltage angle

$\hat{V}_i$	Affine form of the i^{th} bus voltage magnitude
$\hat{f}$	Affine form of the objective function
$\hat{g}_j$	Affine form of the j^{th} equality constraint function
$\hat{h}_k$	Affine form of the k^{th} inequality constraint function
$\nabla(\hat{\chi})$	Lower bound of the affine form $\hat{\chi}$
$\sigma_i(\mathbf{X}\mathbf{X}^T)$	i^{th} eigenvector of the matrix $\mathbf{X}\mathbf{X}^T$
$\Theta_{\hat{\chi}}$	Range of the affine form $\hat{\chi}$
$\varpi(\hat{\chi})$	Radius of the affine form $\hat{\chi}$
C_R	Data compression index
C_r	Complexity reduction factor
f_{low}	Lower boundary of the objective function
f_{up}	Upper boundary of the objective function
$g_{j,low}$	Lower boundary of the j^{th} equality constraint function
$g_{j,up}$	Upper boundary of the j^{th} equality constraint function
$h_{k,low}$	Lower boundary of the k^{th} inequality constraint function
$h_{k,up}$	Upper boundary of the k^{th} inequality constraint function
P_{G_i}	Power generated by the i^{th} generator
P_{loss}	Network active power losses
z_j^k	j^{th} partial deviation of the k^{th} component of the vector $\mathbf{z}$
$\delta_{i,0}$	Central value of the i^{th} bus voltage angle

$\delta_{i,j}^{P}$	Partial deviation of the i^{th} bus voltage angle due to the active power injected at the j^{th} bus
$\delta_{i,k}^{Q}$	Partial deviation of the i^{th} bus voltage angle due to the reactive power injected at the k^{th} bus
$\hat{P}_i$	Affine form of the calculated active power injections in the i^{th} bus
$\hat{Q}_i$	Affine form of the calculated reactive power injections in the i^{th} bus
e^*	Residual error
$P_{i,0}$	Central value of the affine form of the calculated active power injections in the i^{th} bus
$P_{i,h}$	Partial deviation of the i^{th} active power injection associated with the approximation errors due to non-affine operations
$P_{i,j}^{P}$	Partial deviation of the i^{th} active power injection due to the active power injected at the j^{th} bus
$P_{i,k}^{Q}$	Partial deviation of the i^{th} active power injection due to the reactive power injected at the k^{th}
$Q_{i,0}$	Central value of the affine form of the calculated reactive power injections in the i^{th} bus
$Q_{i,h}$	Partial deviation of the i^{th} reactive power injection associated with the approximation errors due to non-affine operations
$Q_{i,j}^{P}$	Partial deviation of the i^{th} reactive power injection due to the active power injected at the j^{th} bus
$Q_{i,k}^{Q}$	Partial deviation of the i^{th} reactive power injection due to the reactive power injected at the k^{th} bus
$V_i\angle\delta_i$	i^{th} bus voltage in polar coordinates

$V_{i,0}$	Central value of the i^{th} bus voltage magnitude
$V_{i,j}^{P}$	Partial deviation of the i^{th} bus voltage magnitude due to the active power injected at the j^{th} bus
$V_{i,k}^{Q}$	Partial deviation of the i^{th} bus voltage magnitude due to the reactive power injected at the k^{th} bus
$\hat{\mathbf{u}}$	Affine form of the control/decision variables vector
$\hat{\mathbf{x}}$	Affine form of the dependent variables vector
$\hat{\mathbf{z}}$	Affine form of the vector ($\mathbf{x}$,$\mathbf{u}$)
$\mathbf{\Omega}$	PCA transformation matrix
$\zeta(K)$	Components of the state vector $\mathbf{x}(K)$ in the transformed domain
$\mathbf{B}$	Interval vector describing the internal uncertainty introduced by the AA computational process
$\mathbf{f}$	Objective function vector
$\mathbf{g}$	Equality constraint function vector
$\mathbf{h}$	Inequality constraint function vector
$\mathbf{J}$	Jacobian of the power flow equations
$\mathbf{J}_{PC}$	Jacobian of the power flow equations in the principal components domain
$\mathbf{r}(K)$	Residual error vector of the domain transformation at the integer time K
$\mathbf{s}(K)$	Principal component vector
$\mathbf{u}$	Vector of the control/decision variables
$\mathbf{x_{med}}$	Mean value of the state variables vector
$\mathbf{x}$	Vector of the dependent variables

Γ^a	Affine approximation of the function Γ
f_i	i^{th} objective function
g_j	j^{th} nonlinear equality constraint function
h_k	k^{th} nonlinear inequality constraint function

Chapter 1

Introduction

1.1 Motivation

Optimal power system operation requires intensive numerical analysis to study and improve system security and reliability. In this context, power system operators need to understand and reduce the impact of system uncertainties. To address this issue, Power Flow (PF) and Optimal Power Flow (OPF) analyses are some of the most important tools, since they represent the mathematical foundations of many power engineering applications such as state estimation, network optimization, unit commitment, voltage control, generation dispatch, and market studies.

For the most common formalization of the PF and OPF problems, all input data are specified using deterministic variables resulting either from a snapshot of the system or defined by the analyst based on several assumptions about the system under study (e.g. expected/desired generation/load profiles). This approach allows to compute PF and OPF solutions for a single system state that is deemed representative of the limited set of system conditions corresponding to the data assumptions. Thus, when the input conditions are uncertain, numerous scenarios need to be analyzed. These uncertainties are due to several internal and external sources in power systems. The most relevant uncertainties are related to the complex dynamics of the active and reactive power supply and demand, which may vary due to, for example:

- the variable nature of generation patterns due to competition [1];
- the increasing number of smaller geographically dispersed generators that could sensibly affect power transactions [1];
- the difficulties arising in predicting and modeling market operators behavior, governed mainly by unpredictable economic dynamics, which introduce considerable uncertainty in short-term power system operation; and
- the high penetration of generation units powered by non-dispatchable renewable energy sources that induce considerable uncertainty in power systems operation [2].

Since uncertainties can affect the PF and OPF solution to a considerable extent, reliable solution paradigms, incorporating the effect of data uncertainties, are required. Such algorithms could allow analysts to estimate both the data tolerance (i.e. uncertainties characterization) and the solution tolerance (i.e. uncertainty propagation assessment), providing, therefore, insight into the level of confidence of PF/OPF solutions. Furthermore, these methodologies could effectively support sensitivity analysis of large variables variations to estimate the rate of change in the solution with respect to changes in input data.

To address the aforementioned problem, this thesis proposes novel solution methodologies based on the use of Affine Arithmetic, which is an enhanced model for self-validated numerical analysis in which the quantities of interest are represented as affine combinations of certain primitive variables representing the sources of uncertainty in the data or approximations made during computations. Compared to existing solution paradigms, this formulation presents greater flexibility, as it allows to find partial solutions and inclusion of multiple equality and inequality constraints, and reduce the approximation errors to obtain better PF and OPF solution enclosures.

To reduce the complexity of the proposed AA-based PF and OPF analysis, and to optimally identify the affine forms describing their uncertain variables, formal methods for knowledge discovery from large quantity of data are proposed. In particular, a knowledge-based process based on Principal Components Analysis (PCA) for PF and OPF analysis is used to extract from operation data-sets complex features, hidden relationships and useful

hypotheses potentially describing regularities in the problem solutions. The structural knowledge extracted by this process is then used to project the PF and OPF equations into a domain in which the cardinality of the PF and OPF problem is sensibly reduced and, consequently, a more efficient algorithm can be used to obtain PF and OPF solutions. In this new domain, it is also possible to define a formal connection between the principal components and the noise symbols of the uncertain variables, which furnish an effective method for the optimal identification of the affine forms.

In this thesis, the application of these techniques to PF and OPF analyses is explained in detail, and several numerical results are presented and discussed, demonstrating the effectiveness of the proposed methodologies, especially in comparison to more traditional techniques.

1.2 Literature Review

Conventional methodologies available in the literature propose the use of sampling, analytical and approximate methods for PF and OPF analysis [3, 4], accounting for the variability and stochastic nature of the input data used. A critical review of the most relevant papers proposing these solution methodologies is presented in the following subsections.

1.2.1 Sampling Methods

Uncertainty propagation studies based on sampling-based methods, such as Monte Carlo, require several model runs that sample various combinations of input values. In particular, the most popular Monte Carlo based algorithm adopted to solve PF and OPF problems is simple random sampling, in which a large number of samples are randomly generated from the probability distribution functions of the input uncertain variables. Although this technique can provide highly accurate results, it has the drawback of requiring high computation resources needed for the large number of repeated PF and OPF solutions [5]. This hinders the application of this solution algorithm, especially for large scale power

system analysis, where the number of simulations may be rather large and the needed computational resources could be prohibitively expensive [6, 7].

The need to reduce the computational costs of Monte Carlo simulations, has stimulated the research for improved sampling techniques aimed at reducing the number of model runs, at the cost of accepting some level of risk. For example, in [8], an efficient Monte Carlo method integrating Latin hypercube sampling and Cholesky decomposition is proposed to solve PF problems. In [9], the unceratin PF problem with statistically correlated input random variables is solved by a hybrid solution algorithm based on deterministic annealing expectation maximization algorithm and Markov chain Monte Carlo. An extended Latin hypercube sampling algorithm aimed at solving PF problems in the presence of correlated wind generators is proposed in [10]. In [11], the uncertain OPF problem is formulated as a chance-constrained programming model, and the stochastic features of its solutions are obtained by combining Monte Carlo based simulations with deterministic optimisation models.

Although the application of the aforementioned techniques lower the computational burden of sampling-based approaches, they reduce the accuracy of the estimation of uncertainty regions of PF and OPF solutions. Therefore, the dichotomy between accuracy and computational efficiency is still an open problem that requires further investigation.

1.2.2 Analytical Methods

Analytical methods are computationally more effective, but they require some mathematical assumptions in order to simplify the problem and obtain an effective characterization of the output random variables [12]. These assumptions are typically based on model multilinearization [13], convolution techniques, and fast Fourier transforms [14]. For example, the cumulant method has been applied to solve the probabilistic PF problem in [15, 16], and the OPF problem in [12]; the performance of this method is enhanced by combining it with the Gram-Charlier expansion in [16], and by integrating the Von Mises functions in [17], to handle discrete distributions.

Furthermore, in [7], a novel OPF formulation based on a chance-constrained programming model is proposed to explore the stochastic features of the OPF solution by means

of a Monte Carlo based probabilistic model, whose parameters are identified by solving a deterministic optimization problem. However, the application of these techniques to solve PF and OPF problems is not straightforward and requires a back-mapping approach and a linear approximation of the non-linear PF equations [18]; this is mainly due to the non-linearities, the multiple uncertain variables, and the multiple output constraints characterizing PF and OPF problems.

Analytical techniques present various shortcomings, as discussed in [19, 20, 21, 22], such as the need to assume statistical independence of the input data, and the problems associated with accurately identifying probability distributions for some input data. This is a problem for PF and OPF analysis, since it is not always feasible to translate imprecise knowledge into probability distributions, as in the case of power generated by wind or photovoltaic generators, due to the inherently qualitative knowledge of the phenomena and the lack of sufficient data to estimate the required probability density distributions. To address this issue, the assumptions of normality and statistical independence of the input variables are often made, but experimental results show that these assumptions are often not supported by empirical evidence. These drawbacks may limit the usefulness of analytical methods in practical applications, especially for the study of large-scale power networks.

1.2.3 Approximate Methods

In order to overcome some of the aforementioned limitations of sampling and analytical methods, the use of approximate methods, such as the first-order second-moment method and point estimate methods, have been proposed in the literature [23]. Rather than computing the exact PF/OPF solution, these methods aim at approximating the statistical proprieties of the output random variables by means of a probability distribution fitting algorithm. In particular, the application of the first-order second-moment method allows to compute the first two moments of the PF/OPF solution by propagating the moments of the input variables by the Taylor series expansion of the model equations [24].

The point estimate methods, represent a more effective strategy, especially if the input parameters uncertainties can be directly estimated or measured. The application of these

solution algorithms allows to estimate the statistical moments of the PF solution by properly amalgamating the solutions of $2m$ deterministic problems, where m is the number of uncertain parameters [25]. This feature could be further enhanced by deploying more sophisticated point estimation schemes, based, for example, on Hong's point estimate method [26]. The application of this enhanced solution strategy allows solving the PF problem in the presence of multiple uncertainty sources characterized by both normal and binomial distributions, which could be particularly useful in modeling generator outages. These papers demonstrate that point estimate methods allow to effectively approximate the PF solution while keeping low the computational burden, which is confirmed in [27], where a comparison between the two-point estimate method proposed in [1] and a cumulant method proposed in [12] for solving the OPF problem in the presence of multiple data uncertainty is presented. The results obtained in this paper show that both approaches give similar results in most cases, and are accurate provided that the OPF has a feasible solution. It also observed that the cumulant method exhibits better performances for higher uncertainty in the input variables; however, since it is based on a linearization around an operation point, its performances rapidly decrease when this approximation is no longer valid. Both of these methods are shown to be computationally signicantly faster than a standard sampling-based approach, since they solve a reduced number of deterministic problems.

Other approaches to solve the uncertain OPF problem are presented in: [28], where a primal-dual interior point method is proposed to compute both the hull of the OPF solutions and their sensitivity with respect to data variation; [29], where a multi-scenario analysis based on the Taguchis orthogonal array testing is used to sample the input data variables; and [30], where the robust design theory is applied to approximate the OPF solutions in the presence of multiple data uncertainty. These papers confirm that the main benefit derived by the application of approximated probabilistic methods in OPF analysis is mainly due to the smaller level of data granularity required to approximate the problem solution [26].

The application of the aforementioned solution methods present several shortcomings. In particular, two-point estimate methods are not suitable to solve large scale problems, since they typically do not provide acceptable results in the presence of a large number

of input random variables. Moreover, the identification of the most effective scheme that should be adopted to select the number of estimated points is still an open problem that requires further investigations [31]; this is a critical issue, since a limited number of estimated points does not allow for an accurate and reliable exploration of the solution space, especially for input uncertainties characterized by relatively large standard deviations, such as in the case of lognormal or exponential distributions [31]. On the other hand, an increased number of estimated points reduces the computational benefits deriving by the application of point estimated methods, which could degenerate into a standard Monte Carlo solution approach.

1.2.4 Non-Probabilistic Methods

Recent research has enriched the spectrum of available techniques to deal with uncertainty in PF and OPF by proposing non-probabilistic formalisms, such as the theory of possibility [32], based on the theory of fuzzy sets, and the theory of evidence [33]. Non probabilistic formalisms are commonly adopted when uncertainty does not originate from unpredictable numerical measurements but stems from imprecise human knowledge about the system [34]; as a consequence, only imprecise estimates of values and relations between variables are available. For example, wind can be locally measured, but it is difficult to estimate the spatial distribution of wind speed in a geographical area using probabilities; also, weather forecasts provide qualitatively information about environmental variables that can hardly be represented in a probabilistic form. Hence, the availability of modeling and simulation tools able to deal with non-probabilistic knowledge can be useful to analysts for PF and OPF studies.

The application of fuzzy set theory to represent imprecise information, rather than using uncertainty associated with a frequency of occurrence, has been proposed in several papers [35, 36, 37]. In this paradigm, the input data and the inequality constraints are modeled by fuzzy numbers, which are special instances of fuzzy sets [38], and the problem solution is computed by deploying efficient linear programming solution algorithms based on Dantzig-Wolfe decomposition and dual simplex [36].

Other studies reported in the literature have proposed the employment of self-validated

computing for uncertainty representation in PF analysis. The main advantage of self-validated computation is that the algorithm itself keeps track of the accuracy of the computed quantities, as part of the process of computing them, without requiring information about the type of uncertainty in the variables [39]. The simplest and most popular of these models is Interval Mathematics (IM), which allows for numerical computation where each quantity is represented by an interval of real numbers without a probability structure [40]. Such intervals are added, subtracted, and/or multiplied in such a way that each computed interval is guaranteed to contain the unknown value of the quantity it represents.

The application of "standard" IM, referred here as interval arithmetic (IA), to PF analysis has been investigated by various authors [21, 20, 41, 42]. However, the adoption of this solution technique presents many drawbacks derived mainly by the so called "dependency problem" and "wrapping effect" [39, 43]; as a consequence, the solution provided by an IA method for PF solution is not always as informative as expected. Thus in [44], we showed that the use of IA for the solution of PF equations may easily yield aberrant solutions, due to the fact that the IA formalism is unable to represent the correlations that the PF equations establishes between the power systems state variables; as a consequence, at each algorithm step spurious values are added to the solutions, which could converge to large domains that include the correct solution. This phenomenon is well known in the simulation of qualitative systems [45, 46], and requires the adoption of specific techniques such as the Interval Gauss elimination, the Krawczyk's method, and the Interval Gauss Seidel iteration procedure. Therefore, the application of these paradigms in the PF solution process leads to realistic solution bounds only for certain special classes of matrices (e.g. M-matrices, H-matrices, diagonally dominant matrices, tri-diagonal matrices) [47]; furthermore, to guarantee convergence, it is necessary to preconditioning the linear PF equations by an M-matrix [48]. These techniques make the application of IA to PF analysis complex and time consuming.

1.2.5 Affine Arithmetic-based Methods

To overcome the aforementioned limitations in IA, in [44], we propose the employment of a more effective self validated paradigm based on Affine Arithmetic (AA) to represent the

uncertainties of the PF state variables, which is one of the topics of the present thesis. In this approach, each state variable is approximated by a first degree polynomial composed by a central value, i.e. the nameplate value, and a number of partial deviations that represent the correlation among various variables. The adoption of AA for uncertainty representation allows expressing the PF equations in a more convenient formalism, so that a reliable estimation of the PF solution hull can be computed taking into account the parameter uncertainty inter-dependencies, as well as the diversity of uncertainty sources. The main advantage of this solution strategy is that it requires neither derivative computations nor interval systems, being thus suitable in principle for large scale PF studies, where robust and computationally efficient solution algorithms are required. These benefits have been confirmed in [49] and in [50], where we proposed AA-based methods to solve uncertain OPF problems, which allows to determine operating margins for thermal generators in systems with uncertain parameters, by representing all the state and control variables with affine forms accounting for forecast, model error, and other sources of uncertainty, without the need to assume a probability density function. These methodologies have been recently recognized as a promising alternative for stochastic information management in bulk generation and transmission systems for smart grids [51].

Based on our own work reported in [44], several papers have explored the application of AA-based computing in power system analysis. In particular, in [52] the state estimation problem in the presence of mixed phasor and conventional power measurements has been addressed, considering the effect of network parameters uncertainty by an iterative weight least square algorithm based on IA and AA processing. In [53], an AA-based model of the uncertain PF problem is proposed, using complementarity conditions to properly represent generator bus voltage controls, including reactive power limits and voltage recovery; the model is then used to obtain operational intervals for the PF variables considering active and reactive power demand uncertainties. In [54], a non-iterative solution scheme based on AA is proposed to estimate the bounds of the uncertain PF solutions by solving an uncertain PF problem, which is formalized by an interval power flow problem and solved by quadratic programming optimization models.

The benefits deriving from the application of AA-based computing to power system planning and operation in the presence of data uncertainty have been assessed in [55], which

confirms that AA represents a fast and reliable computing paradigm that allows planners and operators to cope with high levels of renewable energy penetration, electric vehicle load integration, and other uncertain sources. Moreover, as confirmed in [56, 57, 49, 50], AA allows the analyst to narrow the gap between the upper and lower bounds of the PF and OPF solutions, avoiding the overestimation of bounds resulting from correlation of variables in IA.

Although the aforementioned papers offer considerable insight on the role that AA may play in power systems analysis, several open problems still remain unsolved, particularly:

- Further exploration of the application of AA-based techniques to uncertain OPF analysis.
- Rigorous methodologies aimed at selecting the noise symbols of the affine forms representing the power system state variables.
- More efficient paradigms aimed at reducing the overestimation errors of AA-based PF and OPF problems.

1.3 Objectives

Based on the above literature review, the following are the main thesis objectives:

1. Demonstrate with several realistic test systems that the use IA in PF and OPF analysis leads to over-pessimistic estimation of the solution hull, which are not useful in most practical applications due to the inability of IA to keep track of correlations between the power systems state variables, and analyze the employment of AA to represent the uncertainties of the power systems state variables. The adoption of AA for uncertainty representation will allow to express the PF and OPF models in a more convenient formalism compared to the traditional and widely used linearization frequently used in interval Newton methods.

2. Present and thoroughly test with the help of multiple test systems solution methodologies based on AA for PF and OPF studies with data uncertainties. By using the proposed methodology, a reliable estimation of the PF and OPF solutions hull will be computed, taking into account the parameter uncertainty inter-dependencies as well as the diversity of uncertainty sources. The main advantage of this solution strategy is that it does not require the solution of interval systems of equations, being thus suitable in principle for large scale PF and OPF studies where robust and computationally efficient solution algorithms are required.

3. Conceptualize a unified AA-based computational paradigm aimed at solving both PF and OPF problems in the presence of data uncertainties. These are based on the idea of formulating a generic mathematical programming problem under uncertainty by means of equivalent deterministic problems, defining a coherent set of minimization, equality and inequality operators.

4. Design more effective computing paradigms to reduce computational requirements by knowledge discovery from historical operating data-sets, and use this approach to better identify the noise symbols of the affine forms describing the uncertain variables in the proposed AA-based PF and OPF analyses.

1.4 Content

The thesis is organized as follows:

- Chapter 2 introduces the mathematical preliminaries and the theoretical background on which the presented research is based. In this chapter, the "standard" formalization of PF and OPF, deterministic problems, and the theory of self-validated computing are presented and discussed. The concept of Principal Component Analysis (PCA), which is an advanced technique for knowledge extraction from historical massive data, is also introduced in this chapter, since it represents an enabling methodology to extract actionable information from power system data in order to

determine potential patterns to simplify PF and OPF problems, as well as to properly define affine forms in AA-based techniques.

- Chapter 3 describes a solution methodology based on the use of AA to solve uncertain PF problems. This approach is shown to allow to reliable estimation of the PF solution hull by taking into account the parameter uncertainty inter-dependencies, as well as the diversity of uncertainty sources. Numerical results for a variety of benchmark test systems are presented and discussed in some details to demonstrate the effectiveness of the proposed AA-based PF methodology, especially in comparison to previously proposed techniques.

- Chapter 4 presents a hybrid framework based on the fusion of AA and Range Arithmetic for solving OPF problems, whose input data are specified in real compact intervals. The main idea is to apply the theory of direct interval matching and selection of the extreme value intervals to solve the constrained interval OPF problem, so that this problem can be solved with state-of-the-art NLP solvers. Numerical results for several realistic test systems are presented and discussed, demonstrating the effectiveness of this methodology.

- Chapter 5 describes in detail the theoretical foundations, the mathematical formulation, and the algorithmic deployment of a unified AA-based framework to solve uncertain PF and OPF problems. Compared to existing AA-based solution techniques, this framework is shown to present greater flexibility, as it allows to find partial solutions and inclusion of multiple equality and inequality constraints, and reduce the approximation errors to obtain a better solution enclosure. Detailed numerical results for various test systems are presented and discussed, demonstrating the effectiveness of the proposed methodology and comparing it to the AA-based PF and AA-based OPF presented in Chapters 3 and 4, respectively.

- Chapter 6 discusses the application of the PCA-based knowledge discovery techniques to lower the computational burdens in PF and OPF analysis, and to better represent affine forms in the proposed AA-based PF and OPF methods. The effectiveness of the proposed methodologies is assessed through the detailed simulation studies

presented and discussed in this chapter for various benchmark systems.

- Finally, Chapter 7 summarizes the main conclusions and contributions of the thesis, as well as the future research directions.

Chapter 2

Mathematical Background

2.1 Introduction

In this chapter, the mathematical backbone of the proposed research is presented and discussed. In particular, after the formalization of the deterministic PF and OPF problems is first reviewed. Then alternatives for uncertainty representation based on IA and AA are introduced, presenting the most relevant theorems supporting this techniques. Finally, the main concepts associated with PCA for knowledge extraction from historical data are briefly described.

2.2 Power Flow Analysis

PF analysis deals mainly with the calculation of the steady-state voltage phasor angle and magnitude for each network bus, for a given set of variables such as load demand and real power generation, under certain assumptions such as balanced system operation. Based on this information, the network operating conditions, in particular, real and reactive power flows on each branch, power losses, and generator reactive power outputs, can be determined. Thus, the input (output) variables of the PF problem are typically:

- the real and reactive power (voltage magnitude and angle) at each load bus, i.e. PQ buses;
- the real power generated and the voltage magnitude (reactive power generated and voltage angle) at each generation bus, i.e. PV buses;
- the voltage magnitude and angle (the real and reactive power generated) at the reference or slack bus.

The equations typically used to solve the PF problem are the real power balance equations at the generation and load buses, and the reactive power balance at the load buses. These equations can be written as:

$$\begin{array}{ll} P_i^{SP} = V_i \sum_{j=1}^{N} V_j Y_{ij} \cos\left(\delta_i - \delta_j - \theta_{ij}\right) & \forall i \in \mathcal{N}_{\mathcal{P}} \\ Q_j^{SP} = V_j \sum_{k=1}^{N} V_k Y_{jk} \sin\left(\delta_j - \delta_k - \theta_{jk}\right) & \forall j \in \mathcal{N}_{\mathcal{Q}} \end{array} \tag{2.1}$$

where:

- N is the total number of buses;
- $\mathcal{N}_{\mathcal{P}}$ is the set of the buses in which the active power is specified;
- $\mathcal{N}_{\mathcal{Q}}$ is the set of the buses in which the reactive power is specified;
- P_i^{SP} and Q_j^{SP} are the real and reactive power injections specified at i^{th} and j^{th} bus;
- $V_i \angle \delta_i$ is the unknown i^{th} bus voltage in polar coordinates;
- $Y_{ij} \angle \theta_{ij}$ is the ij^{th} element of the bus admittance matrix.

Due to the nonlinear nature of these equations the solution is not unique, and numerical algorithms, mainly based on Newton-Raphson or fast-decoupled methods, are employed to obtain a solution that is within an acceptable tolerance. These algorithms aim at approximating the non-linear PF equations by linearized Jacobian-matrix equations, which are solved by means of numerical iteration algorithms and sparse factorization techniques.

The PF solution should take into account the limits on certain variables, in particular max/min values of the reactive power at generation buses, to properly model the generator voltage controls. To address this particular issue, the typical solution strategy is to carry out a bus-type "switching", which consists on converting a PV-bus into a PQ-bus with the reactive power set at the limiting value, if the corresponding limits are violated. If at any consequent iteration, the voltage magnitude at that bus is below or above its original set point, depending on whether the generator is respectively underexcited or overexcited, the bus is then reverted back to a PV-bus. An alternative and more effective strategy to represent generator bus voltage controls, including reactive power limits and voltage recovery processes, has been proposed in [58], where a novel OPF-based model of the PF problem using complementarity conditions has been proposed.

2.3 Optimal Power Flow Analysis

Optimal Power Flow (OPF) analysis aims at computing the power system operation state according to, for example, cost, planning, or reliability criteria without violating system and equipment operating limits. The solution of this problem yields for identifying the optimal asset of the control/decision variables $\mathbf{u}$ that minimizes one or more objective functions f_i, subject to a number of nonlinear equality g_j and inequality constraints h_k, where f_i, g_j and h_k are continous and diferrentiable functions. Hence, this problem can be formalized in general by the following constrained, non-linear multi-objective programming problem:

$$\begin{aligned} \min_{(\mathbf{x},\mathbf{u})} \quad & f_i(\mathbf{x},\mathbf{u}) && \forall i \in [1,q] \\ \text{s.t.} \quad & g_j(\mathbf{x},\mathbf{u}) = 0 && \forall j \in [1,n] \\ & h_k(\mathbf{x},\mathbf{u}) < 0 && \forall k \in [1,m] \end{aligned} \tag{2.2}$$

where $\mathbf{x}$ is the vector of dependent variables, q is the number of scalar objective functions, n is the number of equality constraints, and m is the number of inequality constraints.

These equations can be expressed in a more compact vectorial form as follows:

$$\begin{aligned} \min_{(\mathbf{x},\mathbf{u})} \quad & \mathbf{f}(\mathbf{x},\mathbf{u}) \\ \text{s.t.} \quad & \mathbf{g}(\mathbf{x},\mathbf{u}) = 0 \\ & \mathbf{h}(\mathbf{x},\mathbf{u}) < 0 \end{aligned} \tag{2.3}$$

where $\mathbf{f}(.)$ is the q-dimensional objective function vector, and $\mathbf{g}(.)$ and $\mathbf{h}(.)$ are the n-dimensional and m-dimensional vectors representing the equality and inequality constraints, respectively.

The control/decision variables in (2.3) depend on the the specific application domain. These can include both real-valued variables, such as the active power generated by the available generators (i.e. optimal power dispatch), the set points of the primary voltage controllers (i.e. secondary voltage regulation), the optimal location of control/generator resources (i.e. planning studies), the maximum loading factor (i.e. voltage stability analysis), and integer variables, such as the set of the available generators (i.e. unit commitment). As a consequence, the OPF can be in general classified as a non-convex mixed integer/non-linear programming (MINLP) problem.

The dependent variables include the voltage magnitude and phase angle at PQ buses, the voltage phase angle and the reactive power generated at the PV buses, and the active and reactive power generated at the slack bus. The inequality constraints include the maximum allowable power flows for the power lines, the minimum and maximum allowable limits for most control/decision variables, i.e. $u_{min,i} \leq u_i \leq u_{max,i}$, $\forall i \in [1, n_u]$, such as generator voltages, and for some dependent variables, i.e. $x_{min,i} \leq x_i \leq x_{max,i}$, $\forall i \in [1, n_x]$, such as bus voltage limits. In addition, the control/decision and the dependent variables should satisfy the PF equations (2.1), which represent the equality constraints for (2.2) and (2.3).

The objective functions $\mathbf{f}(.)$ could integrate both technical and economic criteria including the minimization of the production costs, the minimization of the transmission line losses, the minimization of the voltage deviations, etc. Because these design objectives are typically competing, and its non-convexity, non-linear charateristics, the OPF problem has no unique solution and a suitable trade-off between the objectives needs to be

identified. To deal with the multi-objective nature of the OPF problem, one of the most common solution approaches used is the weighted global criterion method, in which all objective functions, which are assumed to be non-negative, are combined to form a single utility function expressed as:

$$U(\mathbf{x}, \mathbf{u}) = \sum_{i=1}^{p} \left(\omega_i f_i(\mathbf{x}, \mathbf{u})\right)^r \tag{2.4}$$

where the weights ω_i, so that $\sum_{i=1}^{p} \omega_i = 1$, $\omega_i > 0$, are typically set by the analyst depending on the relative importance of the objective functions.

Many classes of programming algorithms, such as nonlinear programming [59], quadratic programming [60, 61], and linear programming [62], have been proposed to solve the OPF problem. Some methods formalize the problems Karush-Kuhn-Tucker (KKT) optimality conditions, which are a set of nonlinear equations that can be solved by using an iterative Newton-based algorithm. These methods can handle both equality and inequality constraints, with the latter being added as quadratic penalty terms to the objective function and multiplied by proper penalty multipliers [63]. Another useful paradigm to handle inequality constraints is based on the Interior Point method, i.e. barrier method [64]. This approach converts the inequality constraints into equalities by the introduction of non-negative slack variables. A self-concordant barrier function (e.g. logarithmic) of these slack variables is then added to the objective function and multiplied by a barrier parameter, which is gradually reduced to zero during the solution process. A more effective method that does not require the definition of heuristic rules for barrier parameter reduction is based on the unlimited point algorithm [65]. This method aims at converting the KKT conditions to a set of nonlinear equations by implementing a proper transformation of the slack and dual variables of the inequality constraints.

2.4 Self-Validated Computing

2.4.1 Interval Arithmetic

The most intuitive approach to the numerical solution of uncertain PF and OPF problems consists of extending the numerical algorithms for the solution of the corresponding

deterministic problems using IA operators. IA is a range-based formalism for numerical computation, where each real quantity θ is assumed to be "unknown but bounded" in an interval of real numbers $\Theta = [\theta_{inf}, \theta_{sup}]$, also known as the tolerance of θ. The key element of IA based computing is based on the following theorem [40]:

Theorem 1 (Fundamental invariant of range analysis for IA)*:* $\forall\ \Gamma : \Re^p \rightarrow \Re^q$*, globally Lipschitz with bounded slope. There exists an interval extension* $\Gamma^I : \Re^p \rightarrow \Re^q$ *such that:*

$$\forall\,(\theta_1, .., \theta_p) \in (\Theta_1, .., \Theta_p) \Rightarrow \Gamma\,(\theta_1, .., \theta_p) \in \Gamma^I\,(\Theta_1, .., \Theta_p) \qquad \blacksquare$$

The implementation of interval extension Γ^I is generally straightforward for elementary operations, such as sums, products, square roots, since it requires only the identification of the maximum and minimum values of $\Gamma(\theta_1, .., \theta_p)$, when the corresponding arguments vary independently over specified intervals. Examples of simple arithmetic operations between two intervals $\Theta_1 = [\theta_{1,inf}, \theta_{2,sup}]$ and $\Theta_2 = [\theta_{2,inf}, \theta_{2,sup}]$ are:

$$\Theta_1 + \Theta_2 = [\theta_{1,inf} + \theta_{2,inf}, \theta_{1,sup} + \theta_{2,sup}] \tag{2.5}$$

$$\Theta_1 - \Theta_2 = [\theta_{1,inf} - \theta_{2,sup}, \theta_{1,sup} + \theta_{2,inf}] \tag{2.6}$$

$$\begin{aligned} \Theta_1 \cdot \Theta_2 = [&\min(\theta_{1,inf}\theta_{2,inf}, \theta_{1,inf}\theta_{2,sup}, \theta_{1,sup}\theta_{2,inf}, \theta_{1,sup}\theta_{2,sup}), \\ &, \max(\theta_{1,inf}\theta_{2,inf}, \theta_{1,inf}\theta_{2,sup}, \theta_{1,sup}\theta_{2,inf}, \theta_{1,sup}\theta_{2,sup})] \end{aligned} \tag{2.7}$$

$$\Theta_1/\Theta_2 = [\theta_{1,inf}, \theta_{1,sup}] \cdot \left[\tfrac{1}{\theta_{2,sup}}, \tfrac{1}{\theta_{2,inf}}\right] \quad 0 \notin [\theta_{2,inf}, \theta_{2,sup}] \tag{2.8}$$

Computation of interval extensions for more complex functions can be obtained by composing these primitive operators as illustrated in [40, 39]. Based on Theorem 1, it is possible to conclude that if a function is evaluated using these IA-based operators, the resulting interval is guaranteed to enclose the range of function values.

IA-based computing has been applied for solving mathematical problems under uncertainty such as linear systems of equations [66, 67], non-linear systems of equations [68], and optimization problems [69, 70]. The application of these algorithms typically yields to approximate interval solutions, called outer solutions, that are guaranteed to contain the exact interval solution. However, in many cases, these outer solutions are not always

as expected; thus, as shown in [71, 46], the use of IA-based computing in iterative solution algorithms may easily yield aberrant solutions. This is due to the fact that the IA formalism is unable to correctly represent the interaction between the problem variables, due to what is known as the "wrapping problem", as illustrated in Figure 2.1 [46], which plots the state space evolution of the harmonic oscillator, $\dot{\theta}_1 = \theta_2$, $\dot{\theta}_2 = -\theta_1$, whose initial condition (t=0) is represented by the rectangle ABCD with its sides parallel to the axes. In this case, since the initial rectangle does not evolve into another rectangle parallel to the coordinate axes, when one represents the uncertain state of the dynamical system at time t' using the interval notation, the IA solution (rotated rectangle $A'B'C'D'$) adds a set of "spurious states" (black regions), which do not correspond to an evolution of points belonging to ABCD; thus, in a few iterations, the IA solution diverges and covers the entire phase space. Another example is:

$$\Theta_1 \cdot (\Theta_2 + \Theta_3) \subset (\Theta_1 \cdot \Theta_2 + \Theta_1 \cdot \Theta_3) \tag{2.9}$$

As a consequence, the interval solutions produced by IA-based solvers are often much wider than the true range of the corresponding quantities, especially during long computational chains in which the interval width could diverge. This phenomenon is well known in the simulation of qualitative systems [45], and requires the adoption of special techniques.

Another well-known issue which could limit the application of IA-based computing in real world application is the so called "dependency problem", which derives directly from the definition of the interval difference operator (2.6):

$$\Theta - \Theta = [\theta_{inf}, \theta_{sup}] - [\theta_{inf}, \theta_{sup}] = [\theta_{inf} - \theta_{sup}, \theta_{sup} + \theta_{inf}] \neq 0 \tag{2.10}$$

This aberration is due to intrinsic inability of IA to discriminate the uncertainty sources, which are assumed to be independent for each interval variable. In particular, if the interval variables $\Theta_1 = [1, 2]$ and $\Theta_2 = [1, 2]$ describe two independent uncertain sources, then the results computed by applying the IA-based difference operator,$\Theta_1 - \Theta_2 = [-1, 3]$, is correct. On the other hand, if these interval variables describe the same uncertain source, then the corresponding result leads to a large overestimation error.

In [44], we demonstrated that due to the introduction of spurious values in the result of IA-based PF analysis, there is excessive conservatism in the output intervals, especially

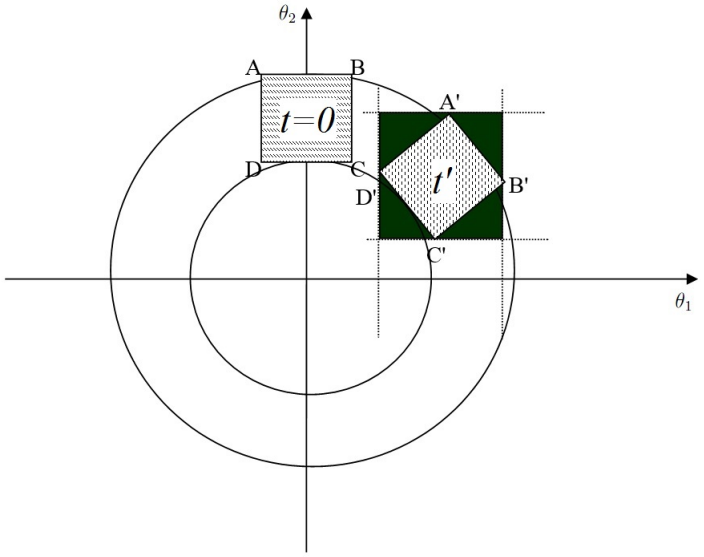

Figure 2.1: IA evolution of the external surface of the region of uncertainty for a 2-nd order oscillatory system ("wrapping" effect).

when solving large scale problems. To address this limitation, it is proposed here the use of more advanced paradigms based on AA, which is discussed next, to solve uncertain PF and OPF problems.

2.4.2 Affine Arithmetic

Affine arithmetic (AA), introduced in [39], is a method for range analysis to manipulate multiple uncertainty sources such as imprecise data, modeling errors, round off and truncation errors. This paradigm is similar to standard IA, but, in addition, it keeps track of correlations between the input and the computed quantities, providing much tighter bounds in the computing process and avoiding the probability for the error explosion problem observed in IA computations [72].

In AA, a partially unknown quantity χ is represented by an affine form that is a first

degree polynomial of the form:

$$\hat{\chi} = \chi_0 + \chi_1\varepsilon_1 + \chi_2\varepsilon_2 + ... + \chi_p\varepsilon_p \tag{2.11}$$

where χ_0 and χ_k are known real coefficients representing the central value and the partial deviations of the affine form $\hat{\chi}$ respectively. The variables ε_k, called the noise symbols, are symbolic quantities whose values are unknown but bounded in the interval [-1,1]. Each noise symbol represents an independent uncertainty source affecting the variable χ, which may be external, if related to the uncertainty of some input quantities, or internal, if originated by round off and truncation errors in the computation of $\hat{\chi}$. Hence, these noise symbols can be used to quantify the uncertainty of all interval quantities, which allows to account for interactions between dependent variables. Thus a formal correlation between AA and IA can be obtained by using the following operators:

$$\varpi_{\hat{\chi}} := \sum_{k=1}^{p} |\chi_k| \tag{2.12}$$

$$\bar{\nabla}(\hat{\chi}) := \chi_0 + \sum_{k=1}^{p} |\chi_k| \tag{2.13}$$

$$\nabla(\hat{\chi}) := \chi_0 - \sum_{k=1}^{p} |\chi_k| \tag{2.14}$$

$$\Theta_{\hat{\chi}} := [\nabla(\hat{\chi}), \bar{\nabla}(\hat{\chi})] \tag{2.15}$$

which define the radius, the upper bound, the lower bound and the range of the affine form $\hat{\chi}$, respectively.

In order to perform AA computations, it is necessary to replace each operation on real numbers by equivalent mappings between affine forms. In particular, given a generic mapping $\Gamma(\chi, \psi)$ the corresponding AA operation $\Gamma(\hat{\chi}, \hat{\psi})$ is a procedure that computes an affine form for $\zeta = \Gamma(\chi, \psi)$, which is coherent with input affine forms $(\hat{\chi}, \hat{\psi})$. If the function Γ is a linear function of its argument χ and ψ, the affine representation of ζ is obtained by expanding and rearranging into an affine form the noise symbols ε_k, as in the case of the following arithmetic operations:

$$\hat{\chi} \pm \hat{\psi} = (\chi_0 \pm \psi_0) + (\chi_1 \pm \psi_1)\varepsilon_1 + (\chi_2 \pm \psi_2)\varepsilon_2 + ... + (\chi_p \pm \psi_p)\varepsilon_p \tag{2.16}$$

$$\lambda\hat{\chi} = (\lambda\chi_0) + (\lambda\chi_1)\varepsilon_1 + (\lambda\chi_2)\varepsilon_2 + ... + (\lambda\chi_p)\varepsilon_p \tag{2.17}$$

$$\hat{\chi} \pm \lambda = (\chi_0 \pm \lambda) + \chi_1\varepsilon_1 + \chi_2\varepsilon_2 + ... + \chi_p\varepsilon_p \tag{2.18}$$

On the other hand, if Γ is a non-affine operation, ζ cannot be expressed exactly as an affine combination of the noise symbols ε_k, i.e.:

$$\hat{\zeta} = \Gamma(\hat{\chi}, \hat{\psi}) = \Gamma(\chi_0 + \chi_1\varepsilon_1 + \chi_2\varepsilon_2 + ... + \chi_p\varepsilon_p, \psi_0 + \psi_1\varepsilon_1 + \psi_2\varepsilon_2 + ... + \psi_p\varepsilon_p) \tag{2.19}$$

In this case, the problem boils down to the identification of an affine function:

$$\Gamma^a(\hat{\chi}, \hat{\psi}) = \zeta_0 + \zeta_1\varepsilon_1 + \zeta_2\varepsilon_2 + ... + \varepsilon_p\zeta_p \tag{2.20}$$

that approximates the function $\Gamma(\hat{\chi}, \hat{\psi})$ reasonably well over its domain:

$$\hat{z} = \Gamma^a(\hat{\chi}, \hat{\psi}) + \zeta_{p+1}\varepsilon_{p+1} = \zeta_0 + \zeta_1\varepsilon_1 + \zeta_2\varepsilon_2 + ... + \zeta_p\varepsilon_p + \zeta_{p+1}\varepsilon_{p+1} \tag{2.21}$$

where the last term represents the residual or approximation error:

$$e^*(\hat{\chi}, \hat{\psi}) = \Gamma(\hat{\chi}, \hat{\psi}) - \Gamma^a(\hat{\chi}, \hat{\psi}) \tag{2.22}$$

The noise symbol ε_{p+1} in (2.21) must be distinct from all other noise symbols that already appeared in the same computation, and its coefficient ζ_{p+1} must be an upper bound on the absolute magnitude of e^*, as follows:

$$\zeta_{p+1} > \max_{(\varepsilon_1, \varepsilon_2, ..., \varepsilon_p)} e^*(\hat{\chi}, \hat{\psi}) \tag{2.23}$$

Furthermore, the affine approximation function Γ^a in (2.20) could assume different structures, depending on the desired degree of accuracy and the available computational resources. A good trade off between these goals could be obtained by assuming the following approximation structure:

$$\Gamma^a(\hat{\chi}, \hat{\psi}) = \alpha\hat{\chi} + \beta\hat{\psi} + \xi \tag{2.24}$$

where the unknown coefficients α, β, and ξ can be identified by the following theorem:

Theorem 2 (Chebyshev approximation theorem for univariate functions)*: Let* Γ *be a bounded and twice differentiable function defined in some interval* $\chi^I = [\chi_{inf}, \chi_{sup}]$*, whose second derivative does not change sign inside* χ*. Let* $\Gamma^a(\hat{\chi}) = \alpha\hat{\chi} + \xi$ *be its Chebyshev affine approximation in* χ^I*. Then:*

$$\alpha = \frac{\Gamma(\chi_{sup}) - \Gamma(\chi_{inf})}{\chi_{sup} - \chi_{inf}} \quad \xi = \frac{\Gamma(u) + r(u)}{2} - \alpha u \quad \frac{d\Gamma(u)}{d\chi} = \alpha \quad r(u) = \alpha u + \Gamma(\chi_{sup}) - \alpha\chi_{sup}$$

and the maximum absolute error is:

$$\zeta_{p+1} = \left|\frac{\Gamma(u) - r(u)}{2}\right| \qquad \blacksquare$$

Observe that α is simply the slope of the line interpolating the points $(\chi_{inf}, f(\chi_{inf}))$ and $(\chi_{sup}, f(\chi_{sup}))$, while the maximum absolute error will occur twice (with the same sign) at the endpoints χ_{inf} and χ_{sup} of the range, and once (with the opposite sign) at every interior point u of χ where $\frac{d\Gamma(u)}{d\chi} = \alpha$. This important result provides an algorithm for finding the optimum coefficients α and ξ of the affine approximation function, and the upper bound ζ_{p+1} of the corresponding approximation error.

The distinguishing propriety of AA compared to other self-validated computation model providing first-order approximations, such as generalized interval arithmetic, first-order Taylor arithmetic, and the ellipsoidal calculus, is that the function is expanded not only in the initial parameters but also in intermediate intervals resulting from the non-linearities. Hence, AA can be considered as an intermediate between Taylor forms and zonotopes, as described in detail in [73], presenting several advantages, including a wider range of applications and a more convenient programming interface [74].

In the next chapter, it will be shown that the adoption of AA-based computing allows to express the power system equations in a more convenient form, to solve them using algorithms that do not require the traditional and widely used linearization approach frequently adopted in IA-based solution methods, thus avoiding the need to invert or factorize matrixes, which introduce significant errors when using intervals to represent uncertainties. This important feature will allow the design of more effective solution techniques for uncertain PF and OPF problems.

2.5 Principal Components Analysis

Effective AA-based computing requires the deployment of formal methods aimed at optimally selecting the noise symbols of the affine forms and reducing the overestimation errors of the solution sets. To address this open problem, novel techniques for knowledge discovery from historical operation data-sets based on Principal Components Analysis (PCA) will be proposed in this research.

PCA aims at discovering the potential relationships among a set of state variables $x_i \quad \forall i \in [1, N_x]$, from the following set of historical observations (usually referred as the knowledge base):

$$\mathbf{x}(K) = [x_1(K)...x_{Nx}(K)]^T \quad \forall K \in [0, \overline{T}] \tag{2.25}$$

where $[0, \overline{T}]$ defines the integer sample time interval of available data. This is accomplished by identifying a suitable domain transformation such that the elements of the knowledge base can be accurately represented by an inverse model of the form:

$$\mathbf{x}(K) = \Pi^{-1}(\zeta(K)) + \mathbf{r}(K) \quad \forall K \in [0, \overline{T}] \tag{2.26}$$

where $\Pi : \Re^{N_x} \rightarrow \Re^{N_\zeta}$ is a continuous function describing the domain transformation mapping; $\zeta(K) = [\zeta_1(K)...\zeta_{N\zeta}(K)]^T$ are the components of the state vector $\mathbf{x}(K)$ in the transformed domain; and $\mathbf{r}(K)$ represents the residual error vector.

In standard PCA, the domain transformation function is composed of a linear combination with a proper number of orthogonal and uncorrelated principal components with decreasing variance, namely [75]:

$$\begin{aligned} \mathbf{x}(K) &= \mathbf{\Omega}\ \mathbf{s}(K) + \mathbf{x_{med}} \quad \forall K \in [0, \overline{T}] \\ \mathbf{x_{med}} &= \tfrac{1}{\overline{T}} \textstyle\sum_{K=0}^{\overline{T}} \mathbf{x}(K) \end{aligned} \tag{2.27}$$

where $\mathbf{s}(K)$ is the principal component vector, and $\mathbf{\Omega}$ is a matrix of dimensions $N_x \times N_{PC}$, which can be determined by solving the following eigenvalue problem:

$$\mathbf{s}(K) = \mathbf{M}(\mathbf{x}(K) - \mathbf{x_{med}}) \quad \forall K \in [0, \overline{T}] \tag{2.28}$$

where the orthonormal matrix $\mathbf{M}$ is defined as:

$$\mathbf{M_i} = \sigma_i(\mathbf{X}\mathbf{X}^T) \tag{2.29}$$

with $\sigma_i(\mathbf{X}\mathbf{X}^T)$ representing the i^{th} eigenvector of the matrix $\mathbf{X}\mathbf{X}^T$, for $\mathbf{X} = [\mathbf{x}(1)...\mathbf{x}(\overline{T})]^T$. This domain transformation mainly consists of translating and rotating the original coordinate axes, in such a way that the first principal component is characterized by the largest variance, and each following component by the highest variance that is orthogonal and uncorrelated with the previous components. As a consequence, each principal component carries different and uncorrelated information to other components, and only a limited number of them are necessary to accurately compute the state variables for highly correlated datasets ($N_{PC} \ll N_x$) [76]. Thanks to this feature, the $N_x\overline{T}$ historical data can be approximated by storing and processing a limited number of variables, namely, the principal components profiles, the static matrix $\mathbf{\Omega}$, and the static vector $\mathbf{x}_{med}$, for a total of $N_{PC}\overline{T} + N_xN_{PC} + N_x$ elements. The ratio between these quantities provides a rough estimation of the data compression capability of the PCA-based knowledge extraction process, which, for a large number of observations, tends to the following value:

$$C_R^{\infty} = \lim_{\overline{T}\to\infty} C_R(\overline{T}) = \lim_{\overline{T}\to\infty} \frac{N_x\overline{T}}{N_{PC}\overline{T} + N_xN_{PC} + N_x} = \frac{N_x}{N_{PC}} \tag{2.30}$$

This result demonstrates the effectiveness of PCA in compressing the knowledge base by extracting only the more relevant information, which mainly depends on the number of principal components N_{PC} assumed in the computation. The latter can be determined by adopting various statistical methods, including:

- Kaiser criterion: it selects principal components with eigenvalues greater than 1.
- Scree test: it is based on the analysis of the scree plot of the available data.
- Cumulative percentage method: it selects the components that cumulatively explain a certain percentage of variation.
- Binary search approach: it selects the components by identifying a proper trade-off between statistical fidelity, i.e. maximizing the variance in the data, and interpretability, i.e. minimizing the coordinate axes.

More details about these methods can be found in [77].

As recently outlined in several papers [78, 79, 80], PCA could be useful in data management for smart grids, where a massive increase of data exchanging and processing is expected in the short/medium term. Furthermore, the described PCA-based knowledge-extraction process, codified in the matrix $\mathbf{\Omega}$, could also be used for selecting the optimal number of noise symbols and reducing the complexities of AA-based PF and OPF analysis, as proposed in this work.

2.6 Summary

In this chapter, the main mathematical background of the proposed research was presented. In particular, the mathematical formalizations of the deterministic PF and OPF problems has been introduced. Also, IA, which can be used to represent uncertainty through intervals, has been reviewed, showing the main limitations of this technique, which results in excessive conservatism, especially when solving large scale problems. To address this limitation, a more effective alternative for uncertainty representation based on AA is proposed in this work, introducing the most relevant theorems supporting this theory has been presented in this chapter. Finally, the PCA-based knowledge discovery paradigm, aimed at solving some open problems in AA-based computing, as discussed in this thesis, has been briefly explained.

Chapter 3

Affine Arithmetic for Uncertain PF Analysis

3.1 Introduction

In this chapter a solution based on the use of AA is presented to solve uncertain PF problems. The adoption of this approach allows expressing the uncertain PF equations in a more convenient formalism, compared to the traditional and widely used linearization frequently adopted in interval Newton methods, and reliably estimating the PF solution hull by taking into account the parameter uncertainty inter-dependencies, as well as the diversity of uncertainty sources. Many numerical results are presented and discussed in some detail to demonstrate the effectiveness of the proposed AA-based PF methodology, especially in comparison to previously proposed interval arithmetics techniques.

3.2 Methodology

AA can be effectively adopted for uncertainty representation in PF analysis. Thus, as described in [44], each state variable, i.e. the voltage magnitude of the load buses and the voltage phase of all buses but the slack, can be expressed by a central value and a set of

partial deviations. These deviations are associated with as many noise variables as those which describe the effect of the various phenomena affecting the system state variables. Without loss of generality, the typical sources of uncertainties considered here are those related to the active and reactive power in loads and the active power in generators, associated with elastic loads and intermittent sources. Therefore, the affine forms representing the power system state variables can be represented as follows:

$$\begin{array}{ll} \hat{V}_i = V_{i,0} + \sum_{j\in\mathcal{N}_\mathcal{P}} V_{i,j}^P \varepsilon_j + \sum_{k\in\mathcal{N}_\mathcal{Q}} V_{i,k}^Q \varepsilon_k & \forall i \in \mathcal{N}_\mathcal{Q} \\ \hat{\delta}_i = \delta_{i,0} + \sum_{j\in\mathcal{N}_\mathcal{P}} \delta_{i,j}^P \varepsilon_j + \sum_{k\in\mathcal{N}_\mathcal{Q}} \delta_{i,k}^Q \varepsilon_k & \forall i \in \mathcal{N}_\mathcal{P} \end{array} \tag{3.1}$$

where ε_j, $j \in \mathcal{N}_\mathcal{P}$, is the noise representing the uncertainty of the active power injection at the j^{th} bus; ε_k, $k \in \mathcal{N}_\mathcal{Q}$, is the noise representing the uncertainty of the reactive power injection at the k^{th} bus; $V_{i,0}$ is the central value of the i^{th} bus voltage magnitude; $\delta_{i,0}$ is the central value of the i^{th} bus voltage angle; $V_{i,j}^P$ is the partial deviation of the i^{th} bus voltage magnitude due to the active power injected at the j^{th} bus; $V_{i,j}^Q$ is the partial deviation of the i^{th} bus voltage magnitude due to the reactive power injected at the j^{th} bus; $\delta_{i,j}^P$ is the partial deviation of the i^{th} bus voltage angle due to the active power injected at the j^{th} bus and $\delta_{i,j}^Q$ is the partial deviation of the i^{th} bus voltage angle due to the reactive power injected at the j^{th} bus.

The central values of the affine forms (3.1) are calculated by solving the conventional PF equations (2.1) for the "nominal" operating point defined by:

$$\begin{cases} P_i^{SP} = \frac{P_{i,max}^{SP} - P_{i,min}^{SP}}{2} & \forall i \in \mathcal{N}_\mathcal{P} \\ Q_i^{SP} = \frac{Q_{i,max}^{SP} - Q_{i,min}^{SP}}{2} & \forall i \in \mathcal{N}_\mathcal{Q} \end{cases} \tag{3.2}$$

and a first estimation of the partial deviations of the affine forms (3.1) can be first approximated by means of the sensitivities of the desired voltage magnitudes and angles with respect to the uncertain inputs at the "nominal" operating point, i.e.

$$\begin{array}{llll} V_{i,j}^P = \left.\frac{\partial V_i}{\partial P_j}\right|_0 \Delta P_j & V_{i,k}^Q = \left.\frac{\partial V_i}{\partial Q_k}\right|_0 \Delta Q_k & \forall j \in \mathcal{N}_\mathcal{P}, \forall \| , \rangle \in \mathcal{N}_\mathcal{Q} \\ \delta_{i,j}^P = \left.\frac{\partial \delta_i}{\partial P_j}\right|_0 \Delta P_j & \delta_{i,k}^Q = \left.\frac{\partial \delta_i}{\partial Q_k}\right|_0 \Delta Q_k & \forall i,j \in \mathcal{N}_\mathcal{P}, \forall \| \in \mathcal{N}_\mathcal{Q} \end{array} \tag{3.3}$$

Observe that if the PF equations would contain only affine expressions, i.e. be a linear system of equations, the obtained affine forms would be the exact solution. However, these

equations are nonlinear expressions, and hence the obtained affine forms are usually an underestimation of the exact result [81]. Thus, to guarantee the inclusion of the solution domain, each partial deviation is multiplied by an amplification coefficient [81]. Starting from this initial affine solution, a "domain contraction" based method for narrowing its bounds is used. Hence, the algorithm first starts by plugging (3.1), with the initial partial deviation approximations defined in (3.3), in the right-hand side of the PF equations (2.1) to compute the following AA form of the injected powers:

$$\begin{array}{rl} \hat{Q}_i = Q_{i,0} + \sum_{j\in\mathcal{N}_\mathcal{P}} Q^P_{i,j}\varepsilon_j + \sum_{k\in\mathcal{N}_\mathcal{Q}} Q^Q_{i,k}\varepsilon_k + \sum_{h\in\mathcal{N}_\mathcal{N}} Q_{i,h}\varepsilon_h & \forall i \in \mathcal{N}_\mathcal{Q} \\ \hat{P}_i = P_{i,0} + \sum_{j\in\mathcal{N}_\mathcal{P}} P^P_{i,j}\varepsilon_j + \sum_{k\in\mathcal{N}_\mathcal{Q}} P^Q_{i,k}\varepsilon_k + \sum_{h\in\mathcal{N}_\mathcal{N}} P_{i,h}\varepsilon_h & \forall i \in \mathcal{N}_\mathcal{P} \end{array} \tag{3.4}$$

where $\hat{P}_i$ and $\hat{Q}_i$ are the affine forms of the calculated active and reactive power injections in the i^{th} bus; ε_h are new noise variables introduced in the computational process due to the presence of non affine operations (N_N denotes the set of these new noise variables); $Q_{i,0}$, $Q^P_{i,j}$, $Q^Q_{i,k}$, $P_{i,0}$, $P^P_{i,j}$, and $P^Q_{i,k}$ are the computed central values and the partial deviations of the affine forms of the calculated active and reactive powers injected in the i^{th} node; and $Q_{i,h}$ and $P_{i,h}$ are the coefficients of the noise symbols ε_h, associated with the approximation errors due to non-affine operations.

The AA operators (2.16)-(2.18) and affine approximations of the sinusoidal functions described in [39] are used to obtain $Q^P_{i,j}$, $Q^Q_{i,k}$, $Q_{i,h}$,$P^P_{i,j}$,$P^Q_{i,k}$, and $P_{i,h}$. The obtained affine forms (3.4) can then be arranged in the following matrix form:

$$
\begin{bmatrix} \hat{Q}_1 \\ ... \\ \hat{Q}_{N_Q} \\ \hat{P}_1 \\ ... \\ \hat{P}_{N_P} \end{bmatrix} = \begin{bmatrix} Q_{1,0} \\ ... \\ Q_{N_Q,0} \\ P_{1,0} \\ ... \\ P_{N_P,0} \end{bmatrix} +
$$

$$
+ \begin{bmatrix} Q^P_{1,1} & ... & Q^P_{1,N_P} & Q^Q_{1,1} & ... & Q^Q_{1,N_Q} \\ ... & ... & ... & ... & ... & ... \\ Q^P_{N_Q,1} & ... & Q^P_{N_Q,N_P} & Q^Q_{N_Q,1} & ... & Q^Q_{N_Q,N_Q} \\ P^P_{1,1} & ... & P^P_{1,N_P} & P^Q_{1,1} & ... & P^Q_{1,N_Q} \\ ... & ... & ... & ... & ... & ... \\ P^P_{N_P,1} & ... & P^P_{N_P,N_P} & P^Q_{N_P,1} & ... & P^Q_{N_P,N_Q} \end{bmatrix} \begin{bmatrix} \varepsilon_1 \\ ... \\ \varepsilon_{N_P} \\ \varepsilon_{N_P+1} \\ ... \\ \varepsilon_{N_P+N_Q} \end{bmatrix} + \tag{3.5}
$$

$$
+ \begin{bmatrix} Q_{1,1} & ... & Q_{1,N_N} \\ ... & ... & ... \\ Q_{N_Q,1} & ... & Q_{N_Q,N_N} \\ P_{1,1} & ... & P_{1,N_N} \\ ... & ... & ... \\ P_{N_P,1} & ... & P_{N_P,N_N} \end{bmatrix} \begin{bmatrix} \varepsilon_{N_P+N_Q+1} \\ ... \\ ... \\ ... \\ ... \\ \varepsilon_{N_P+N_Q+N_N} \end{bmatrix}
$$

where N_P and N_Q represent the number of PV buses and PQ buses and N_N is the number of the noise symbols. In a more general form, (3.5) can be written as:

$$
\mathbf{F}(\mathbf{X}) = \mathbf{A}\mathbf{X} + \mathbf{B} \tag{3.6}
$$

where

$$
\mathbf{A} = \begin{bmatrix} Q^P_{1,1} & ... & Q^P_{1,N_P} & Q^Q_{1,1} & ... & Q^Q_{1,N_Q} \\ ... & ... & ... & ... & ... & ... \\ Q^P_{N_Q,1} & ... & Q^P_{N_Q,N_P} & Q^Q_{N_Q,1} & ... & Q^Q_{N_Q,N_Q} \\ P^P_{1,1} & ... & P^P_{1,N_P} & P^Q_{1,1} & ... & P^Q_{1,N_Q} \\ ... & ... & ... & ... & ... & ... \\ P^P_{N_P,1} & ... & P^P_{N_P,N_P} & P^Q_{N_P,1} & ... & P^Q_{N_P,N_Q} \end{bmatrix} \tag{3.7}
$$

$$\mathbf{X} = \begin{bmatrix} \varepsilon_1 \\ ... \\ \varepsilon_{N_P} \\ \varepsilon_{N_p+1} \\ ... \\ \varepsilon_{N_P+N_Q} \end{bmatrix} \tag{3.8}$$

$$\mathbf{B} = \begin{bmatrix} Q_{1,0} \\ ... \\ Q_{N_Q,0} \\ P_{1,0} \\ ... \\ P_{N_P,0} \end{bmatrix} + \begin{bmatrix} Q_{1,1} & ... & Q_{1,N_N} \\ ... & ... & ... \\ Q_{N_Q,1} & ... & Q_{N_Q,N_N} \\ P_{1,1} & ... & P_{1,N_N} \\ ... & ... & ... \\ P_{N_P,1} & ... & P_{N_P,N_N} \end{bmatrix} \begin{bmatrix} \varepsilon_{N_P+N_Q+1} \\ ... \\ ... \\ ... \\ ... \\ \varepsilon_{N_P+N_Q+N_N} \end{bmatrix} \tag{3.9}$$

Note that, $\mathbf{A}$ is a matrix of computed real coefficients; $\mathbf{X}$ is the vector that needs to be contracted, with initial values for each of its components set at [-1,1]; and $\mathbf{B}$ is an interval vector, since the new noise variables vary in the interval [-1,1] and hence it is not possible to contract them, because these represent internal noise introduced by the AA computational process. The PF solution can then be obtained by contracting the vector $\mathbf{X}$ so that:

$$\mathbf{AX} + \mathbf{B} = \mathbf{F}^{SP} \tag{3.10}$$

where $\mathbf{F}^{SP}$ is the following interval vector defining the specified range of the active and reactive powers:

$$\mathbf{F}^{SP} = \begin{bmatrix} \left[Q^{SP}_{1,min}, Q^{SP}_{1,max}\right] \\ ... \\ [Q^{SP}_{N_Q,min}, Q^{SP}_{N_Q,max}] \\ [P^{SP}_{1,min}, P^{SP}_{1,max}] \\ ... \\ [P^{SP}_{N_P,min}, P^{SP}_{N_P,max}] \end{bmatrix} \tag{3.11}$$

The problem is thus reduced to solving the IA problem:

$$\mathbf{AX} = \mathbf{C} \tag{3.12}$$

where $C = \mathbf{F}^{SP} - \mathbf{B}$, and $\mathbf{A}$ is a real matrix. The linear IA problem (3.12) can be effectively solved using the following $N_P + N_Q$ constrained linear optimization problems:

$$\begin{aligned} \min \quad & (\varepsilon_k, \varepsilon_j) \quad \forall k \in \mathcal{N}_\mathcal{Q}, \forall j \in \mathcal{N}_\mathcal{P} \\ \text{s.t.} \quad & -1 \leq \varepsilon_k \leq 1, \quad -1 \leq \varepsilon_j \leq 1 \\ & inf(\mathbf{C}) \leq \mathbf{AX} \leq sup(\mathbf{C}) \end{aligned} \tag{3.13}$$

$$\begin{aligned} \max \quad & (\varepsilon_k, \varepsilon_j) \quad \forall k \in \mathcal{N}_\mathcal{Q}, \forall j \in \mathcal{N}_\mathcal{P} \\ \text{s.t.} \quad & -1 \leq \varepsilon_k \leq 1, \quad -1 \leq \varepsilon_j \leq 1 \\ & inf(\mathbf{C}) \leq \mathbf{AX} \leq sup(\mathbf{C}) \end{aligned} \tag{3.14}$$

These are standard linear programming (LP) problems which can be readily and efficiently solved by using an LP solver such as CPLEX [82]. The desired PF solution is then obtained as:

$$\begin{aligned} V_i &= V_{i,0} + \textstyle\sum_{j \in \mathcal{N}_\mathcal{P}} V_{i,j}^P[\varepsilon_{j,min}, \varepsilon_{j,max}] + \sum_{k \in \mathcal{N}_\mathcal{Q}} V_{i,k}^Q[\varepsilon_{k,min}, \varepsilon_{k,max}] \quad \forall i \in \mathcal{N}_\mathcal{Q} \\ \delta_i &= \delta_{i,0} + \textstyle\sum_{j \in \mathcal{N}_\mathcal{P}} \delta_{i,j}^P[\varepsilon_{j,min}, \varepsilon_{j,max}] + \sum_{k \in \mathcal{N}_\mathcal{Q}} \delta_{i,k}^Q[\varepsilon_{k,min}, \varepsilon_{k,max}] \quad \forall i \in \mathcal{N}_\mathcal{P} \end{aligned} \tag{3.15}$$

Observe that the proposed solution procedure represents an alternative to the traditional and widely used linearization formalism adopted in IA approaches, which is based on the Interval Newton method and consist on solving the following IA problem:

$$\mathbf{F}(\mathbf{x}_0 + \Delta\mathbf{x}) \in \mathbf{F}(\mathbf{x}) + \mathbf{J}(\mathbf{x}_0)\Delta\mathbf{x} \quad \forall \mathbf{x} \in \mathbf{x}_0 \tag{3.16}$$

where $\mathbf{x}_0$ is a vector of intervals, the Jacobian matrix $\mathbf{J}(x_0)$ is an interval matrix, and $\mathbf{F}(\mathbf{x})$ is a real vector defined by $\mathbf{x}$, which is typically the midpoint of $\mathbf{x}_0$. Solving (3.16) requires the "inversion" of the interval matrix $\mathbf{J}(\mathbf{x}_0)$, which is a nontrivial problem [83, 84], and, as pointed out in [48, 47], this is the main impediment in the application of IA to PF studies. On the other hand, the solution of (3.12) does not require an interval matrix inversion, making it computationally efficient and hence readily applicable to real size systems.

The described AA-based solution methodology can be improved to account for reactive power limits and properly model the generators voltage regulators. This is done here by using the standard PV- and PQ-bus switching as described in Section 2.2.

3.3 Numerical Results

This section discusses the application of the presented AA-based PF to three IEEE test systems. The PF solution bounds obtained by the proposed AA-based technique are compared to those calculated using a Monte Carlo simulation with a uniform distribution, which is typically assumed to yield the "correct" solution intervals. For the latter, 5000 different values of the input variables within the assumed input bounds were randomly selected, and a conventional PF solution was obtained for each one; this procedure yielded the desired interval solutions defined by the largest and the smallest values of the bus voltage magnitudes and angles as well as line flows. It should be noted that increasing the number of Monte Carlo simulations beyond 5000 did not yield any significant changes to the solution intervals.

Since all computational tasks were performed using Matlab^{TM}, for the representation of affine forms, a vectorial-based approach was adopted, which is computationally more efficient in Matlab^{TM}. Thus, each affine form is represented as a vector whose first element represents the central value while the other vector components describe the partial deviations with respect to the corresponding noise variable.

Without loss of generality, a $\pm 20\%$ (40%) tolerance on load and generator powers was assumed, since this would define an interval wide enough to represent, for example, uncertain wind and solar generation. Based on the assumed load and generator power bounds to represent input data uncertainty, the proposed AA-based PF was applied to estimate the bounds of the PF solution. All the simulation studies were developed on a PC workstation equipped with an Intel Core Duo CPU @ 3 GHz with 3 GB RAM, the obtained results are presented and discussed in the following sections.

3.3.1 IEEE 30-bus test system

The IEEE 30-bus test case represents a portion of the American Electric Power System composed by 30 buses, 3 generators, 3 synchronous condensers, 24 loads, and 41 lines [85]. The power profiles used to simulate the network are shown in Figures 3.1 and 3.2. The computed AA-based solution is compared with the one obtained by using the Monte

Carlo approach, in the profiles depicted in Figures 3.3-3.4, which depict the bus voltages magnitude and angle bounds, respectively. For this case study, the solution algorithm detected that the upper bound of the reactive power on the 4th generator, connected at the Bus 27, violated the upper limit. Consequently, the solution algorithm first switched this bus from PV to PQ, then fixed the corresponding reactive power to the maximum allowable value and, finally, proceeded to calculate the final PF solution. The corresponding reactive power generated at the PV buses after the bus-type switches is depicted in Figure 3.5.

3.3.2 IEEE 57-bus test system

The IEEE 57-bus Test system represents a portion of the American Electric Power System composed by 57 buses, 7 generators, 42 loads, and 80 lines [85]. The power profiles adopted to simulate the network are shown in Figures 3.6 and 3.7. In this case, after the first iteration, the solution algorithm detected that the upper bound of the reactive power on both the 4th and the 6th generator, connected at Buses 6 and 8 respectively, violated the upper limit. Consequently, the solution algorithm first switched these buses from PV to PQ, then fixed the corresponding reactive powers to the maximum allowable values and, finally, proceeded to calculate the final PF solution. The computed AA-based solution is compared with that obtained by using the Monte Carlo approach, as shown in the profiles depicted in Figures 3.8-3.10, with Figure 3.8 depicting the bus voltages magnitude bounds, Figure 3.9 showing the bus voltages angle bounds, and Figure 3.10 depicting the reactive power generated at the PV buses after the bus-type switches.

3.3.3 IEEE 118-bus test system

The IEEE 118 Bus Test Case represents a portion of the Midwestern American Electric Power System composed by 118 bus, 54 generators, 64 loads and 186 lines [85]. The power profiles adopted to simulate the network are shown in Figures 3.11 and 3.12. The computed AA-based solution is compared with that obtained by using the Monte Carlo approach, as shown in the profiles depicted in Figures 3.13 and 3.14, with Figure 3.13 depicting the bus voltages magnitude bounds, while Figure 3.14 shows the corresponding bus voltages

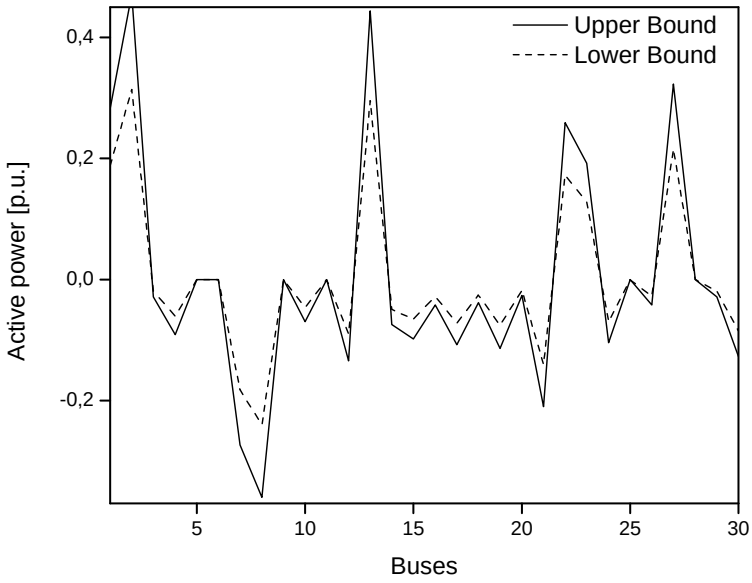

(a)

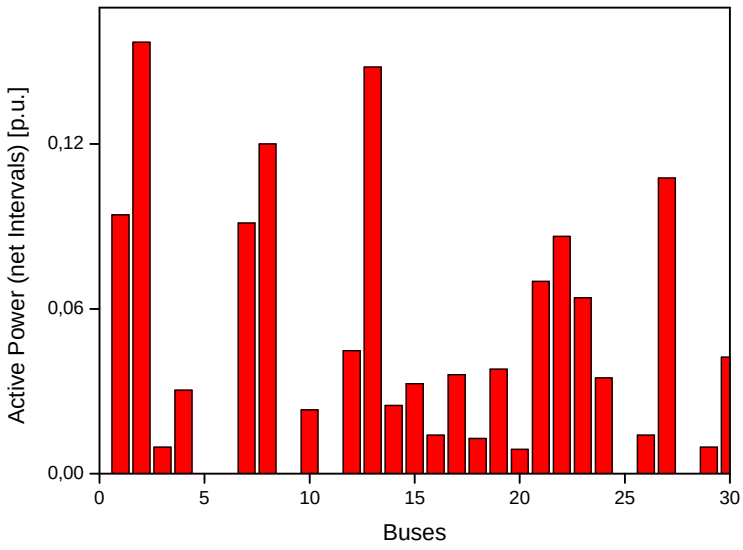

(b)

Figure 3.1: Active power (a) bounds and (b) net intervals for the IEEE 30-bus test system.

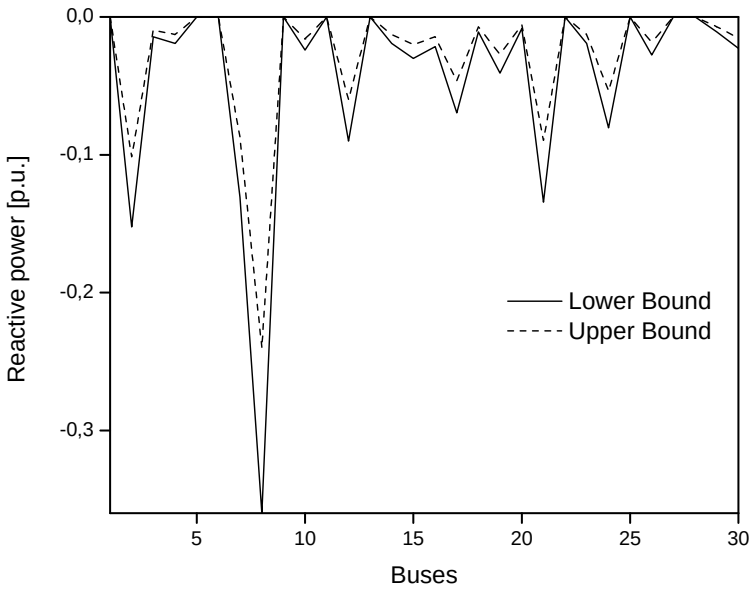

(a)

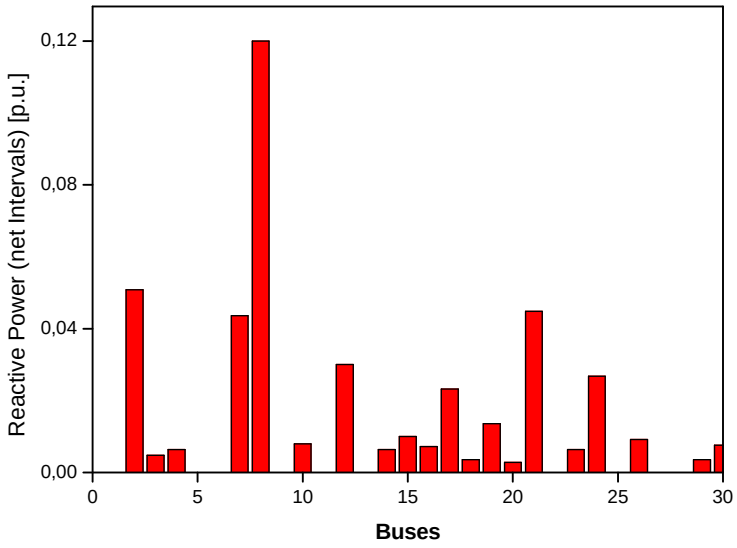

(b)

Figure 3.2: Reactive power (a) bounds and (b) net intervals for the IEEE 30-bus test system.

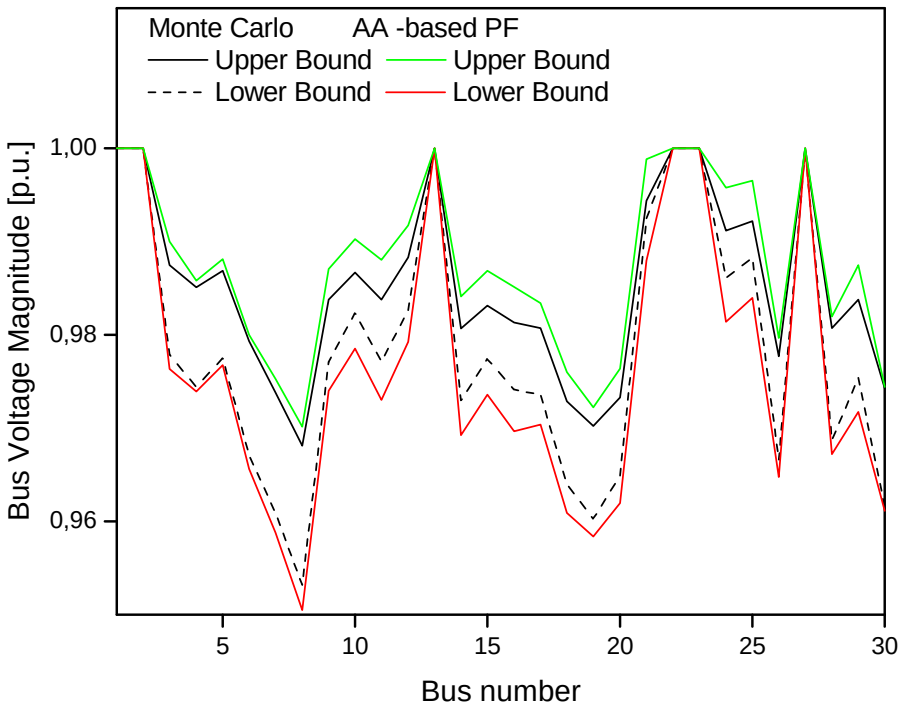

Figure 3.3: Obtained bus voltage magnitude bounds for the IEEE 30-bus test system.

angle bounds. For this case study, the solution algorithm didn't detect any violations of the reactive power constraints.

3.3.4 Discussion

From the obtained results summarized in Table 3.1, comparing the average errors in the difference of the upper and lower bounds for bus voltage magnitudes and angles between the proposed AA method and Monte Carlo, it is worth observing that the AA-based methodology gives fairly good approximations of the PF solution bounds, when compared to the benchmark intervals obtained with the Monte Carlo approach; this is mainly due to the intrinsic characteristic of AA, which keeps track of correlations between the power systems state variables. It is important to notice that the solution bounds are slightly conservative, which is due to the fact that AA, like IA, yields "worst case" bounds, which

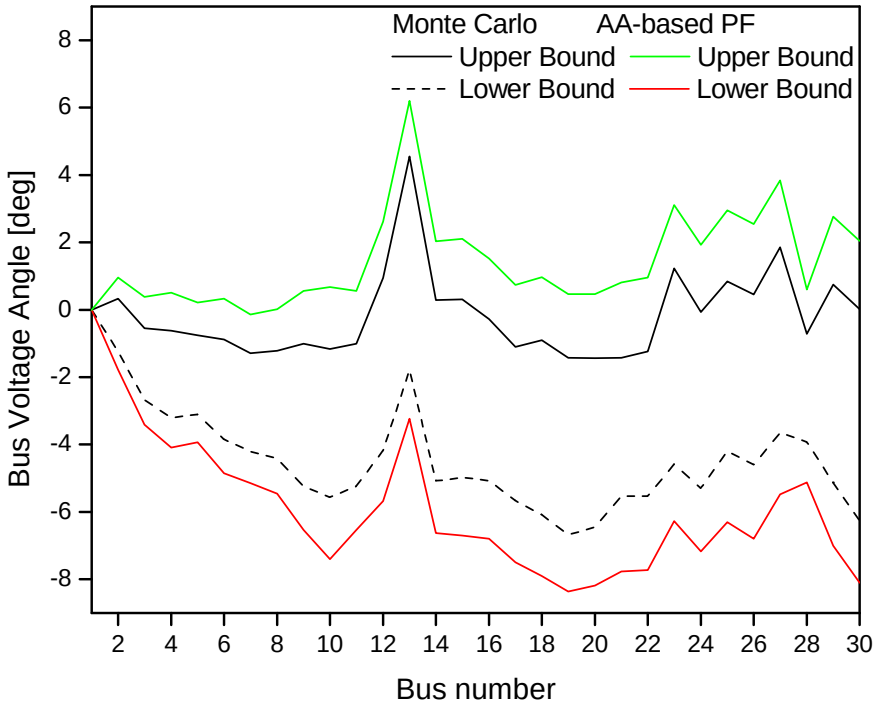

Figure 3.4: Obtained bus voltage angle bounds for the IEEE 30-bus test system.

take into account any uncertainties in the input data. This is to be expected, since, as stated in [86], the random, uniformly distributed variation of variables (with mean equal zero) assumed in the Monte Carlo approach tends to underestimate the worst case variations. This can be considered as an advantage of the proposed approach, since no assumptions regarding the probability distribution of load and generator power variations are required.

In order to assess the benefits of uncertainty representation by AA compared to IA, further studies aimed at characterizing the solution domain of the PF equations were performed for the IEEE 57-bus test system. These results are summarized in Figures 3.15 and 3.16, with Figure 3.15 showing the solution domain for Buses 2 and 6 voltage angles assessed by IA, AA, and the Monte Carlo approach, and Figure 3.16 depicting the active power bounds at the PV and PQ buses obtained by applying IA to the PF equations 2.1 using the solution bounds obtained from the Monte Carlo formulations as IA intervals.

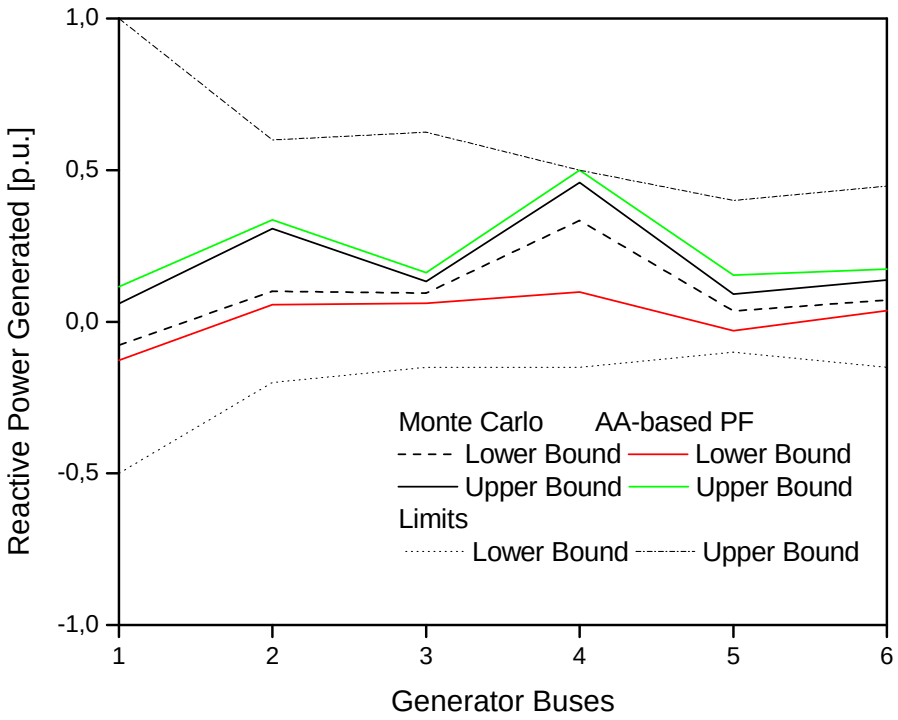

Figure 3.5: Obtained reactive power bounds at PV buses for the IEEE 30-bus test system.

Observe that AA yields a more realistic elliptical approximation of the solution domain compared to the typical "hyper box" (rectangle) used in IA, which may result on missing some salient features of the actual variations of the power systems state variables. This in turn leads to a large overestimation of the complex power bus injections, as confirmed by the wide IA-based bounds shown in Figure 3.16. Note that, although these bounds were obtained by processing the best available approximation of the state variable solution bounds, the calculated active power bus injection bounds are significantly larger than the assumed $\pm 20\%$ (40%) interval.

Finally, it is worth observing that the AA-based methodology allows to compute a reliable and fast estimation of the PF solution bounds compared to the sampling-based approach. This is clearly observed in Table 3.2, which summarizes the execution times observed in the simulation studies.

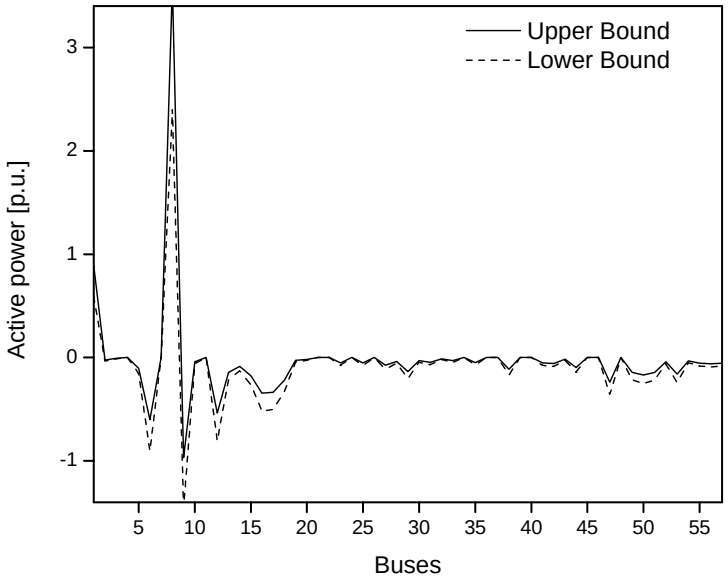

(a)

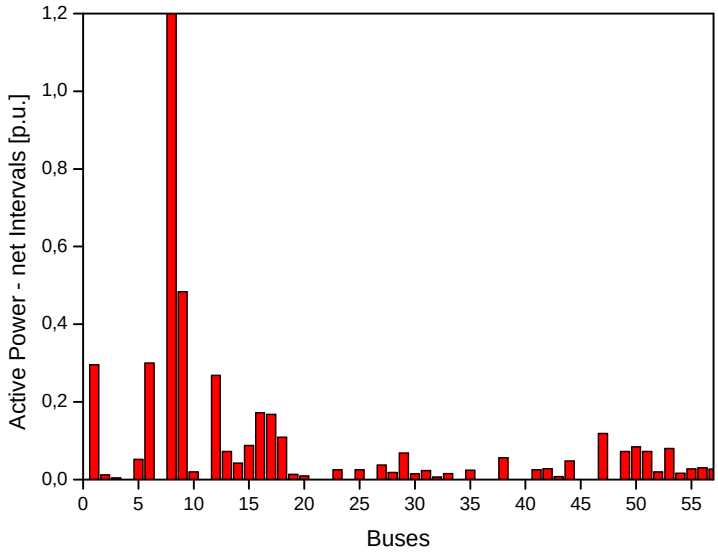

(b)

Figure 3.6: Active power (a) bounds and (b) net intervals for the IEEE 57-bus test system.

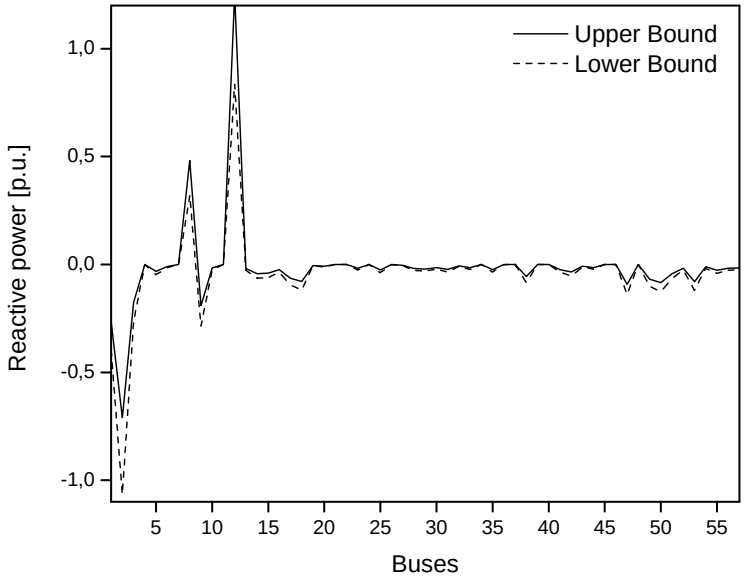

(a)

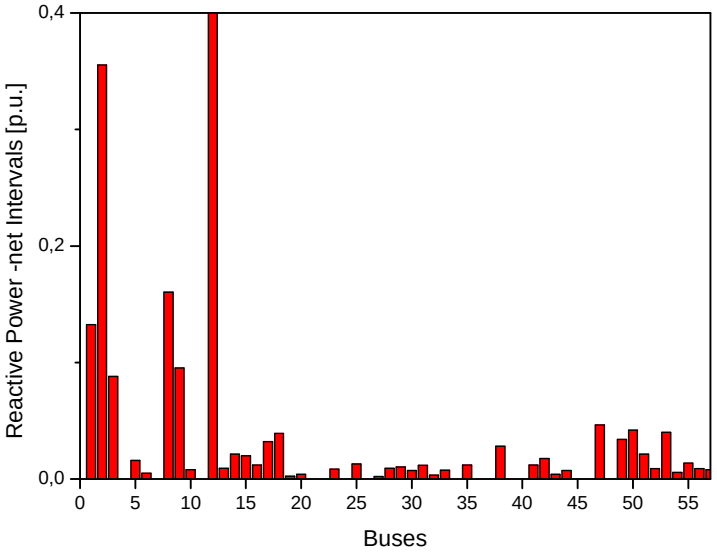

(b)

Figure 3.7: Reactive power (a) bounds and (b) net intervals for the IEEE 57-bus test system.

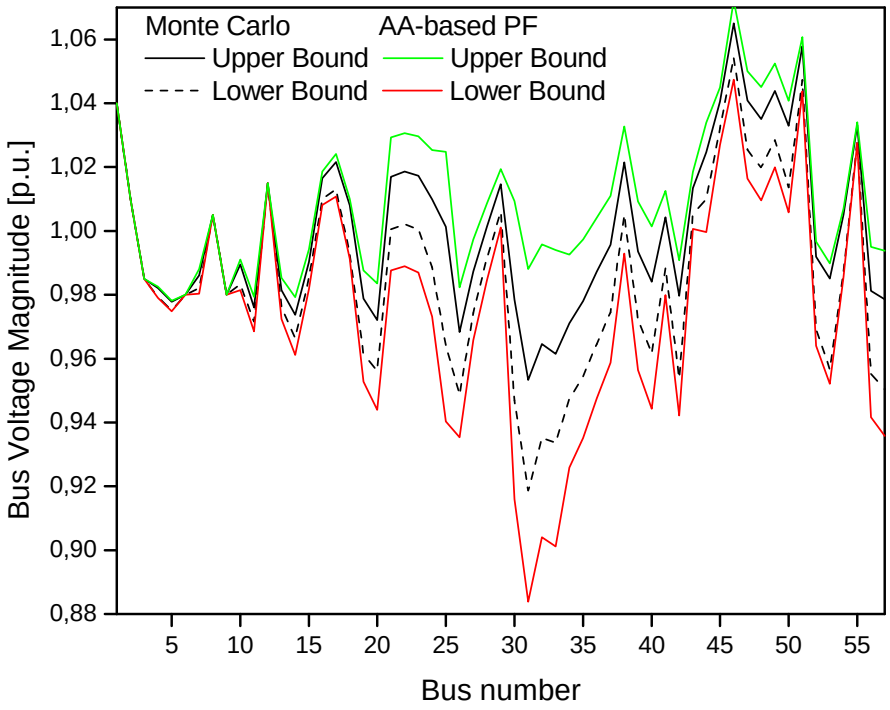

Figure 3.8: Obtained bus voltage magnitude bounds for the IEEE 57-bus test system.

3.4 Summary

In this chapter, a methodology for AA-based PF analysis that allows to better handle uncertainty compared to the traditional and widely used IA approaches has been explained. Based on this AA formalism, the PF solution bounds were readily obtained by solving a limited number of linear optimization problems. It was shown, with the help of various tests run on several power test systems, that using AA allows addressing effectively the "wrapping effect" and the "dependency problem" of IA, leading to a better characterization of the effects of input data uncertainty in PF solutions, and a more realistic approximation of the solution domain compared to the typical "hyper box" form obtained with IA approaches. It was also illustrated that the AA-based technique is computationally more efficient than the Monte Carlo simulation sampling-based method. The presented analysis and results demonstrate that the AA-based approach is well suited for the assessment of uncertainty

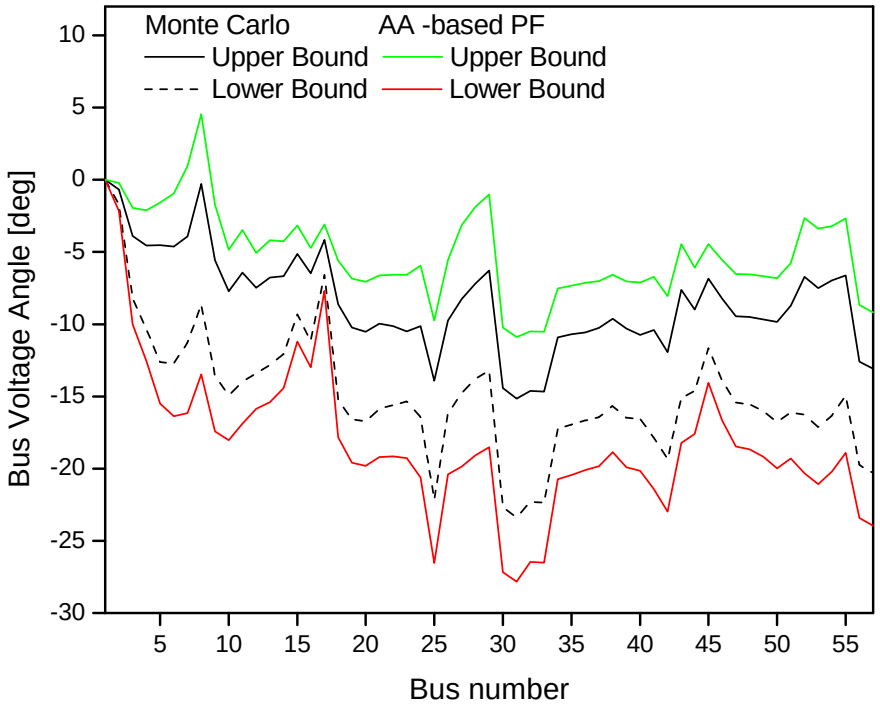

Figure 3.9: Obtained bus voltage angle bounds for the IEEE 57-bus test system.

propagation in PF solutions, independent of the types and levels of uncertainties in the input data.

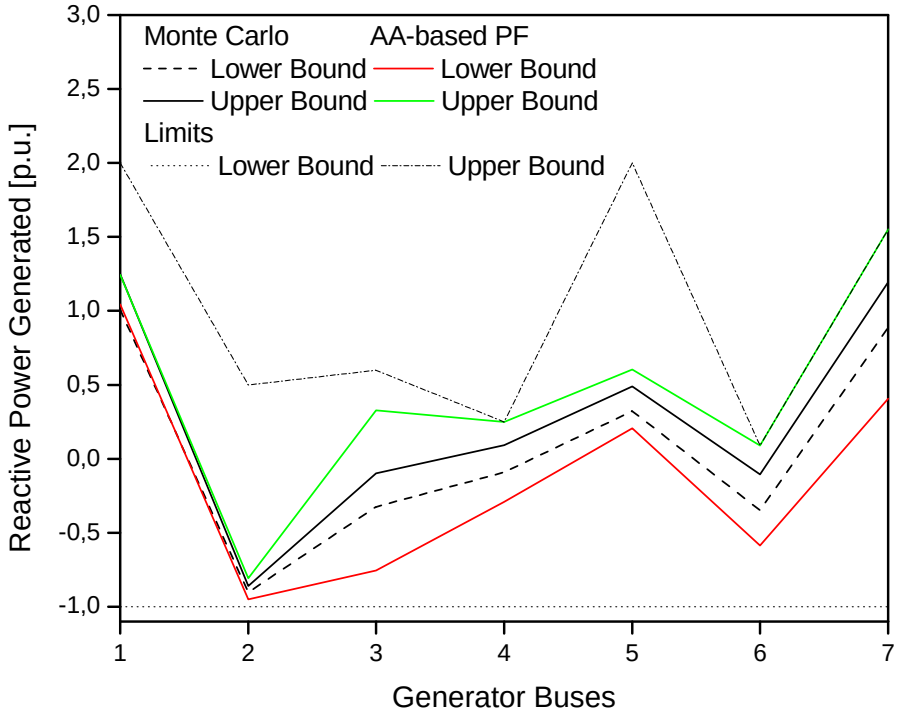

Figure 3.10: Obtained reactive power bounds at PV buses for the IEEE 57-bus test system.

Table 3.1: Average Errors

	30 bus		57 bus		118 bus	
	Upper	Lower	Upper	Lower	Upper	Lower
Bus Voltage Angle [deg]	0.65	0.97	3.32	3.33	3.18	3.16
Bus Voltage Magnitude [p.u.]	0.0055	0.0046	0.009	0.0088	0.0102	0.0101

Table 3.2: Execution Times (seconds)

	30 bus	57 bus	118 bus
Monte Carlo (5000 trials) [s]	149.9	211.8	603.1
AA-based PF [s]	1.7	2.5	5.7

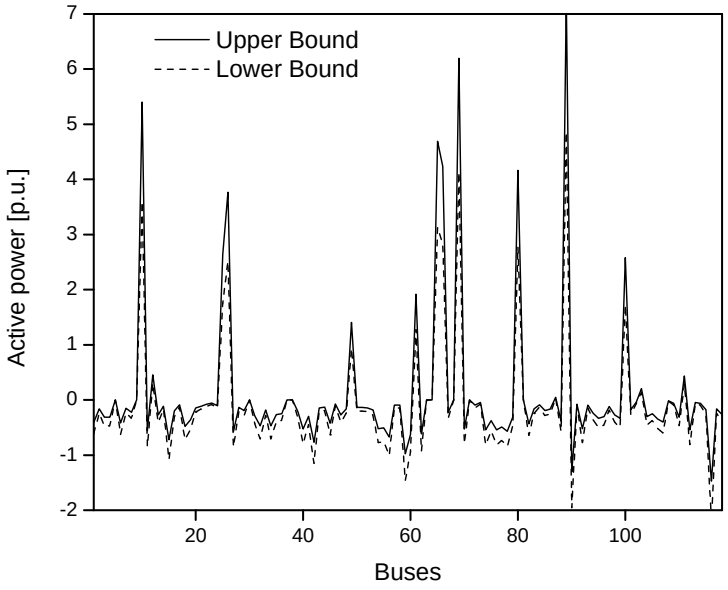

(a)

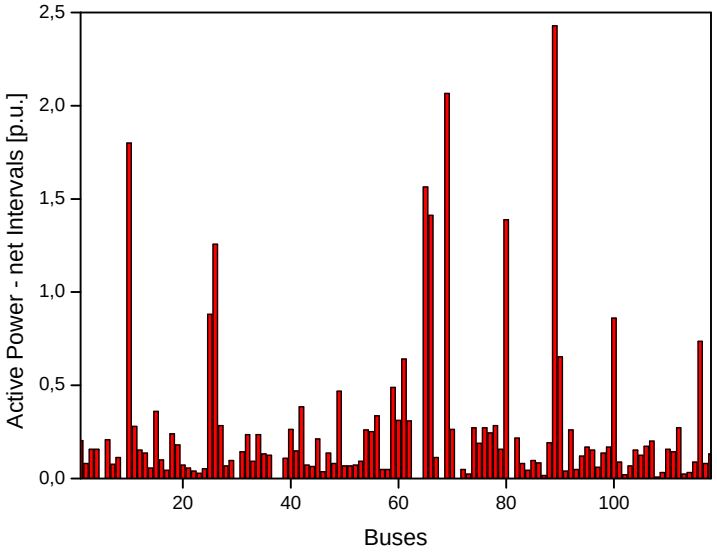

(b)

Figure 3.11: Active power (a) bounds and (b) net intervals for the IEEE 118-bus test system.

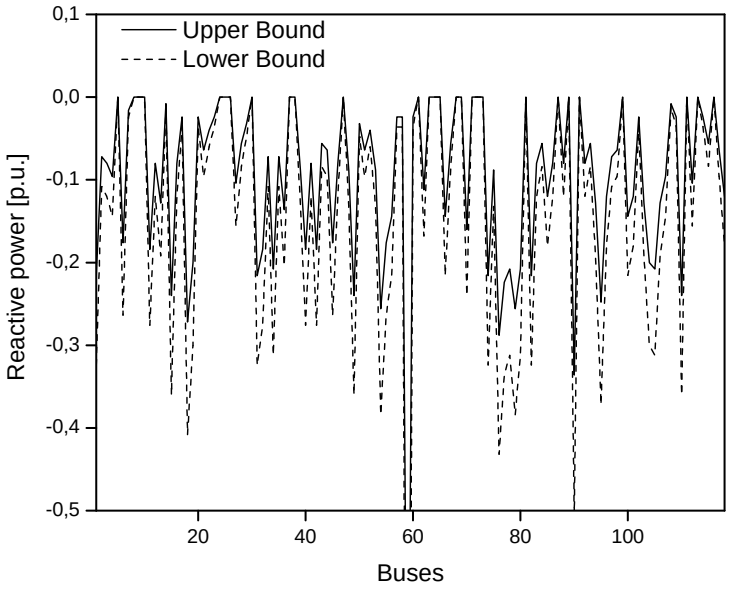

(a)

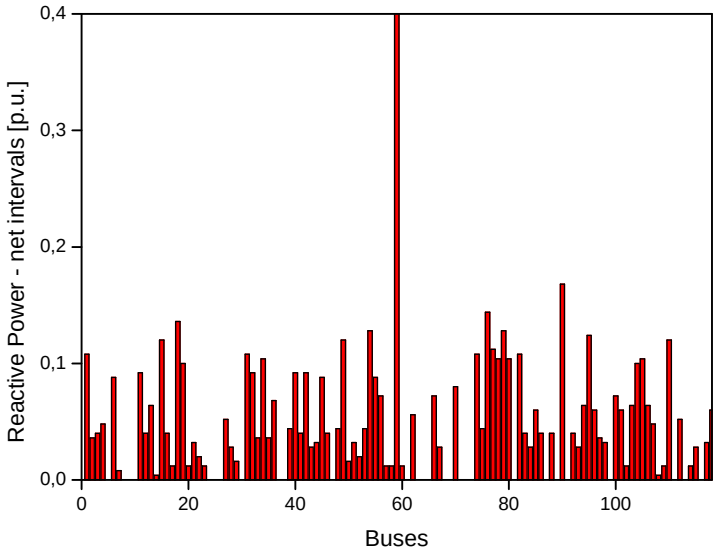

(b)

Figure 3.12: Reactive power (a) bounds and (b) net intervals for the IEEE 118-bus test system.

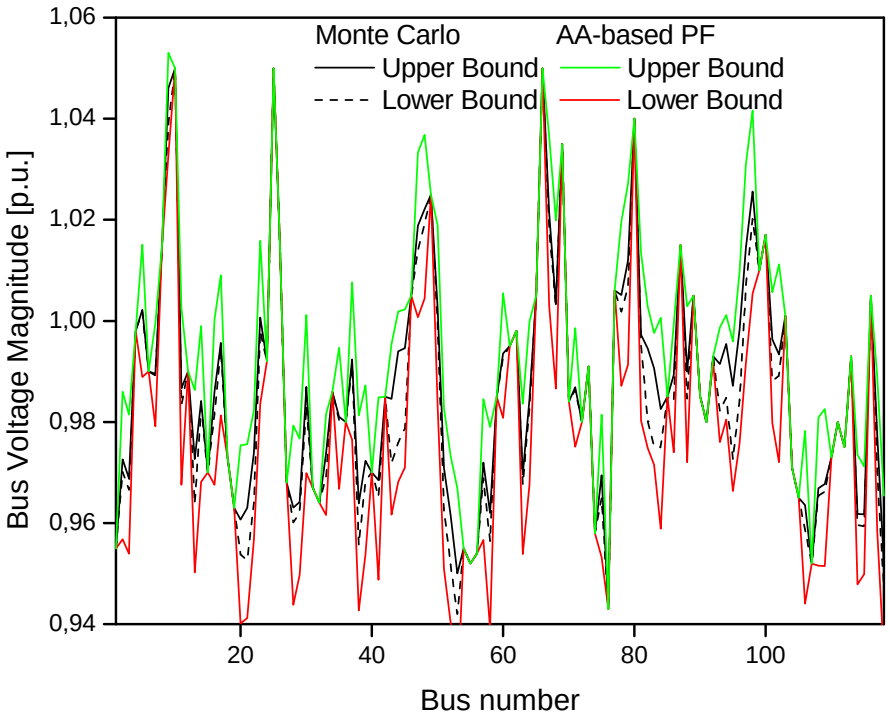

Figure 3.13: Obtained bus voltage magnitude bounds for the IEEE 118-bus test system.

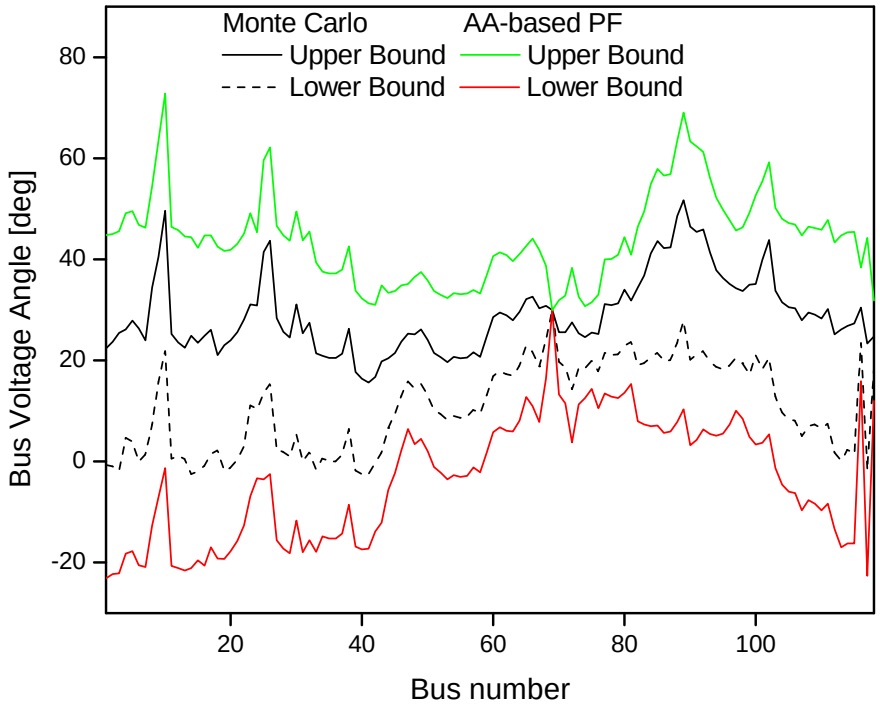

Figure 3.14: Obtained bus voltage angle bounds for the IEEE 118-bus test system.

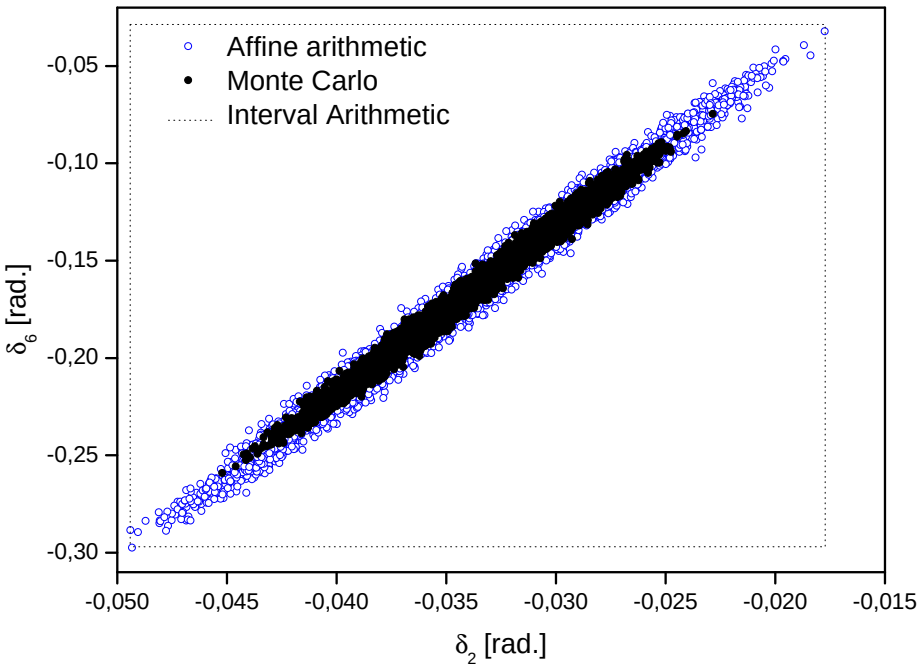

Figure 3.15: Solution boundary of the Bus 2 and Bus 6 voltage angles for the IEEE 57-bus test system.

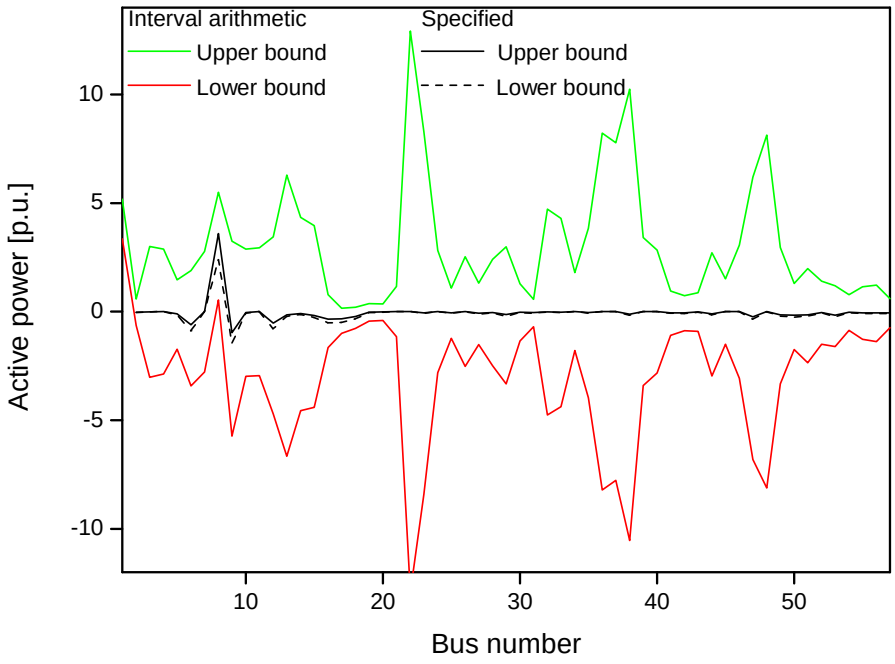

Figure 3.16: Active powers at the PV and PQ buses obtained by IA using the bounds computed by Mote Carlo simulations for the IEEE 57-bus test system.

Chapter 4

Range Arithmetic for Uncertain OPF Analysis

4.1 Introduction

This chapter presents a hybrid framework based on the fusion of AA and Range Arithmetic for solving OPF problems whose input data are specified within real compact intervals. Reliable interval bounds are computed for the OPF problem, which is represented as an optimization model with complementary constraints to properly represent generator bus voltage controls, including reactive power limits and voltage recovery processes. It is demonstrated that the lower and upper bounds of the OPF solutions can be obtained by solving two determinate optimization problems. Several numerical results are presented and discussed for several test system and the standard cost minimization and voltage deviation minimization OPF problems, demonstrating the effectiveness of the proposed methodology.

4.2 Methodology

As proposed in [49], an "uncertain" OPF can be expressed as a class of nonlinear interval optimization problems that can be defined as follows, based on the mathematical model (2.2):

$$\begin{aligned} \min_{\hat{\mathbf{z}}} \quad & \hat{f}(\hat{\mathbf{z}}) \\ \text{s.t.} \quad & \hat{g}_j(\hat{\mathbf{z}}) = 0 \ \forall j \in [1, n] \\ & \hat{h}_k(\hat{\mathbf{z}}) < 0 \ \forall k \in [1, m] \end{aligned} \tag{4.1}$$

where $\hat{\mathbf{z}} = (\hat{\mathbf{x}}, \hat{\mathbf{u}})$, and the locally convex objective function $\hat{f}(\hat{\mathbf{z}})$, the n equality constrained continuous functions $\hat{g_j}(\hat{\mathbf{z}})$, and the m inequality constrained functions $\hat{h_k}(\hat{\mathbf{z}})$, are defined on closed intervals as follows:

$$\hat{f}(\hat{\mathbf{z}}) = [f_{low}(\hat{\mathbf{z}}), f_{up}(\hat{\mathbf{z}})] \tag{4.2}$$

$$\hat{g}_j(\hat{\mathbf{z}}) = [g_{j,low}(\hat{\mathbf{z}}), g_{j,up}(\hat{\mathbf{z}})] \quad \forall j \in [1, n] \tag{4.3}$$

$$\hat{h}_k(\hat{\mathbf{z}}) = [h_{k,low}(\hat{\mathbf{z}}), h_{k,up}(\hat{\mathbf{z}})] \quad \forall k \in [1, m] \tag{4.4}$$

Here, $f_{low}(\hat{\mathbf{z}})$, $g_{j,low}(\hat{\mathbf{z}})$ $\forall j \in [1, n]$ and $h_{k,low}(\hat{\mathbf{z}})$ $\forall k \in [1, m]$ are lower boundary functions, while $f_{up}(\hat{\mathbf{z}})$, $g_{j,up}(\hat{\mathbf{z}})$ $\forall j \in [1, n]$ and $h_{k,up}(\hat{\mathbf{z}})$ $\forall k \in [1, m]$ are corresponding upper boundary functions. If (4.2), (4.3) and (4.4) are assumed to be represented in affine form, the inclusion isotonicity property of AA solves the nonlinear optimization problem under interval uncertainty (4.1). This fundamental property can be expressed with the following theorem [87]:

Theorem 3 (Fundamental Theorem of Range Analysis)*: For the convex interval function* $\hat{\Gamma}(\hat{\chi}) = [\Gamma_{low}(\hat{\chi}), \Gamma_{up}(\hat{\chi})]$ *to take the minimum (maximum) value at* χ^* *in its compact domain* G*, it is necessary and sufficient that the boundary functions* $\Gamma_{low}(\hat{\chi})$ *and* $\Gamma_{up}(\hat{\chi})$ *take the minimum (maximum) value at the same point:*

$$\hat{\Gamma}(\chi^*) = [\Gamma_{low}(\chi^*), \Gamma_{up}(\chi^*)] = \min_{\hat{\chi} \in G} \quad \hat{\Gamma}(\hat{\chi}) = [\Gamma_{low}(\hat{\chi}), \Gamma_{up}(\hat{\chi})] \Leftrightarrow \begin{cases} \Gamma_{low}(\chi^*) = \min\limits_{\hat{\chi} \in G} & \Gamma_{low}(\hat{\chi}) \\ \Gamma_{up}(\chi^*) = \min\limits_{\hat{\chi} \in G} & \Gamma_{up}(\hat{\chi}) \end{cases}$$

$$\hat{\Gamma}(\chi^*) = [\Gamma_{low}(\chi^*), \Gamma_{up}(\chi^*)] = \max_{\hat{\chi} \in G} \quad \hat{\Gamma}(\hat{\chi}) = [\Gamma_{low}(\hat{\chi}), \Gamma_{up}(\hat{\chi})] \Leftrightarrow \begin{cases} \Gamma_{low}(\chi^*) = \max\limits_{\hat{\chi} \in G} & \Gamma_{low}(\hat{\chi}) \\ \Gamma_{up}(\chi^*) = \max\limits_{\hat{\chi} \in G} & \Gamma_{up}(\hat{\chi}) \end{cases}$$

∎

This theorem reduces the search for the extreme of an interval function in a given domain to the search for the extrema of its lower and upper boundary functions in the same domain. In other words, the interval problem associated with (4.1) is reduced to two ordinary optimization problems, namely, the lower and upper boundary problems [88, 89]. Therefore, the solution to (4.1) can be restated as the solution of the following two NLP problems [90], [88], [89]:

$$\begin{aligned} \min_{\hat{\mathbf{z}}} \quad & f_{low}(\hat{\mathbf{z}}) \\ \text{s.t.} \quad & g_{j,low}(\hat{\mathbf{z}}) = 0 \ \forall j \in [1, n] \\ & h_{k,up}(\hat{\mathbf{z}}) < 0 \ \forall k \in [1, m] \end{aligned} \tag{4.5}$$

$$\begin{aligned} \min_{\hat{\mathbf{z}}} \quad & f_{up}(\hat{\mathbf{z}}) \\ \text{s.t.} \quad & g_{j,up}(\hat{\mathbf{z}}) = 0 \ \forall j \in [1, n] \\ & h_{k,up}(\hat{\mathbf{z}}) < 0 \ \forall k \in [1, m] \end{aligned} \tag{4.6}$$

Thus, Theorem 3 yields the problems (4.5) and (4.6) for determining the lower and upper bounds of the interval objective function $\hat{f}(\hat{\mathbf{z}}) = [f_{low}(\hat{\mathbf{z}}), f_{up}(\hat{\mathbf{z}})]$ of the OPF problem (4.1), with the respective constraints obtained from the upper and lower bound of the system of equality constraints of the interval problem $\hat{g_j}(\hat{\mathbf{z}}) = [g_{j,low}(\hat{\mathbf{z}}), g_{j,up}(\hat{\mathbf{z}})] \ \forall j \in [1, n]$, and from the upper bound of the system of inequality constraints of the interval problem $\hat{h}_k(\hat{\mathbf{z}}) = [h_{k,low}(\hat{\mathbf{z}}), h_{k,up}(\hat{\mathbf{z}})] \ \forall k \in [1, m]$.

These formulae are deterministic optimization problems with point (non-interval) data, which could significantly simplify the solution to the interval OPF problem (4.1), as proposed in [49]. Thus, to find the OPF solution interval the following solution algorithm is adopted:

1. Compute an outer estimation of the uncertain OPF problem solution (i.e. by using the sensitivity-based approach described in (3.3)):

$$\hat{\mathbf{z}}_{outer} = \mathbf{z}_0 + \mathbf{z}_1\varepsilon_1 + ... + \mathbf{z}_p\varepsilon_p \tag{4.7}$$

2. Solve the lower boundary problem (4.5) using any appropriate solver for determinate nonlinear programming problems, obtaining a solution $\varepsilon_{i,low}$ $\forall i \in [1, p]$.

3. Solve the upper boundary problem (4.6) using the same solver as in Step 1, obtaining a solution $\varepsilon_{i,up}$ $\forall i \in [1, p]$.

4. Compute the solution set as:

$$\hat{\mathbf{z}} = \mathbf{z}_0 + \mathbf{z}_1\varepsilon_{1,opt} + ... + \mathbf{z}_p\varepsilon_{p,opt} \tag{4.8}$$

where

$$\varepsilon_{i,opt} = [-\varepsilon_{i,up}, \varepsilon_{i,up}] \cap [-\varepsilon_{i,low}, \varepsilon_{i,low}] \ \forall i \in [1, p] \tag{4.9}$$

4.2.1 Optimal Economic Dispatch

Economic dispatch analysis aims at assessing the optimal output of a number of power generators which meets the system load, at the lowest possible cost, and assures a secure a reliable power system operation. The overall problem can be formalized by the following constrained nonlinear optimization programming problem [91]:

$$\begin{aligned} \min_{(P_{G_1},...,P_{G_{NGA}})} \quad & \sum_{i=1}^{N_{GA}} (a_i + b_i P_{G_i} + c_i P_{G_i}^2) \\ \text{s.t.} \quad & \sum_{i=1}^{N_G} P_{G_i} = P_D + P_{loss}(P_{G_1}, ..., P_{G_{Nga}}) \\ & P_{G_i,min} \leq P_{G_i} \leq P_{G_i,max} \qquad \forall i \in [1, N_{GA}] \end{aligned} \tag{4.10}$$

where P_D is the power demand; N_G is the total number of generators; N_{GA} is the number of dispatchable generators; P_{G_i} is the power generated by the i^{th} generator; $P_{G_i,min}$ and $P_{G_i,max}$ are the minimum and maximum generation limits respectively; a_i b_i and c_i are the corresponding cost coefficients; and $P_{loss}(P_{G_1}, ..., P_{G_{NGA}})$ denotes the network active power losses that can be computed by using the following simplified equations:

$$P_{loss}(P_{G_1}, ..., P_{G_{NGA}}) = \sum_{i=1}^{N_G} B_i \ P_{G_i}^2 \tag{4.11}$$

where B_i are fixed loss coefficients.

The solution paradigm formalized in (4.5) and (4.6) can be adopted to solve this problem in the presence of interval uncertainty. To this aim, controllable generators are treated as intervals, as follows:

$$\hat{P}_i = P_{G_{i,0}} + P_{G_{i,1}}\varepsilon_1 + ... + P_{G_{i,p}}\varepsilon_p \; \forall i \in [1, N_{GA}] \tag{4.12}$$

Which yields the following upper and lower bounds:

$$\begin{aligned} \hat{P}_{G_i,up} &= P_{G_{i,0}} + P_{G_{i,1}}\varepsilon_{1,up} + ... + P_{G_{i,p}}\varepsilon_{p,up} \; \forall i \in [1, N_{GA}] \\ \hat{P}_{G_i,low} &= P_{G_{i,0}} + P_{G_{i,1}}\varepsilon_{1,low} + ... + P_{G_{i,p}}\varepsilon_{p,low} \; \forall i \in [1, N_{GA}] \end{aligned} \tag{4.13}$$

where the noise symbols bounds $\varepsilon_{j,up}$ and $\varepsilon_{j,low}$, $\forall j \in [1, p]$, can be obtained by solving the following deterministic OPF problems:

$$\begin{aligned} \min_{(\varepsilon_{1,up},...,\varepsilon_{p,up})} \quad & \bar{\nabla}\left(\sum_{i=1}^{N_{GA}} (a_i + b_i\hat{P}_{G_{i,up}} + c_i\hat{P}^2_{G_{i,up}})\right) \\ \text{s.t.} \quad & \sum_{i=1}^{N_G} P_{G_{i,0}} + \sum_{i=1}^{N_G}\sum_{j=1}^{p} \left|P_{G_{i,j}}\ \varepsilon_{j,up}\right| = \bar{\nabla}\left(P_{D,max} + P_{loss}(\hat{P}_{G_{i,up}}, ..., \hat{P}_{G_{N_{GA},up}})\right) \\ & P_{G_{i,0}} + \sum_{j=1}^{p} \left|P_{G_{i,j}}\ \varepsilon_{j,up}\right| \leq P_{G_{i,max}} \; \forall i \in [1, N_{GA}] \\ & P_{G_{i,min}} \leq P_{G_i,0} - \sum_{j=1}^{p} \left|P_{G_{i,j}}\ \varepsilon_{j,up}\right| \; \forall i \in [1, N_{GA}] \end{aligned} \tag{4.14}$$

$$\begin{aligned} \min_{(\varepsilon_{1,low},...,\varepsilon_{p,low})} \quad & \nabla\left(\sum_{i=1}^{N_{GA}} (a_i + b_i\hat{P}_{Gi,low} + c_i\hat{P}^2_{Gi,low})\right) \\ \text{s.t.} \quad & \sum_{i=1}^{N_G} P_{Gi,0} - \sum_{i=1}^{N_G}\sum_{j=1}^{p} |P_{Gi,j}\ \varepsilon_{j,low}| = \nabla\left(P_{D,min} + P_{loss}(\hat{P}_{G1,low}, ..., \hat{P}_{GN_{GA},low})\right) \\ & P_{Gi,0} + \sum_{j=1}^{p} |P_{Gi,j}\ \varepsilon_{j,low}| \leq P_{Gi,max} \; \forall i \in [1, N_{GA}] \\ & P_{Gi,min} \leq P_{Gi,0} - \sum_{j=1}^{p} |P_{Gi,j}\ \varepsilon_{j,low}| \; \forall i \in [1, N_{GA}] \end{aligned} \tag{4.15}$$

where $\bar{\nabla}$ and ∇ are the upper and lower bound operator for affine forms defined in (2.13) and (2.14), respectively.

4.2.2 Reactive Power Dispatch

Reactive power dispatch in power systems aims to identify, for each network state, the set-points of the primary generator voltage controllers that minimize an objective function subject to a number of equality and inequality constraints. The overall problem can be formalized by the following constrained non-linear programming problem [91]:

$$\begin{aligned}
\min_{(V_i\ \forall i\in[1,N],\delta_i\ \forall i\in\mathcal{N}_{\mathcal{P}},\mathcal{Q}_i\ \forall i\in\mathcal{N}_{\mathcal{PV}})} \quad & \frac{1}{N}\sum_{i=1}^{N}(V_i-1)^2 \\
\text{s.t. } & P_i^{SP} - V_i\sum_{j=1}^{N} V_j Y_{ij}\cos\left(\delta_i-\delta_j-\theta_{ij}\right)=0 && \forall i\in\mathcal{N}_{\mathcal{P}} \\
& Q_j^{SP} - V_j\sum_{k=1}^{N} V_k Y_{jk}\sin\left(\delta_j-\delta_k-\theta_{jk}\right)=0 && \forall j\in\mathcal{N}_{\mathcal{Q}} \\
& Q_i - V_i\sum_{k=1}^{N} V_k Y_{ik}\sin\left(\delta_i-\delta_k-\theta_{ik}\right)=0 && \forall i\in\mathcal{N}_{\mathcal{PV}} \\
& V_{i,min}\le V_i\le V_{i,max} && \forall i\in[1,N] \\
& Q_{i,min}\le Q_i\le Q_{i,max} && \forall i\in\mathcal{N}_{\mathcal{PV}}
\end{aligned} \tag{4.16}$$

where $\mathcal{N}_{\mathcal{PV}}$ is the set of voltage controlled buses.

The solution paradigm formalized in (4.5) and (4.6) can also be adopted to solve this problem in the presence of interval uncertainty. To this aim, all optimization variables are treated as affine forms as follows:

$$\begin{aligned}
\hat{V}_i &= V_{i,0}+V_{i,1}\varepsilon_1+...+V_{i,p}\varepsilon_p\ \forall i\in[1,N] \\
\hat{\delta}_i &= \delta_{i,0}+\delta_{i,1}\varepsilon_1+...+\delta_{i,p}\varepsilon_p\ \forall i\in\mathcal{N}_{\mathcal{P}} \\
\hat{Q}_i &= Q_{i,0}+Q_{i,1}\varepsilon_1+...+Q_{i,p}\varepsilon_p\ \forall i\in\mathcal{N}_{\mathcal{PV}}
\end{aligned} \tag{4.17}$$

where each noise symbol represents an independent source of uncertainty affecting the input variables. This affine based representation yields the following upper and lower bounds:

$$\begin{aligned}
\hat{V}_{i,low} &= V_{i,0} + V_{i,1}\varepsilon_{1,low} + ... + V_{i,p}\varepsilon_{p,low} \ \forall i \in [1,N] \\
\hat{V}_{i,up} &= V_{i,0} + V_{i,1}\varepsilon_{1,up} + ... + V_{i,p}\varepsilon_{p,up} \ \forall i \in [1,N] \\
\hat{\delta}_{i,low} &= \delta_{i,0} + \delta_{i,1}\varepsilon_{1,low} + ... + \delta_{i,p}\varepsilon_{p,low} \ \forall i \in \mathcal{N}_{\mathcal{P}} \\
\hat{\delta}_{i,up} &= \delta_{i,0} + \delta_{i,1}\varepsilon_{1,up} + ... + \delta_{i,p}\varepsilon_{p,up} \ \forall i \in \mathcal{N}_{\mathcal{P}} \\
\hat{Q}_{i,low} &= Q_{i,0} + Q_{i,1}\varepsilon_{1,low} + ... + Q_{i,p}\varepsilon_{p,low} \ \forall i \in \mathcal{N}_{\mathcal{PV}} \\
\hat{Q}_{i,up} &= Q_{i,0} + Q_{i,1}\varepsilon_{1,up} + ... + Q_{i,p}\varepsilon_{p,up} \ \forall i \in \mathcal{N}_{\mathcal{PV}}
\end{aligned} \tag{4.18}$$

where the noise symbols bounds $\varepsilon_{j,up}$ and $\varepsilon_{j,low}$ $\forall j \in [1,p]$ can be obtained by solving the following deterministic OPF problems:

$$\begin{aligned}
\min_{(\varepsilon_{1,up},...,\varepsilon_{p,up})} \quad & \bar{\nabla}\left(\frac{1}{N}\sum_{i=1}^{N}(\hat{V}_{i,up}-1)^2\right) \\
\text{s.t. } & \bar{\nabla}\left(P_i^{SP} - \hat{V}_{i,up}\sum_{j=1}^{N}\hat{V}_{j,up}Y_{ij}\cos\left(\hat{\delta}_{i,up}-\hat{\delta}_{j,up}-\theta_{ij}\right)\right) = 0 \qquad \forall i \in \mathcal{N}_{\mathcal{P}} \\
& \bar{\nabla}\left(Q_j^{SP} - \hat{V}_{j,up}\sum_{k=1}^{N}\hat{V}_{k,up}Y_{jk}\sin\left(\hat{\delta}_{j,up}-\hat{\delta}_{k,up}-\theta_{jk}\right)\right) = 0 \qquad \forall j \in \mathcal{N}_{\mathcal{Q}} \\
& \bar{\nabla}\left(Q_i - \hat{V}_{i,up}\sum_{k=1}^{N}\hat{V}_{k,up}Y_{ik}\sin\left(\hat{\delta}_{i,up}-\hat{\delta}_{k,up}-\theta_{ik}\right)\right) = 0 \qquad \forall i \in \mathcal{N}_{\mathcal{PV}} \\
& V_{i,0} + \sum_{j=1}^{p}|V_{i,j}\ \varepsilon_{j,up}| \leq V_{i,max} \qquad \forall i \in [1,N] \\
& V_{i,min} \leq V_{i,0} + \sum_{j=1}^{p}|V_{i,j}\ \varepsilon_{j,up}| \qquad \forall i \in [1,N] \\
& Q_{i,0} + \sum_{j=1}^{p}|Q_{i,j}\ \varepsilon_{j,up}| \leq Q_{i,max} \qquad \forall i \in \mathcal{N}_{\mathcal{PV}} \\
& Q_{i,min} \leq Q_{i,0} + \sum_{j=1}^{p}|Q_{i,j}\ \varepsilon_{j,up}| \qquad \forall i \in \mathcal{N}_{\mathcal{PV}}
\end{aligned} \tag{4.19}$$

$$
\begin{aligned}
\min_{(\varepsilon_{1,low},\ldots,\varepsilon_{p,low})} \quad & \nabla\left(\frac{1}{N}\sum_{i=1}^{N}(\hat{V}_{i,up}-1)^2\right) \\
\text{s.t. } & \nabla\left(P_i^{SP}-\hat{V}_{i,low}\sum_{j=1}^{N}\hat{V}_{j,low}Y_{ij}\cos\left(\hat{\delta}_{i,low}-\hat{\delta}_{j,low}-\theta_{ij}\right)\right)=0 && \forall i\in\mathcal{N}_{\mathcal{P}} \\
& \nabla\left(Q_j^{SP}-\hat{V}_{j,low}\sum_{k=1}^{N}\hat{V}_{k,low}Y_{jk}\sin\left(\hat{\delta}_{j,low}-\hat{\delta}_{k,low}-\theta_{jk}\right)\right)=0 && \forall j\in\mathcal{N}_{\mathcal{Q}} \\
& \nabla\left(Q_i-\hat{V}_{i,low}\sum_{k=1}^{N}\hat{V}_{k,low}Y_{ik}\sin\left(\hat{\delta}_{i,low}-\hat{\delta}_{k,low}-\theta_{ik}\right)\right)=0 && \forall i\in\mathcal{N}_{\mathcal{PV}} \\
& V_{i,0}-\sum_{j=1}^{p}|V_{i,j}\ \varepsilon_{j,low}|\leq V_{i,max} && \forall i\in[1,N] \\
& V_{i,min}\leq V_{i,0}-\sum_{j=1}^{p}|V_{i,j}\ \varepsilon_{j,low}| && \forall i\in[1,N] \\
& Q_{i,0}-\sum_{j=1}^{p}|Q_{i,j}\ \varepsilon_{j,low}|\leq Q_{i,max} && \forall i\in\mathcal{N}_{\mathcal{PV}} \\
& Q_{i,min}\leq Q_{i,0}-\sum_{j=1}^{p}|Q_{i,j}\ \varepsilon_{j,low}| && \forall i\in\mathcal{N}_{\mathcal{PV}}
\end{aligned}
\tag{4.20}
$$

4.3 Numerical Results

4.3.1 Optimal Economic Dispatch

To assess the benefits of the range-arithmetic-based method for solving uncertain OPF problems, two case studies are analyzed here. First, the presented methodology is applied to solve the optimal active power dispatch of a 53 generators system proposed in [92], in the presence of demand uncertainty, which is described by the following affine form:

$$
\hat{P}_D = P_{D0} + P_{D1}\epsilon_1 + P_{D2}\epsilon_2 = 75 + 7.5\epsilon_1 + 3.75\epsilon_2 \tag{4.21}
$$

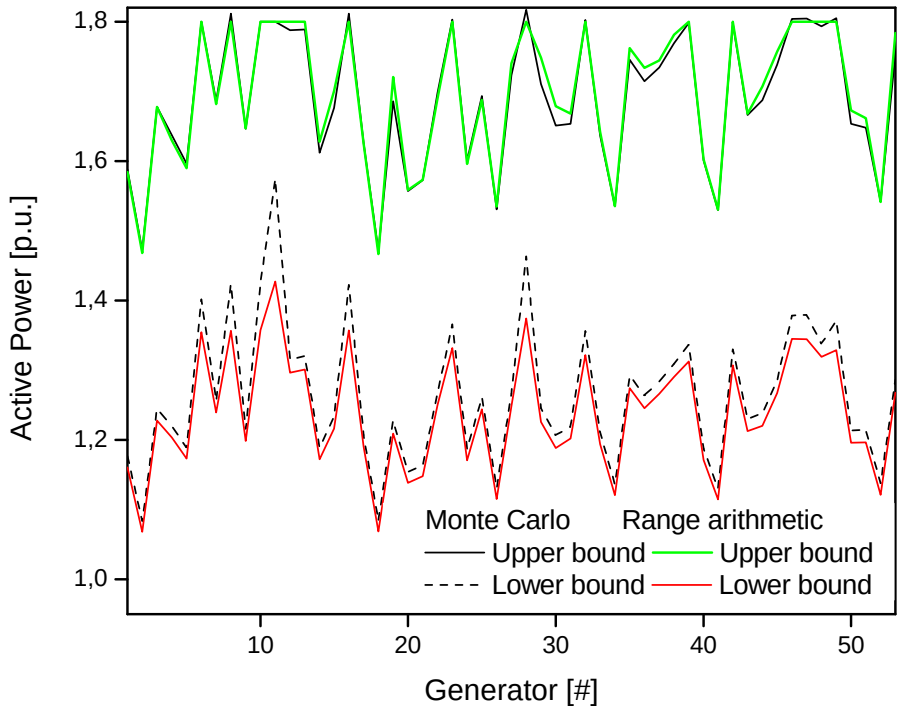

Figure 4.1: Bounds of the computed economic dispatch solutions.

where the noise symbols ϵ_1 and ϵ_2 can be used to model uncertain power demand and generation injections from wind and solar power sources (e.g. the forecasting errors in renewable generators). The main goal of this study is to determine the bounds of the active power generated, namely $P_{Gi} = [P_{Gi,low}, P_{Gi,up}]$ with $0.8 \leq P_{Gi} \leq 1.8 \ \forall i \in [1, 53]$, which minimize the total generation cost. Therefore, the solution algorithm discussed in Section 4.2.1 is applied, and the computed solution bounds are compared with those obtained by applying a Monte Carlo approach with 5000 simulations. The obtained results are summarized in Figure 4.1.

4.3.2 Reactive Power Dispatch

The second case study analyzes the solution of the reactive power dispatch in the presence of a $\pm 20\%$ tolerance on load and generator powers for the IEEE 118-bus test system [85]; the test power network is composed of 54 voltage controllable generators, 186 lines, and 64 load buses.

The control variables of the OPF problem are the set-points of the voltage magnitude at the generator buses, while the dependent variables are the reactive power at the generators, the voltage magnitude at the load buses, and the voltage phase angle at all buses except the slack bus. The voltage magnitudes at each bus are constrained to lie in the following range:

$$0.95 \leq V_i \leq 1.05 \, \forall i \in [1, 118] \tag{4.22}$$

Hence the data uncertainty characterizing the control and dependent variables of the OPF problem are represented by the following affine forms:

$$\begin{aligned} \hat{V}_i &= V_{i,0} + \sum_{k=1}^{117} V_{i,k} \varepsilon_k \; \forall i \in [1, N] \\ \hat{\delta}_i &= \delta_{i,0} + \sum_{k=1}^{117} \delta_{i,k} \varepsilon_k \; \forall i \in \mathcal{N}_{\mathcal{P}} \\ \hat{Q}_i &= Q_{i,0} + \sum_{k=1}^{117} Q_{i,k} \varepsilon_k \; \forall i \in \mathcal{N}_{\mathcal{PV}} \end{aligned} \tag{4.23}$$

where the central values and the partial deviations were obtained by the same sensitivity analysis used in Chapter 3 to define the affine forms. The obtained results have been summarized in Figures 4.2 and 4.3.

4.3.3 Discussions

From the obtained results, it can be observed that the range-arithmetic-based OPF technique yields fairly good approximations of the OPF solution bounds when compared to the benchmark intervals obtained using the Monte Carlo approach. Note that the OPF solution

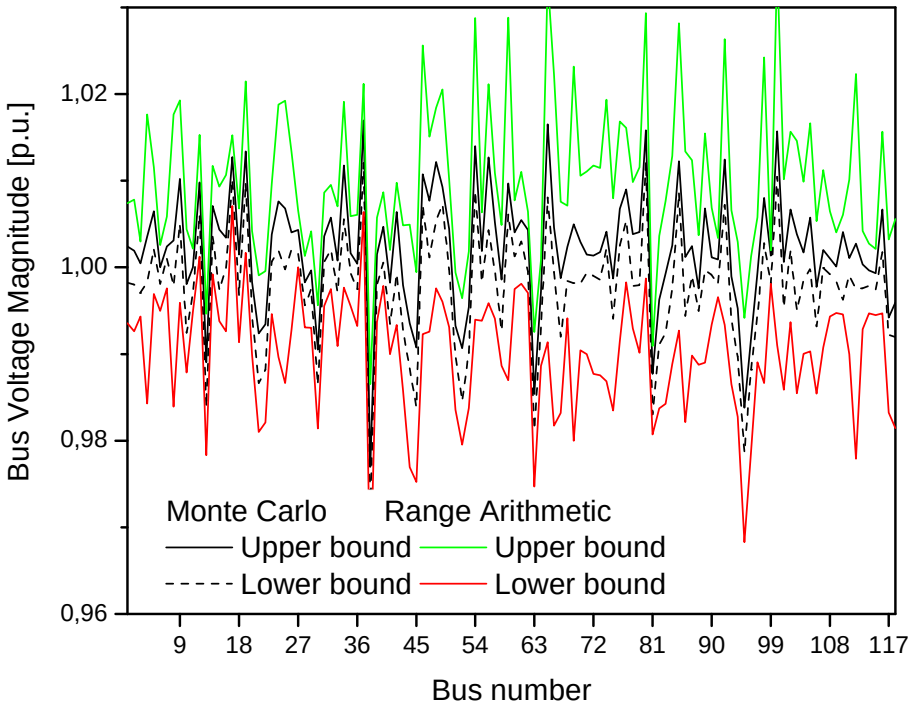

Figure 4.2: Bounds of the computed reactive power dispatch: Voltage magnitudes.

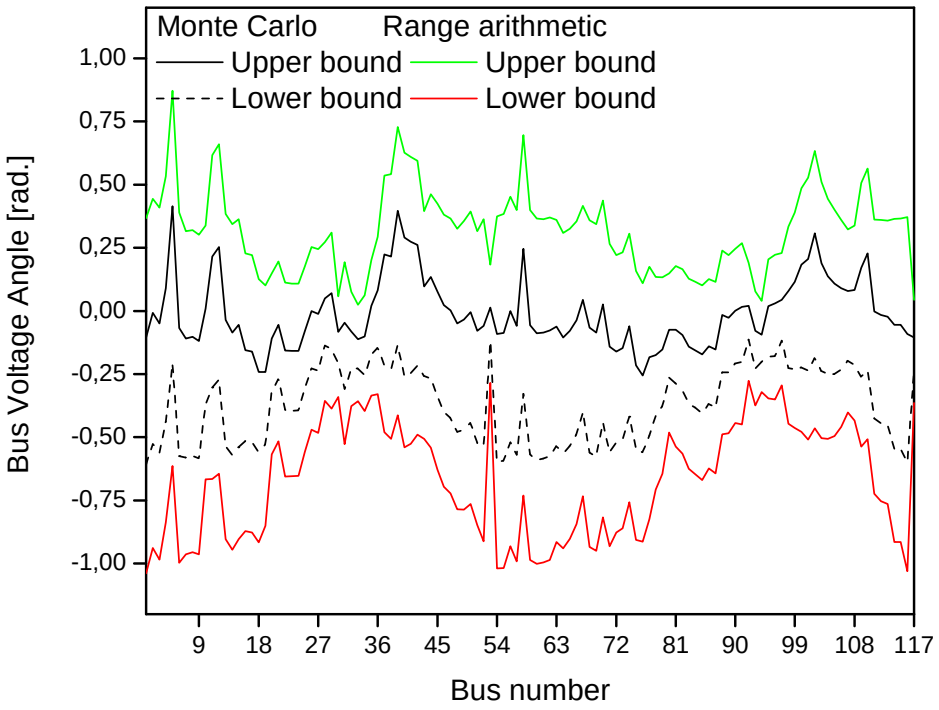

Figure 4.3: Bounds of the computed reactive power dispatch: Voltage angles.

bounds are slightly conservative, which is due to the fact that the AA-based methodology yields "worst case" bounds, as mentioned in Chapter 3, that take into account any uncertainties in input data. This can be argued to be an advantage of AA, as widely discussed in the reliable computing literature, since probabilistic methods that deal with non probabilistic uncertainty could neglect solutions that present a very low probability, but whose possibility of realization is greater than zero.

In terms of computational requirements, it should be noted that the range-arithmetic-based OPF is significantly cheaper than the Monte Carlo approach, since it only requires the solution of 2 OPF problems, as opposed to computing hundred to thousands of OPF solutions.

4.4 Summary

A novel optimization framework for OPF analysis with uncertainty variables represented as intervals was analyzed in this chapter. To solve the uncertain OPF, which is a constrained nonlinear interval optimization programming problem, a solution strategy based on a fundamental theorem of Range Arithmetic theory was presented. This allowed to compute the range of OPF solutions associated with input interval uncertainties by solving two determinate problems of the same type, namely, the lower and the upper boundary problems, which can be readily solved using state-of-the-art NLP solvers. The main benefits of the AA-based technique were assessed on several power test systems, demonstrating the effectiveness of the proposed approach in solving uncertain OPF analysis, independent of the types and levels of uncertainties in the input data.

Chapter 5

Unified AA-based Framework for Uncertain PF and OPF Analysis

5.1 Introduction

In this chapter a novel AA-based computing paradigm aimed at achieving more efficient computational processes and better enclosures of PF and OPF solution sets is conceptualized. The main idea is to formulate a generic mathematical programming problem under uncertainty by means of equivalent deterministic problems, defining a coherent set of minimization, equality, and inequality operators. Compared to existing AA and Range-Arithmetic-based solution paradigms, this formulation is expected to present greater flexibility, as it would allow to find partial solutions and include of multiple equality and inequality constraints, and reduce the approximation errors to obtain a better solution enclosure. Detailed numerical results are presented and discussed, demonstrating the effectiveness of the proposed methodology and comparing it to the AA-based PF and Range Arithemtic-based OPF presented in Chapters 3 and 4, respectively.

5.2 Theoretical Framework

In this section, a theoretical framework is developed aimed at effectively solving linear and nonlinear systems of equations for constrained optimizations problems, under multiple and heterogeneous source of data uncertainty, based on a unified AA-based formalism. Thus, the main aim is to solve the following non-linear constrained optimization problem in the presence of data uncertainties represented in affine forms:

$$\begin{aligned} \min_{(\hat{\mathbf{x}},\hat{\mathbf{u}})} \quad & f(\hat{\mathbf{x}},\hat{\mathbf{u}}) \\ \text{s.t.} \quad & g_j(\hat{\mathbf{x}},\hat{\mathbf{u}}) = 0 \quad \forall j \in [1,n] \\ & h_k(\hat{\mathbf{x}},\hat{\mathbf{u}}) < 0 \quad \forall k \in [1,m] \end{aligned} \tag{5.1}$$

where:

- $\hat{\mathbf{x}}$ and $\hat{\mathbf{u}}$ are the unknown affine forms describing the dependent and independent variables, respectively;
- f is the scalar, continuous and differentiable function describing the problem objectives;
- and g_j and h_k are the continuous and differentiable functions describing the j^{th} equality and k^{th} inequality constraints respectively.

To solve (5.1), novel AA-based mathematical operators are defined here aimed at extending to affine functions and affine forms the minimization operator and the main comparison operators $<$, $>$, $\leq$, $\geq$, and $==$, respectively. To accomplish this, starting from the definition of these novel operators and according to the Invariance Theorem of Affine Arithmetic, it will be shown that (5.1) can be recasted as a dual deterministic problem, which can be solved employing a traditional numerical programming technique. In particular, the mathematical definitions introduced in Section 2.4.2 allow stating the following propriety of affine forms, which directly results from the definition of the difference operator:

Definition 1 (Equality operator for affine forms $\stackrel{A}{=}$) *Two affine forms* $\hat{\chi} = \chi_0 + \sum_{k=1}^{p_\chi} \chi_k \varepsilon_k^\chi$ *and* $\hat{\psi} = \psi_0 + \sum_{k=1}^{p_\psi} \psi_k \varepsilon_k^\psi$ *are equal, i.e.* $\hat{\chi} \stackrel{A}{=} \hat{\psi}$*, if and only if:*

$$\hat{\chi} - \hat{\psi} = \chi_0 - \psi_0 + \sum_{k=1}^{p_\chi} \chi_i \varepsilon_k^\chi - \sum_{k=1}^{p_\psi} \psi_k \varepsilon_k^\psi = 0 \tag{5.2}$$

∎

That is, two affine forms are equal if they have the same central value and share the same noise symbols with the same partial deviations, namely:

$$\hat{\chi} \stackrel{A}{=} \hat{\psi} \Leftrightarrow \begin{cases} \chi_0 = \psi_0 \\ \varepsilon_k^\chi = \varepsilon_k^\psi \quad \forall k \in [1, p] \\ \chi_k = \psi_k \quad \forall k \in [1, p] \\ p = p_\chi = p_\psi \end{cases} \tag{5.3}$$

These rigorous equality conditions can be rarely satisfied when solving (5.1), due to the presence of non-affine operations, which introduce approximation and computational errors. For example, consider the following equality constraint:

$$(\chi_0 + \chi_1 \varepsilon_1)^2 \stackrel{A}{=} 1 + 0.1\varepsilon_1 \tag{5.4}$$

Hence, there is no way to satisfy this constraint, since the square function is a non-affine operation, which introduces a new and distinct noise symbol ε_2 as follows:

$$\chi_0^2 + 2\chi_0\chi_1\varepsilon_1 + \chi_2\varepsilon_2 \stackrel{A}{=} 1 + 0.1\varepsilon_1 \tag{5.5}$$

This issue affects the handling of the equality constraints in the OPF analysis, which are typically described by non-linear equations of the form:

$$\begin{aligned} g_i(\hat{\mathbf{z}}) &= \hat{P}_i(\hat{\mathbf{z}}) - \hat{P}_i^{SP} \quad \forall i \in \mathcal{N}_\mathcal{P} \\ g_j(\hat{\mathbf{z}}) &= \hat{Q}_j(\hat{\mathbf{z}}) - \hat{Q}_j^{SP} \quad \forall j \in \mathcal{N}_\mathcal{Q} \end{aligned} \tag{5.6}$$

where $\hat{\mathbf{z}} = (\hat{\mathbf{x}}, \hat{\mathbf{u}}) = (z_0^1 + \sum_{k=1}^p z_k^1 \varepsilon_k, ..., z_0^{N_x+N_u} + \sum_{k=1}^p z_k^{N_x+N_u} \varepsilon_k)$ is the affine state vector; while $P_i^{SP} = P_{i,0}^{SP} + \sum_{k=1}^p P_{i,k}^{SP} \varepsilon_k$ and $Q_j^{SP} = Q_{j,0}^{SP} + \sum_{k=1}^p Q_{j,k}^{SP} \varepsilon_k$ are fixed affine forms.

Since $\hat{P}_i(\hat{\mathbf{z}})$ and $\hat{Q}_j(\hat{\mathbf{z}})$ are non-linear functions of the affine vector $\hat{\mathbf{z}}$, from (2.1) it follows that:

$$\begin{array}{l} \hat{P}_i(\hat{\mathbf{z}}) = P_{i,0} + \sum_{k=1}^{p} P_{i,k}\varepsilon_k + \sum_{k=p+1}^{p+p_{na}} P_{i,k}\varepsilon_k \quad \forall i \in \mathcal{N}_{\mathcal{P}} \\ \hat{Q}_j(\hat{\mathbf{z}}) = Q_{i,0} + \sum_{k=1}^{p} Q_{j,k}\varepsilon_k + \sum_{i=p+1}^{p+p_{na}} Q_{j,k}\varepsilon_k \quad \forall j \in \mathcal{N}_{\mathcal{Q}} \end{array} \tag{5.7}$$

where the presence of the additional p_{na} noise symbols deriving by the approximation of non-affine operations, makes the application of the rigorous equality operator $\overset{A}{=}$ infeasible. Consequently, alternative operators aimed at assessing the similarity, rather than the equality, between affine forms should be defined.

To address the aforementioned issue, a similarity criteria, which is based on the equality of the partial deviations of the "primitive" noise symbols, denoted here as ε_k $\forall k \in [1, p]$, and on the definition of an approximation degree based on the radius of the uncertainties generated by the approximation of the non-affine operations, denoted here as ε_k $\forall k \in [p+1, p+p_{na}]$, is defined:

Definition 2 (Similarity operator for affine forms $\overset{A}{\approx}$) *Two affine forms* $\hat{\chi} = \chi_0 + \sum_{k=1}^{p+p_{na}} \chi_k \varepsilon_k$ *and* $\hat{\psi} = \psi_0 + \sum_{k=1}^{p+p_{na}} \psi_k \varepsilon_k$ *are similar with an approximation degree* $Ł_{\chi,\psi}$ *, i.e.* $\hat{\chi} \overset{A}{\approx} \hat{\psi}$*, if and only if:*

$$\Big(\chi_k = \psi_k \ \forall k \in [0, p]\Big) \wedge \Big(Ł_{\chi,\psi} = \sum_{k=p+1}^{p+p_{na}} (|\chi_k| + |\psi_k|)\Big) \tag{5.8}$$

∎

The adoption of this operator is particularly useful in solving OPF problems in the presence of interval uncertainties, where the bounds of the uncertain variables are the only available information. In this case, the equality constraints between the affine forms describing the computed and the fixed quantities can be formalized as follows:

$$\begin{array}{l} \hat{P}_i(\hat{\mathbf{z}}) \overset{A}{\approx} \hat{P}_i^{SP} \quad \forall i \in \mathcal{N}_{\mathcal{P}} \\ \hat{Q}_j(\hat{\mathbf{z}}) \overset{A}{\approx} \hat{Q}_j^{SP} \quad \forall j \in \mathcal{N}_{\mathcal{Q}} \end{array} \tag{5.9}$$

and the corresponding approximation degrees depend on the non-affine operations needed to compute $\hat{P}_i(\hat{\mathbf{z}})$ and $\hat{Q}_j(\hat{\mathbf{z}})$.

By following the same approach, it is possible to define an inequality operator for affine forms as follows:

Definition 3 (Inequality operator for affine forms $\overset{A}{<}$) *Given two affine forms* $\hat{\chi} = \chi_0 + \sum_{k=1}^{p_\chi} \chi_k \varepsilon_k^\chi$ *and* $\hat{\psi} = \psi_0 + \sum_{k=1}^{p_\psi} \psi_k \varepsilon_k^\psi$*, then* $\hat{\chi} \overset{A}{<} \hat{\psi}$ *if and only if:*

$$\chi_0 + \sum_{k=1}^{p_\chi} |\chi_k| < \psi_0 - \sum_{k=1}^{p_\psi} |\psi_k| \tag{5.10}$$

∎

This definition directly follows from the basic theory of interval analysis, since this stats that the upper bound of $\hat{\chi}$ is less than the lower bound of $\hat{\psi}$.

Once the aforementioned relational operators are introduced, the problem of the minimization of a scalar and non-linear affine function could be effectively addressed by defining the following operator:

Definition 4 (Minimization operator for functions of affine forms) *Given a non-linear function* $f : \Re \to \Re$*, and the affine form* $\hat{\chi} = \chi_0 + \sum_{k=1}^{p} \chi_k \varepsilon_k$*, then the following AA-based minimization problem:*

$$\min_{\substack{A \\ \hat{\chi}}} \quad f(\hat{\chi}) = f_0(\hat{\chi}) + \sum_{k=1}^{p} f_k(\hat{\chi}) \varepsilon_k + \sum_{k=p+1}^{p+p_{na}} f_k(\hat{\chi}) \varepsilon_k \tag{5.11}$$

is equivalent to the following deterministic multi-objective programming problem:

$$\min_{(\chi_0, \chi_1, ..., \chi_p)} \quad \{ f_0(\chi_0, \chi_1, ..., \chi_p), \sum_{k=1}^{p+p_{na}} |f_k(\chi_0, \chi_1, ..., \chi_p)| \} \tag{5.12}$$

∎

This definition follows from the AA-based robust circuit design approach proposed in [93], and with the principles of risk-based programming theory, since the minimization of the affine central value aims at identifying the most effective solutions, without considering the uncertainty represented by the noise symbols, while the minimization of the affine radius aims at identifying the most reliable solutions that exhibit the lowest tolerance to data uncertainty. The tradeoff between these two conflicting objectives basically represents the

decision maker's risk. Based on this, the minimization of an affine function should be equivalent to finding an affine form which minimizes both its central value and its radius.

From (5.12), problem (5.1) can be solved by solving to the following deterministic multi-objective constrained optimization problem:

$$\begin{aligned} \min_{\hat{\mathbf{z}}} \quad & \{f_0(\hat{\mathbf{z}}), \sum_{k=1}^{p+p_{na}} |f_k(\hat{\mathbf{z}})|\} \\ \text{s.t.} \quad & g_j(\hat{\mathbf{z}}) \overset{A}{\approx} 0 \qquad\qquad \forall j \in [1,n] \\ & h_k(\hat{\mathbf{z}}) \overset{A}{<} 0 \qquad\qquad \forall k \in [1,m] \end{aligned} \tag{5.13}$$

To solve this problem, a two stage solution algorithm is proposed here. In the first stage, the main idea is to identify the central values of the unknown state vector by first considering the system operating at its nominal condition, which defines these central values. In this case, which is referred here as the "nominal state", uncertainties are not considered and thus the corresponding solution can be computed by solving the following deterministic optimization problem:

$$\begin{aligned} \min_{(z_0^1,...,z_0^{N_x+N_u})} \quad & f_0(z_0^1,...,z_0^{N_x+N_u}) \\ \text{s.t.} \quad & g_j(z_0^1,...,z_0^{N_x+N_u}) = 0 \qquad \forall j \in [1,n] \\ & h_k(z_0^1,...,z_0^{N_x+N_u}) < 0 \qquad \forall k \in [1,m] \end{aligned} \tag{5.14}$$

In the second stage, referred here as the "perturbed state", the effect of data uncertainty is considered, computing the partial deviations of the unknown state vector by solving the following deterministic optimization problem:

$$\begin{aligned} \min_{(z_1^1,..,z_1^{N_x+N_u},..,z_p^1,..,z_p^{N_x+N_u})} \quad & \sum_{k=1}^{p+p_{na}} |f_k(z_1^1,...,z_1^{N_x+N_u},...,z_p^1,...,z_p^{N_x+N_u})| \\ \text{s.t.} \quad & g_j(z_1^1,...,z_1^{N_x+N_u},...,z_p^1,...,z_p^{N_x+N_u}) \overset{A}{\approx} 0 \qquad \forall j \in [1,n] \\ & h_k(z_1^1,...,z_1^{N_x+N_u},...,z_p^1,...,z_p^{N_x+N_u}) \overset{A}{<} 0 \qquad \forall k \in [1,m] \end{aligned} \tag{5.15}$$

To clarify the aforementioned approach consider the following example:

$$\begin{aligned} \min_{(\hat{\chi},\hat{\psi})} \quad & f(\hat{\chi},\hat{\psi}) = \hat{\chi}^2 + 4\hat{\psi}^2 - (3 + 0.1\epsilon_1 + 0.1\epsilon_2) \\ \text{s.t.} \quad & g(\hat{\chi},\hat{\psi}) = 4\hat{\chi}^2 - 16\hat{\chi} + \hat{\psi}^2 \overset{A}{\approx} -12 + 0.2\epsilon_1 \end{aligned} \tag{5.16}$$

where the central values and the partial deviations of the unknown affine forms $\hat{\chi} = \chi_0 + \chi_1\epsilon_1 + \chi_2\epsilon_2$ and $\hat{\psi} = \psi_0 + \psi_1\epsilon_1 + \psi_2\epsilon_2$ can be identified by solving the optimization problem in the "nominal" and "perturbed" state, namely:

$$\begin{aligned} \min_{(\chi_0,\psi_0)} & \chi_0^2 + 4\psi_0^2 - 3 \\ \text{s.t.} \quad & 4\chi_0^2 - 16\chi_0 + \psi_0^2 + 12 = 0 \end{aligned} \tag{5.17}$$

$$\begin{aligned} \min_{(\chi_1,\chi_2,\psi_1,\psi_2)} \quad & |(2\chi_0\chi_1 + 8\psi_0\psi_1 - 0.1)| + |2\chi_0\chi_2 + 8\psi_0\psi_2 - 0.1| + (|\chi_1| + |\chi_2|)^2 + 4(|\psi_1| + |\psi_2|)^2 \\ \text{s.t.} \quad & 8\chi_0\chi_1 - 16\chi_1 + 2\psi_0\psi_1 = 0.2 \\ & 8\chi_0\chi_2 - 16\chi_2 + 2\psi_0\psi_2 = 0 \end{aligned} \tag{5.18}$$

The solution of these problems leads to the following results:

$$\begin{gathered} \hat{\chi_s} = 1 - 0.026\epsilon_1 = [0.9750, 1.0259] \\ \hat{\psi_s} = 0 \\ f(\hat{\chi_s},\hat{\psi_s}) = -2 - 0.15\epsilon_1 - 0.1\epsilon_2 + 0.00062\epsilon_3 = [-2.25, -1.75] \\ g(\hat{\chi_s},\hat{\psi_s}) = -12 + 0.2\epsilon_1 + 0.0025\epsilon_3 = [-12.2025, -11.7975] \end{gathered} \tag{5.19}$$

To check the consistency of these results, the same problem has been solved by a Monte Carlo-based simulation, obtaining the following results:

$$\begin{gathered} \chi_s = [0.9753, 1.0253] \\ \psi_s = 0; \\ f(\chi_s,\psi_s) = [-2.2443, -1.7535] \end{gathered} \tag{5.20}$$

Observe that the adoption of the proposed AA-based computing paradigm allows obtaining accurate intervals. Hence, thanks to the definition of rigorous relational and minimization operators, it is possible to obtain more precise solution bounds compared to those obtained

by applying others AA-based solution paradigms, as those described in Chapters 3 and 4, which typically employ approximated minimization operators (i.e. domain contraction).

It should be noted that the solution of the AA-based optimization problem for the "perturbed state" requires the identification of a larger number of state variables, i.e., $p \times (N_x + N_u)$. However, the number of the noise symbols describing the affine forms of the state vector, which sensible influences the problem cardinality, can be significantly reduced by exploring the statistical correlation between the uncertainty sources, as explained in the next chapter.

5.3 Applications

5.3.1 PF Problem

The uncertain PF problem can be effectively solved by applying the proposed framework, since, as proposed in [58], it can be stated as a particular instance of the optimal power flow problem (5.1), as follows:

$$
\begin{aligned}
\min_{(\hat{V}_i, \hat{\delta_k}, \hat{V}_{aj}, \hat{V}_{bj})} \quad & \sum_{i \in \mathcal{N}_\mathcal{P}} (\hat{P}_i^{SP} - \hat{P}_i)^2 + \sum_{j \in \mathcal{N}_\mathcal{Q}} (\hat{Q}_j^{SP} - \hat{Q}_j)^2 \\
\text{s.t.} \quad & \hat{P}_i = \hat{V}_i \sum_{j=1}^{N} \hat{V}_j Y_{ij} \cos\left(\hat{\delta}_i - \hat{\delta}_j - \theta_{ij}\right) && \forall i \in \mathcal{N}_\mathcal{P} \\
& \hat{Q}_j = \hat{V}_j \sum_{k=1}^{N} \hat{V}_k Y_{jk} \sin\left(\hat{\delta}_j - \hat{\delta}_k - \theta_{jk}\right) && \forall j \in \mathcal{N}_\mathcal{Q} \\
& \hat{V}_i = V_{i0} + \hat{V}_{ai} - \hat{V}_{bi} && \forall i \in \mathcal{N}_{\mathcal{PV}} \\
& 0 \overset{A}{\leq} (\hat{Q}_i - \hat{Q}_{i,min}) \nabla \hat{V}_{ai} \overset{A}{\geq} 0 && \forall i \in \mathcal{N}_{\mathcal{PV}} \\
& 0 \overset{A}{\leq} (\hat{Q}_{i,max} - \hat{Q}_i) \nabla \hat{V}_{bi} \overset{A}{\geq} 0 && \forall i \in \mathcal{N}_{\mathcal{PV}} \\
& \hat{V}_i, \hat{V}_{ai}, \hat{V}_{bi} \overset{A}{\geq} 0 && \forall i \in \mathcal{N}_{\mathcal{PV}}
\end{aligned}
\tag{5.21}
$$

where, as in Chapter 4, $\mathcal{N}_{\mathcal{PV}}$ is the set of voltage controlled buses, where the injected active power and the voltage magnitude are specified; $\hat{V}_i = V_0^i + \sum_{k=1}^{p} V_k^i \epsilon_k$ is the affine

form describing the voltage magnitude of the i^{th} load bus; $\hat{\delta}_i = \delta_0^i + \sum_{k=1}^{p} \delta_k^i \epsilon_k$ is the affine form describing the voltage angle for the i^{th} bus (different from the slack); and p is the number of noise symbols representing the source of uncertainties affecting the power system operation. Consequently, the dependent variables of the AA-based PF problem are:

- $[V_0^i, V_1^i, ..., V_p^i]$ for each load bus
- $[V_{a,0}^j, V_{a,1}^j, ..., V_{a,p}^j, V_{b,0}^j, V_{b,1}^j, ..., V_{b,p}^j]$ for each generation bus
- $[\delta_0^k, \delta_1^k, ..., \delta_{nN}^k]$ for each bus except the slack bus.

5.3.2 OPF Problem

The application of the proposed AA-based framework for OPF analysis is straightforward, since the dependent variables are the affine forms of the voltage magnitudes at the load buses, and the voltage angles at all buses except the slack bus, namely:

$$\begin{array}{cc} [V_0^i, V_1^i, ..., V_{nN}^i] & \forall i \in \mathcal{N}_{\mathcal{PQ}} \\ [\delta_0^k, \delta_1^k, ..., \delta_{nN}^k] & \forall k \in \mathcal{N}_{\mathcal{P}} \subset \mathcal{N}_{\mathcal{PV}} \cup \mathcal{N}_{\mathcal{PQ}} \end{array} \tag{5.22}$$

on the other hand the control variables depends on the particular application domain; thus for example, in optimal economic dispatch analysis they include the active power generated by the dispatchable generators, namely $[P_0^i, P_1^i, ..., P_{nN}^i] \;\; \forall i \in \mathcal{N}_{\mathcal{PV}}$.

The equality constraints are described by the PF equations, while the inequality constraints typically include in practice the maximum allowable apparent power flow P_l on

each line. Consequently, the AA-based formulation of the OPF problem is:

$$
\begin{aligned}
\min_{(\hat{V}_i,\hat{\delta}_k,\hat{P}_j)} \quad & f(\hat{V}_i,\hat{\delta}_k,\hat{P}_j) \\
\text{s.t.} \quad & \hat{P}_i^{SP} - \hat{V}_i \sum_{j=1}^{N} \hat{V}_j Y_{ij} \cos\left(\hat{\delta}_i - \hat{\delta}_j - \theta_{ij}\right) \overset{A}{\approx} 0 && \forall i \in \mathcal{N}_{\mathcal{P}} \\
& \hat{Q}_j^{SP} - \hat{V}_j \sum_{k=1}^{N} \hat{V}_k Y_{jk} \sin\left(\hat{\delta}_j - \hat{\delta}_k - \theta_{jk}\right) \overset{A}{\approx} 0 && \forall i \in \mathcal{N}_{\mathcal{Q}} \\
& V_i^{min} \overset{A}{\leq} \hat{V}_i \overset{A}{\leq} V_i^{max} && \forall i \in \mathcal{N}_{\mathcal{PQ}} \\
& P_i^{min} \overset{A}{\leq} \hat{P}_i \overset{A}{\leq} P_i^{max} && \forall i \in \mathcal{N}_{\mathcal{PV}} \\
& P_l^{min} \overset{A}{\leq} \hat{P}_l(\hat{V}_1,...,\hat{V}_N,\hat{\delta}_1,...,\hat{\delta}_N) \overset{A}{\leq} P_l^{max} \quad \forall l \in \mathcal{N}_{\mathcal{L}}
\end{aligned}
\tag{5.23}
$$

where $\mathcal{N}_{\mathcal{L}}$ is the set of the constrained lines.

5.4 Numerical Results

To assess the benefits of the unified AA method for solving both uncertain PF and OPF problems, the same case studies presented in Chapters 3 and 4 are considered here, in order to make a direct comparison with the results obtained for the previous proposed PF and OPF AA-based techniques. These results are discussed in the next sections.

5.4.1 PF Analysis

The uncertain power flow problems formalized in Chapter 3 are solved here using the unified AA formulation presented in (5.21). The obtained results are summarized in Figures 5.1-5.3 for the IEEE 30-bus test system; in Figures 5.4-5.6 for the IEEE 57-bus test system; and in Figures 5.7-5.8 for the IEEE 118-bus test system. In all these figures, observe that the unified AA method is characterized by an improved accuracy compared to the previous methods. This is also confirmed by analyzing the average errors in the upper and lower bounds for the bus voltage magnitudes and angles, as reported in Tables 5.1 and 5.2.

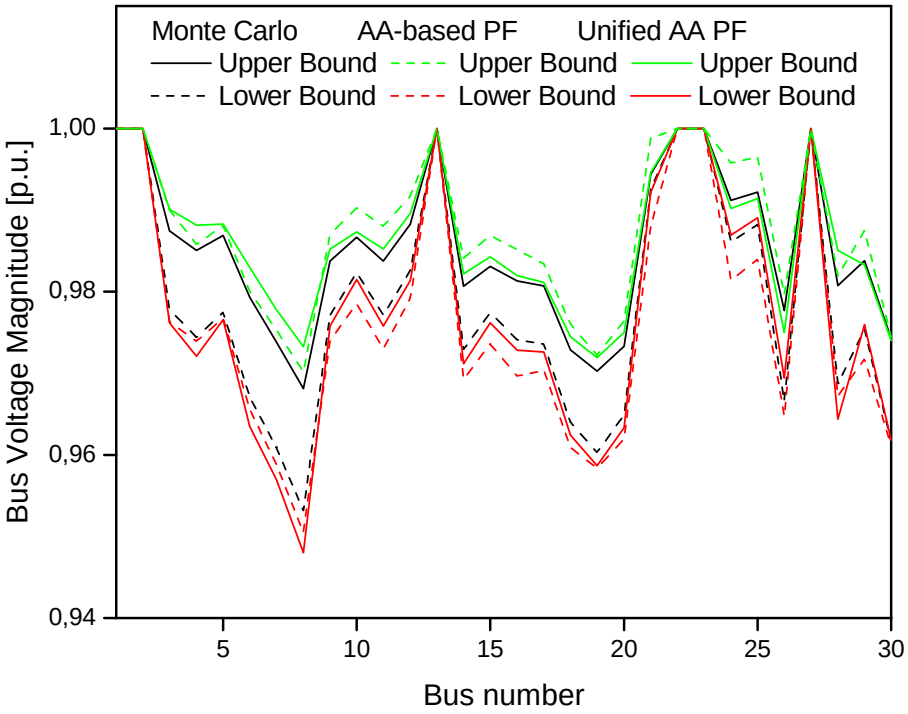

Figure 5.1: Bus voltage magnitude bounds obtained for the IEEE 30-bus test system for both AA-PF methods.

As expected, this accuracy improvement is obtained at the cost of increased computational burden, as confirmed in Table 5.3, which depicts the execution times registered for the simulations. This issue is addressed in Chapter 6, based on a novel PCA-based approach.

5.4.2 Economic Dispatch

To assess the benefits of the unified AA method for solving uncertain OPF problems, the uncertain optimal economic dispatch described in Chapter 4 is studied here using the proposed unified OPF approach. Thus, this problem can be formalized as the following

Table 5.1: Average Errors (Bus Voltage Magnitude Bounds

	30 bus		57 bus		118 bus	
	Upper	Lower	Upper	Lower	Upper	Lower
AA-based PF [p.u.]	0.0055	0.0046	0.009	0.0088	0.0102	0.0101
Unified AA method [p.u.]	0.002	0.003	0.0047	0.0071	0.0062	0.0065

Table 5.2: Average Errors (Bus Voltage Angle Bounds)

	30 bus		57 bus		118 bus	
	Upper	Lower	Upper	Lower	Upper	Lower
AA-based PF [deg]	0.65	0.97	3.32	3.33	3.18	3.16
Unified AA method [deg]	0.26	0.10	0.96	0.98	0.99	0.01

Table 5.3: Execution Times (seconds)

	30 bus	57 bus	118 bus
Monte Carlo (5000 trials) [s]	149.9	211.8	603.1
AA-based PF [s]	1.7	2.5	5.7
Unified AA method	110.72	167.8	406.5

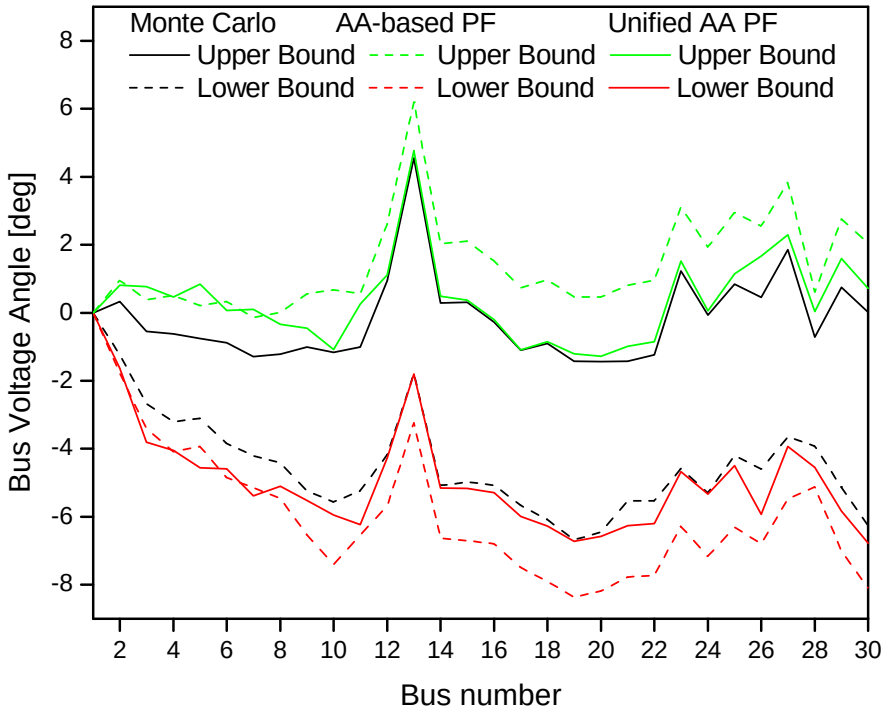

Figure 5.2: Bus voltage angle bounds obtained for the IEEE 30-bus test system for both AA-PF methods.

non-linear AA-based constrained optimization problem:

$$\begin{aligned} \min_{(\hat{P}_{G_1},\ldots,\hat{P}_{G_{53}})} \quad & \sum_{i=1}^{53} (a_i + b_i \hat{P}_{G_i} + c_i \hat{P}_{G_i}^2) \\ \text{s.t.} \quad & \sum_{i=1}^{53} \hat{P}_{G_i} \overset{A}{\approx} \hat{P}_D + \sum_{i=1}^{53} B_i \hat{P}_{G_i}^2 \\ & 0.8 \overset{A}{\leq} \hat{P}_{G_i} \overset{A}{\leq} 1.8 \qquad\qquad \forall i \in [1, 53] \end{aligned} \tag{5.24}$$

To solve this problem, the solution paradigm formalized in (5.23) is applied, and the obtained results are summarized in Figure 4.1. Observe that, compared to the range-arithmetic-based approach, the unified AA method is able to compute solution bounds which are closer to the Monte Carlo solution. However, this improvement also involves a sensible increase in the computational times, which is addressed in Chapter 6.

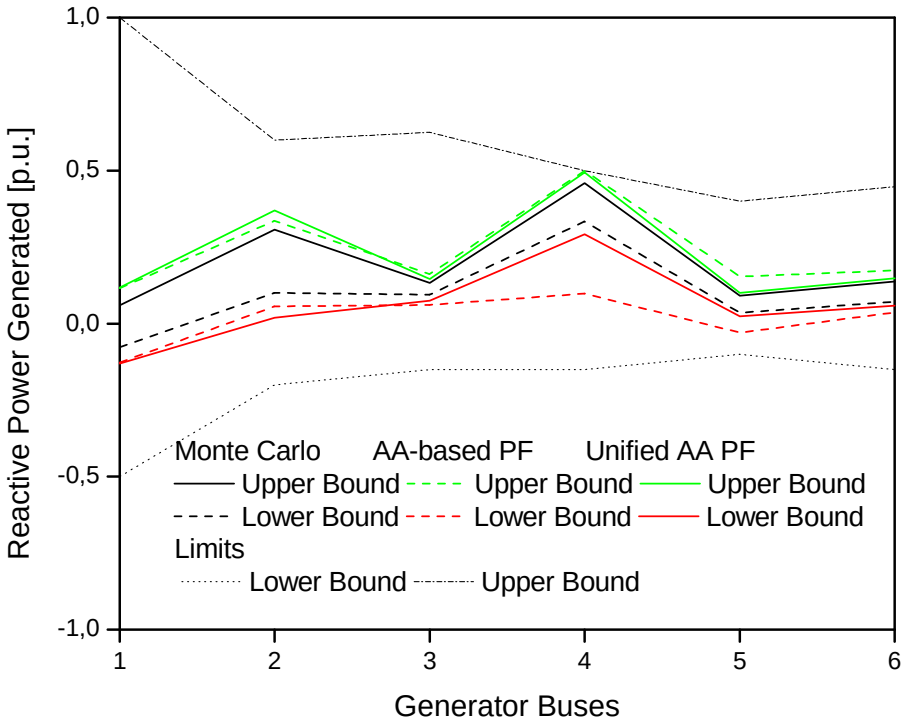

Figure 5.3: Reactive power bounds at the generation buses for the IEEE 30-bus test system for both AA-PF methods.

5.4.3 Reactive Power Dispatch

To confirm the benefits deriving from the application of the unified AA method to solve a complex OPF problem, the uncertain optimal reactive power dispatch defined in Chapter 4 is analyzed here. To solve this problem, the solution paradigm formalized in (5.23) is applied, and the obtained results are summarized in Figures 5.10 and 5.11, which depict the bounds of the bus voltage magnitudes and angles, respectively. Note that compared to the range-arithmetic-based approach, the unified AA method is able to compute more accurate enclosures of the OPF solution bounds but, at a sensible increase again in the computational times, which is addressed in Chapter 6.

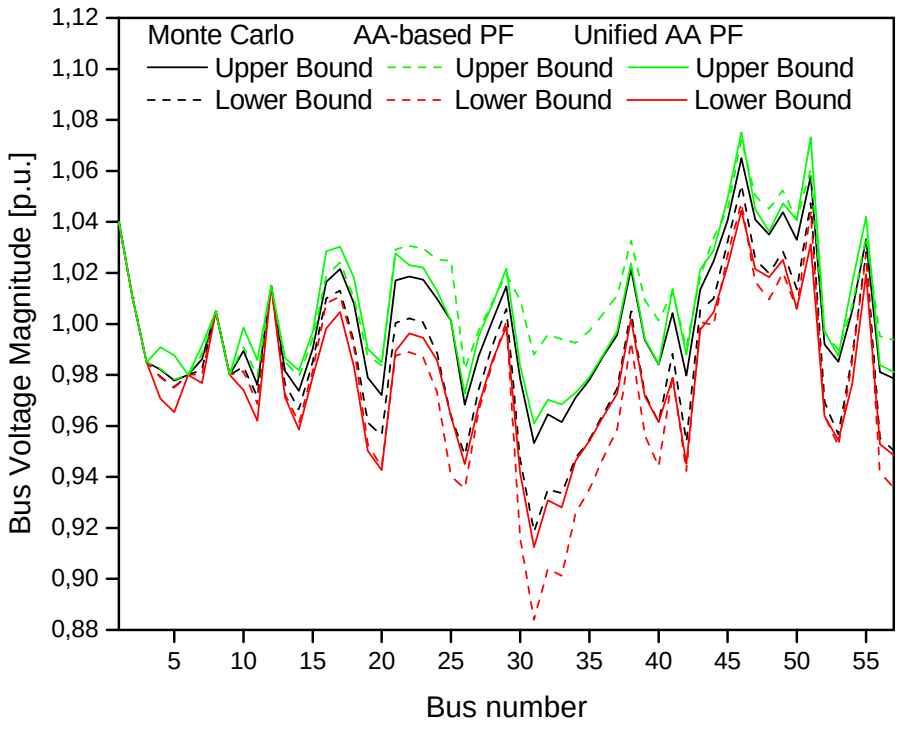

Figure 5.4: Bus voltage magnitude bounds obtained for the IEEE 57-bus test system for both AA-PF methods.

5.5 Computational Requirements

In terms of computational requirements, the following observations can be made:

1. The AA-based PF and the range-arithmetic-based methods are the fastest techniques for uncertain PF and OPF analysis, respectively.

2. The computational cost of Monte Carlo and its accuracy is related to the number of required simulations.

3. Although the unified AA framework gives the more accurate enclosures for the solution bounds, it is the costliest heaviest approach in terms of computational times,

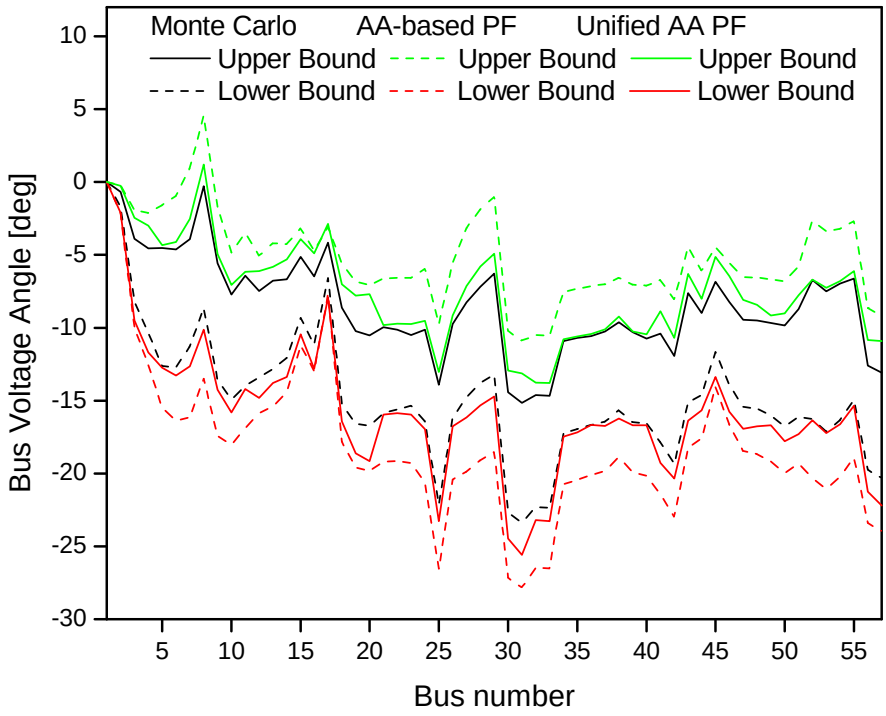

Figure 5.5: Bus voltage angle bounds obtained for the IEEE 57-bus test system for both AA-PF methods.

since this is mainly influenced by the large number of control variables, which depend on the number of noise symbols characterizing the parameter uncertainties. This poses computational difficulties for addressing uncertain PF and OPF analysis in large scale power systems.

To overcome this limitation, it is necessary to design techniques aimed at identifying the optimal number of independent uncertainties (i.e. the optimal number of noise symbols) affecting the system variables. To address this issue, knowledge discovery paradigms from historical operation data can be used as explained in the next chapter.

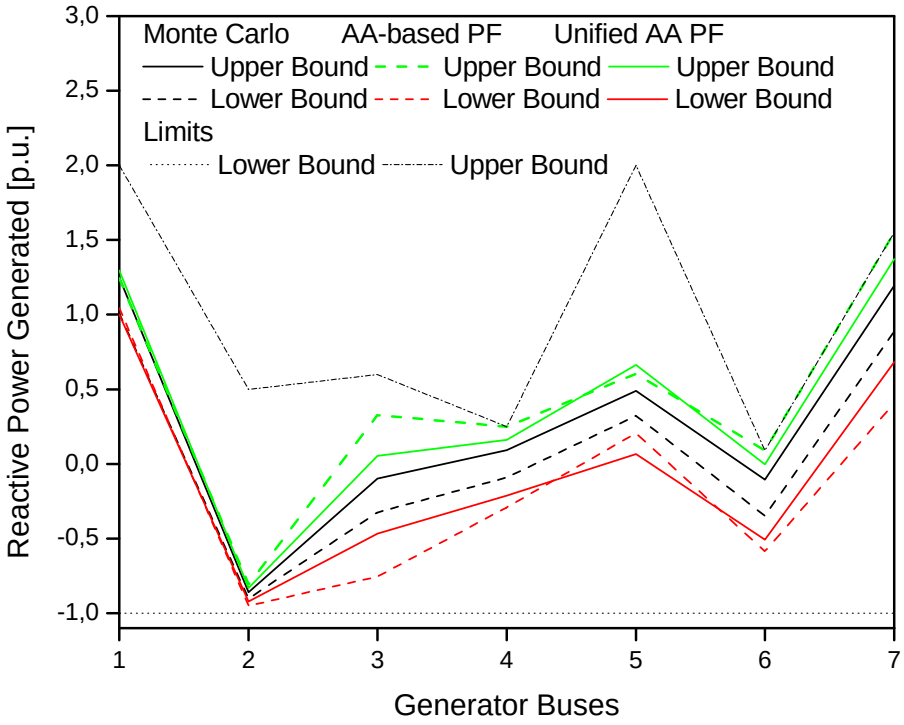

Figure 5.6: Reactive power bounds at the generation buses for the IEEE 57-bus test system for both AA-PF methods.

5.6 Summary

In this chapter a novel AA-based computing paradigm aimed at achieving better enclosures for AA PF and OPF solution sets was defined. Compared to existing AA-based solution paradigms for uncertain PF an OPF analysis, this formulation allowed to drastically reduce the approximation errors by obtaining a better estimation of the PF and OPF solution sets. However, compared to the previous proposed AA-based PF and range-arithmetic-based OPF, this approach resulted in higher computational costs, mainly due to the large number of control variables required to solve the "perturbed state" problem. This could pose some computational difficulties for large scale power system applications. To address this problem, PCA-based paradigms for knowledge discovery from historical operation data-sets is proposed in the next chapter, to identify the optimal affine forms describing

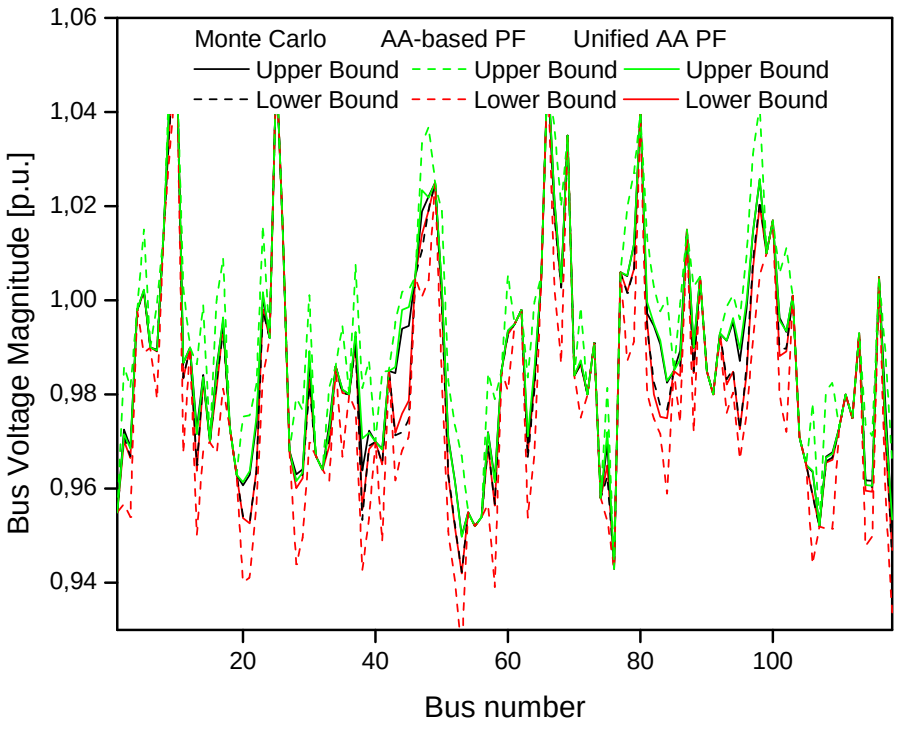

Figure 5.7: Bus voltage magnitude bounds obtained for the IEEE 118-bus test system for both AA-PF methods.

the uncertain variables in the proposed AA framework.

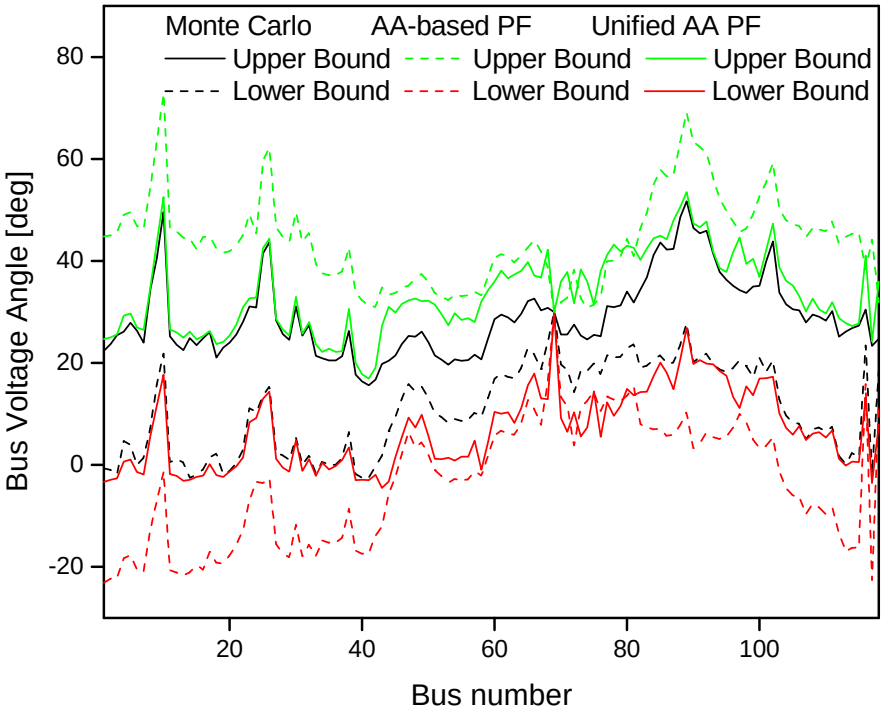

Figure 5.8: Bus voltage angle bounds obtained for the IEEE 118-bus test system for both AA-PF methods.

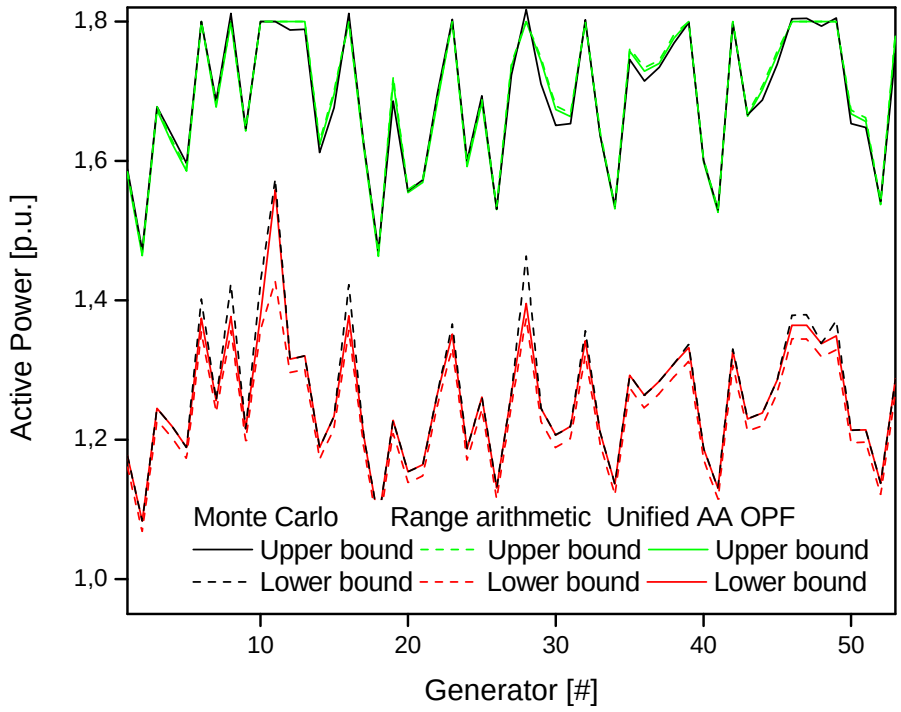

Figure 5.9: Bounds of the computed economic dispatch solutions.

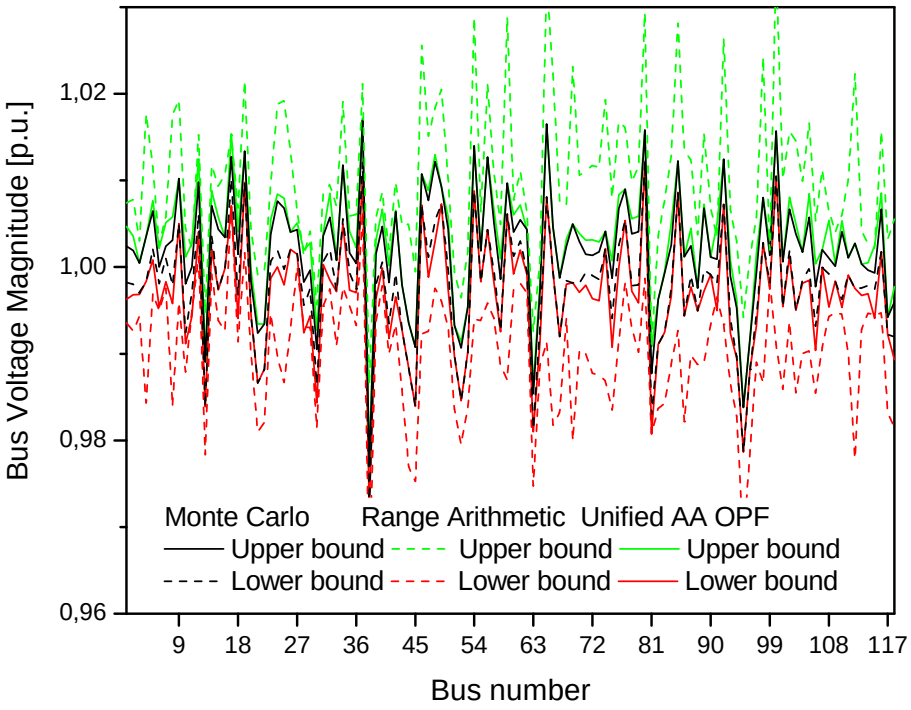

Figure 5.10: Voltage magnitude bounds of the computed reactive power dispatch solutions for the 118-bus test system.

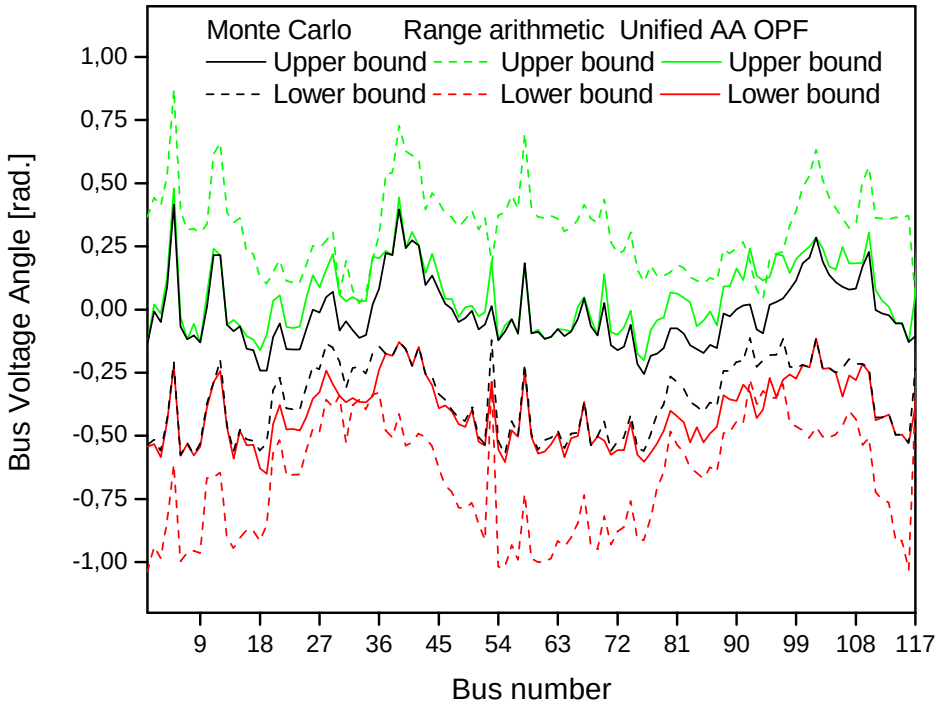

Figure 5.11: Voltage angle bounds of the computed reactive power dispatch solutions for the 118-bus test system.

Chapter 6

PCA-based Knowledge Discovery Paradigms

6.1 Introduction

This chapter proposes formal methods for knowledge discovery from large quantity of data as an enabling methodology for reducing the complexity of PF and OPF problems, and for the optimal identification of the affine forms describing their uncertain variables. In particular, a knowledge-based paradigm for PF and OPF analyses is used to extract from operation data-sets complex features, hidden relationships, and useful hypotheses potentially describing regularities in the problem solutions. This is realized by designing a knowledge-extraction process based on PCA. The structural knowledge extracted by this process is then used to project the PF equations into a domain in which these equations can be solved more effectively. In this new domain, the cardinality of the PF and OPF problem is sensibly reduced and, consequently, PF and OPF solutions can be obtained more efficiently. Furthermore, in this new domain, it is also possible to define a formal connection between the principal components and affine forms used to describe the uncertain variables, furnishing an effective method for the optimal identification of the relevant noise symbols. The effectiveness of the proposed framework is demonstrated with numerical results obtained for small and large power networks for many operating conditions.

6.2 Proposed PCA Applications

PCA-based paradigms for knowledge discovery from historical operation data-sets are proposed here to simplify the computational burden of PF and OPF problems by reducing their complexity. The underlying principle is to extract actionable information aimed at determining potential patterns to reduce the cardinality of these problems.

6.2.1 PF Analysis

The main idea of the PCA-based PF is to generalize the mathematical formulation defined in (2.27) by extrapolating the linear mapping between the power system state variables and the principal components as follows:

$$\mathbf{x}(K) = \mathbf{\Omega}\ \mathbf{s}(K) + \mathbf{x}_{med} \quad \forall K > \overline{T} \tag{6.1}$$

This linear extrapolation allows to solve the PF problem for each $K > \overline{T}$, by identifying the unknown principal components $\mathbf{s}(K) = [s_1(K)...s_{N_{PC}}(K)]^T$, such that:

$$\begin{aligned} P_i^{SP}(K) &= P_i(\mathbf{x}(K)) = P_i(\mathbf{\Omega}\ \mathbf{s}(K) + \mathbf{x}_{med}) \quad \forall i \in \mathcal{N}_{\mathcal{P}} \\ Q_j^{SP}(K) &= Q_j(\mathbf{x}(K)) = Q_j(\mathbf{\Omega}\ \mathbf{s}(K) + \mathbf{x}_{med}) \quad \forall j \in \mathcal{N}_{\mathcal{Q}} \end{aligned} \tag{6.2}$$

A noticeable benefit deriving from this mathematical formulation is the drastic reduction of the problem cardinality, since the number of design variables that should be identified at each time step is reduced from N_x to N_{PC}. This important feature should improve the convergence properties of the solution algorithm and lower its complexity and computational burden, based on the reduction of the asymptotic complexity of the solution algorithm, which is $O(N_x N_{PC}^2)$, due to the pseudo inverse of the Jacobian matrix of dimension $N_x \times N_{PC}$ of the PF equations in the principal component domain. However, the sparsity of the Jacobian is reduced with respect to the "standard" PF Jacobian, since the latter roughly depends on the number of power system elements, whereas the former would have more intertwining variables. Nevertheless, the complexity reduction of the solution algorithm could be noticeable, given the significant Jacobian size reduction, especially in the presence of variable load/generation patterns, which may require multiple PF solutions (e.g. Monte Carlo simulations).

Observe that the integration of the proposed solution paradigm on existing power systems analysis toolboxes is straightforward, since the Jacobian of the PF equations in the principal components domain can be easily computed as:

$$\mathbf{J}_{PC} = \frac{\partial \mathbf{F}}{\partial \mathbf{s}} = \frac{\partial \mathbf{F}}{\partial \mathbf{x}} \frac{\partial \mathbf{x}}{\partial \mathbf{s}} = \mathbf{J}\ \mathbf{\Omega} \tag{6.3}$$

where $\mathcal{F}$ is the set of PF equations and $\mathbf{J}$ is the corresponding Jacobian matrix. Observe as well that the reactive power generation limits in conventional PF programs can be readily integrated in the proposed framework by properly redimensioning the matrix $\mathbf{\Omega}$ when a PV to PQ bus switch, or vice-versa, takes place.

6.2.2 OPF Analysis

The benefits deriving by the formalization of the PF equations in the principal components domain, can be easily extended to OPF analysis. In this context, the main idea is to extrapolate a linear mapping between the variables of the OPF problem z and the principal components $\mathbf{s}(K)$ as follows:

$$\mathbf{z}(K) = \mathbf{\Omega}\ \mathbf{s}(K) + \mathbf{z}_{med} \quad \forall K > \overline{T} \tag{6.4}$$

This linear extrapolation allows to solve the OPF problem for each $K > \overline{T}$, by identifying the unknown principal components $\mathbf{s}(K)$ such that:

$$\begin{aligned} \min_{\mathbf{s}(K)} \quad & f(\mathbf{\Omega}\ \mathbf{s}(K) + \mathbf{z}_{med}) \\ \text{s.t.} \quad & g(\mathbf{\Omega}\ \mathbf{s}(K) + \mathbf{z}_{med}) = 0 \\ & h(\mathbf{\Omega}\ \mathbf{s}(K) + \mathbf{z}_{med}) < 0 \end{aligned} \tag{6.5}$$

observe again the drastic reduction of the problem cardinality, since the number of variables has been reduced from N_z to N_{PC}. Moreover, the gradient of the cost and constraints functions in the principal components domain can be easily computed according to (6.3).

6.2.3 AA Analysis

The proposed PCA-based paradigm can also be used to better identify the noise symbols adopted for uncertainty representation in PF and OPF analyses. The main idea is to

exploit the capacity of PCA in detecting potential relations among a set of power systems data, which allows to describe the evolution of a large number of statistically correlated variables by a linear combination of a limited number of "primitive" variables. This feature is particularly useful in solving uncertain PF and OPF analyses using AA as explained in Chapters 3,4 and 5, where the hypothesis of statistically independence of the active and reactive power injections involves the definition of a large number of noise symbols, which increases the complexities of the AA-based computations. To discover the potential patterns among these data, the following set of historical observations should be analyzed:

$$[P_i^{SP}(K), Q_j^{SP}(K)]^T \quad \forall i \in \mathcal{N}_{\mathcal{P}},\ | \in \mathcal{N}_{\mathcal{Q}},\ \mathcal{K} \in [\imath, \overline{\mathcal{T}}] \tag{6.6}$$

the application of PCA to this data set allows to represent the injected active and reactive powers with a linear combination of a proper number of orthogonal and uncorrelated principal components, namely:

$$\begin{array}{rl} P_i^{SP}(K) = \mathbf{\Omega}^P\ \mathbf{s}(K) + P_{i,med}^{SP} & \forall i \in \mathcal{N}_{\mathcal{P}},\ \mathcal{K} \in [\imath, \overline{\mathcal{T}}] \\ Q_j^{SP}(K) = \mathbf{\Omega}^Q\ \mathbf{s}(K) + Q_{j,med}^{SP} & \forall j \in \mathcal{N}_{\mathcal{Q}},\ \mathcal{K} \in [\imath, \overline{\mathcal{T}}] \\ P_{i,med}^{SP} = \frac{1}{\overline{T}} \sum_{K=1}^{\overline{T}} P_i^{SP}(K) & \forall i \in \mathcal{N}_{\mathcal{P}} \\ Q_{j,med}^{SP} = \frac{1}{\overline{T}} \sum_{K=1}^{\overline{T}} Q_j^{SP}(K) & \forall j \in \mathcal{N}_{\mathcal{Q}} \end{array} \tag{6.7}$$

based on this, it can be argued that the evolution of the injected powers in the power system is governed by N_{PC} "primitive" variables. Hence, based on (3.4), the following number of noise symbols describing the injected power uncertainties can be set to N_{PC}, and the corresponding affine forms can be defined as follows:

$$\begin{array}{ll} \hat{P}_i^{SP} = P_{i,0}^{SP} + \sum_{k=1}^{N_{PC}} P_{i,k}\varepsilon_k & \forall i \in \mathcal{N}_{\mathcal{P}} \\ \hat{Q}_j^{SP} = Q_{j,0}^{SP} + \sum_{k=1}^{N_{PC}} Q_{j,k}\varepsilon_k & \forall j \in \mathcal{N}_{\mathcal{Q}} \end{array} \tag{6.8}$$

where the noise symbols $\varepsilon_k\ \forall k \in [1, N_{PC}]$ represent the uncertainty affecting the principal components. Compared to (3.4), this should yield a significant reduction in the number of noise symbols.

The unknown parameters of the affine forms defined in (6.8) can be identified by solving the system of linear interval equations describing the relationships between the bounds of

the uncertain power injections and the bounds of the principal components, as follows:

$$\begin{array}{l} [P^{SP}_{i,min}, P^{SP}_{i,max}] = \mathbf{\Omega}^P\ [\mathbf{s}_{min}, \mathbf{s}_{max}] + P^{SP}_{i,med} \quad \forall i \in \mathcal{N}_\mathcal{P} \\ [Q^{SP}_{j,min}, Q^{SP}_{j,max}] = \mathbf{\Omega}^Q\ [\mathbf{s}_{min}, \mathbf{s}_{max}] + Q^{SP}_{j,med} \quad \forall j \in \mathcal{N}_\mathcal{Q} \end{array} \tag{6.9}$$

which directly follows from (6.7). Thus, by comparing (6.8) and (6.9), the unknown affine form parameters can be identified as follows:

$$\begin{array}{rl} P_{i,0} = P^{SP}_{i,med} + \sum_{k=1}^{N_{PC}} \Omega^P_{i,k}\ \frac{s_{k,max}+s_{k,min}}{2} & \forall i \in \mathcal{N}_\mathcal{P} \\ P_{i,k} = \Omega^P_{i,k}\ \frac{s_{k,max}-s_{k,min}}{2} & \forall i \in \mathcal{N}_\mathcal{P} \\ Q_{j,0} = Q^{SP}_{j,med} + \sum_{k=1}^{N_{PC}} \Omega^Q_{j,k}\ \frac{s_{k,max}+s_{k,min}}{2} & \forall j \in \mathcal{N}_\mathcal{Q} \\ Q_{j,k} = \Omega^Q_{i,k}\ \frac{s_{k,max}-s_{k,min}}{2} & \forall j \in \mathcal{N}_\mathcal{Q} \end{array} \tag{6.10}$$

based on these equations, it is possible to identify the proper number of noise symbols, and the optimal parameters of the affine forms describing the uncertain PF and OPF variables, which is an issue in AA applications.

6.3 Numerical Results

This section describes the results obtained by applying the proposed framework to solve PF and/or OPF problems for several power networks, namely, the IEEE 30 bus test system, the IEEE 118 bus test system, and the 2383-bus Polish power system, for varying realistic operating conditions.

6.3.1 IEEE 30-bus System PF

For the 30-bus test system, 24 load buses are clustered in 5 different classes characterized by the bi-weekly 15 min profiles depicted in Figure 6.1 for $K \in [0, 1343]$; these profiles correspond to realistic commercial, residential, and 3 different kinds of industrial load patterns obtained from [94]. The corresponding generation profiles are defined for each time sample K as follows:

$$P_{G_i}(K) = \alpha_{G_i} \sum_{j=1}^{N} P_{D_j}(K) \quad \forall i \in [1, n_G] \tag{6.11}$$

where α_{G_i} are dispatch factors for the base case, i.e.

$$\alpha_{G_i} = \frac{P_{G_i}(0)}{\sum_{j=1}^{N} P_{D_j}(0)} \quad \forall i \in [1, n_G] \tag{6.12}$$

n_G is the number of generators; and $P_{D_j}(0)$ and $P_{G_i}(0)$ are the active power demands at the j^{th} bus and the active power generated by the i^{th} generator, respectively. This approach yields 1343 power flow problems, which, when solved using standard Newton-Raphson, generate the voltage magnitudes and angles depicted in Figures 6.2 and 6.3, respectively.

The power flow results are arranged in two data sets, namely, a knowledge base composed of 500 sample points, and a validation set composed of 843 sample points. Processing the first 500 solutions using the PCA knowledge extraction process described in Chapter 2, identifies the principal components of bus voltage phasors, the matrix Ω and the vector x_{med}. The second data set is used to validate the accuracy of the power flow solutions computed by the proposed algorithm based on the calculated Ω and x_{med}. The knowledge extraction process is then applied to a variable number of principal components N_{PC} in the interval $[1, 18]$. The obtained results are summarized in Figure 6.4 using a semi-logarithmic scale to plot the norm of the approximation error e_{app} versus N_{PC}, where:

$$\begin{aligned} \mathbf{e}_{app}^{(K)}(N_{PC}) &= \mathbf{x}(K) - \mathbf{x}_{PC}(N_{PC}, K) = \qquad \forall N_{PC} \in [1, 18],\ K \in [0, 500] \\ &= \mathbf{x}(K) - [\mathbf{\Omega}(N_{PC})\ \mathbf{s}(K) + \mathbf{x}_{med}(K)] \\ \Rightarrow \mathbf{e}_{app}(N_{PC}) &= [\mathbf{e}_{app}^{(1)}(N_{PC}), ..., \mathbf{e}_{app}^{(500)}(N_{PC})] \end{aligned} \tag{6.13}$$

This figure shows that when the principal components number N_{PC} increases, the approximation error drastically decreases approaching a saturation threshold. This allows to identify the adequate number of principal components needed to properly solve the power flow problem for a given approximation error tolerance. Thus, assuming an approximation tolerance of 10^{-4}, 8 principal components are needed in this case, which yelds Figure 6.5 depicting the profiles of these components for the first 500 data samples of the knowledge base. It is then possible to reconstruct the profiles of 53 state variables with a compression ratio $C_R(500)$ of 5.91.

In order to prove the extrapolation features of the proposed approach, the PF problem was then solved in the principal components domain $\forall K \in [500, 1343]$, and the obtained

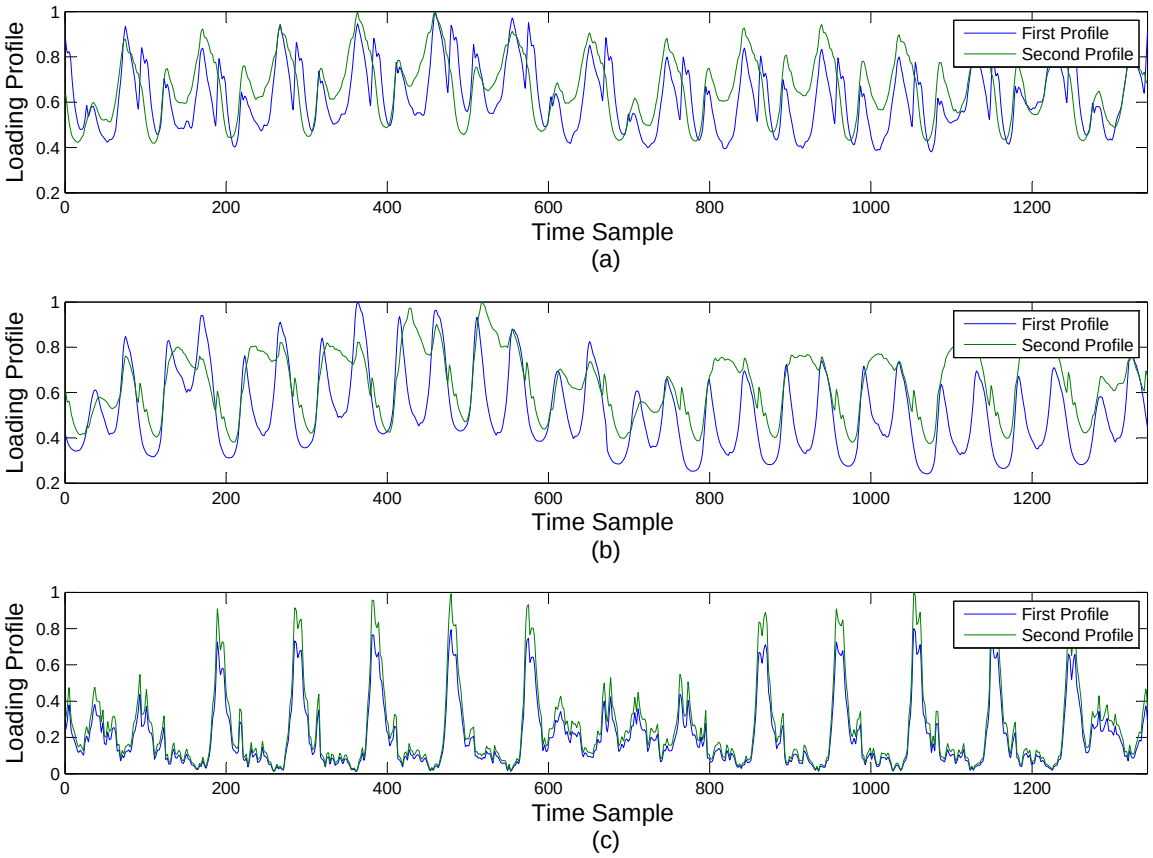

Figure 6.1: Assumed load profiles for the power flow analysis of the IEEE 30-bus test system: (a) residential, (b) commercial, and (c) industrial.

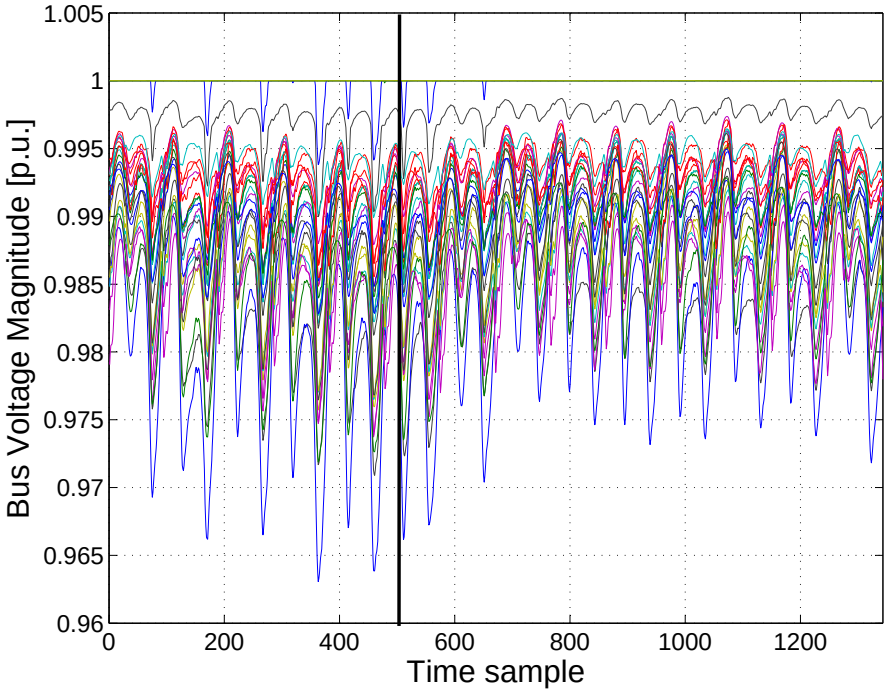

Figure 6.2: Power flow solutions for the IEEE 30-bus test system: bus voltage magnitudes.

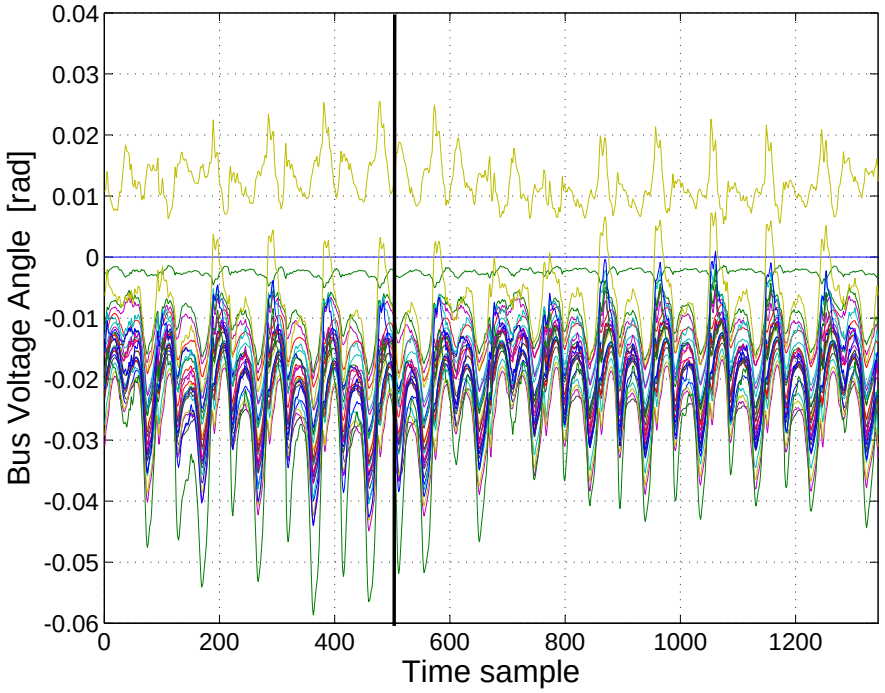

Figure 6.3: Power flow solutions for the IEEE 30-bus test system: bus voltage angles.

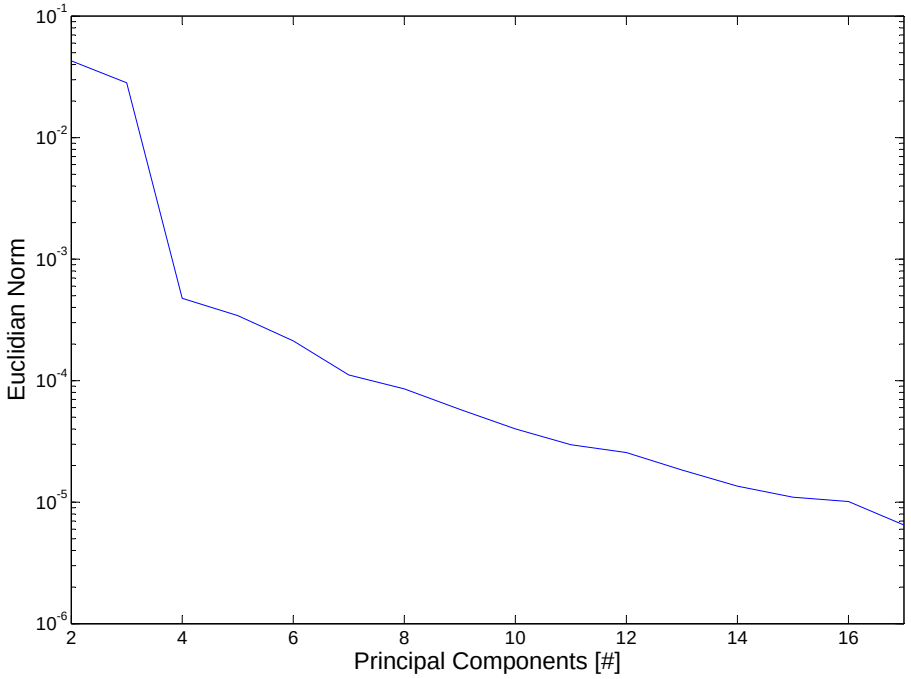

Figure 6.4: Norm of the approximation error $\|\mathbf{e}_{app}(N_{PC})\|_2$, in semi-logarithmic scale, versus the number of principal components for the IEEE 30-bus test system.

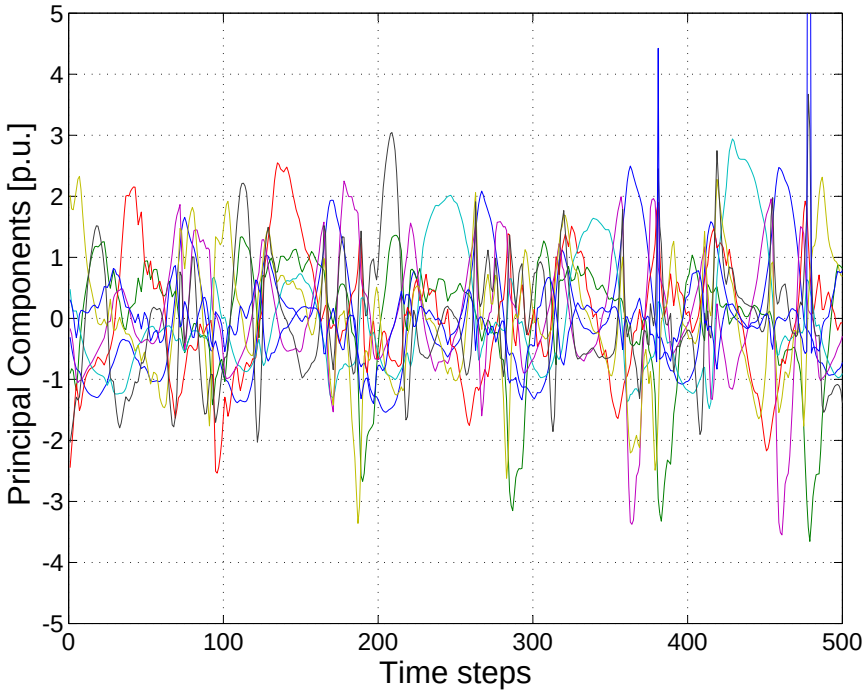

Figure 6.5: Principal components' profile for the IEEE 30-bus test system.

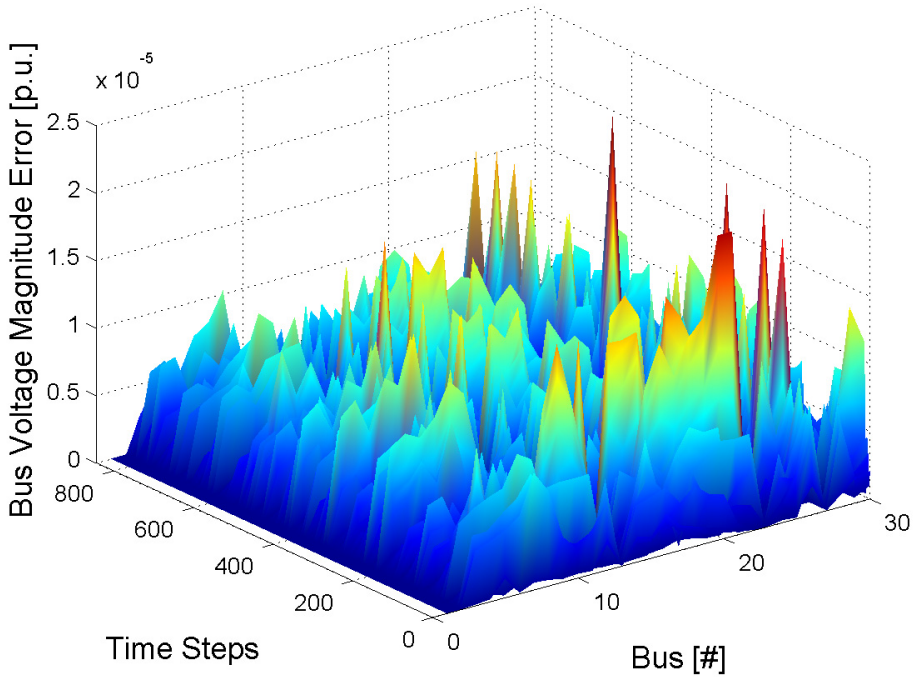

Figure 6.6: Approximation errors of the proposed PCA technique versus the true power flow solution for the IEEE 30-bus test system: bus voltage magnitude error.

results were then compared with those computed by applying the traditional PF solution algorithm. The corresponding error surfaces are shown in Figures 6.6 and 6.7, where one can to observe the high accuracy of the solutions computed by the proposed solution framework.

6.3.2 2383-bus Polish Power System PF

In order to further test the proposed technique, a large scale power system is also studied. Thus, the bi-weekly 15min load profiles shown in Figure 6.8 are assumed for the 2383-bus Polish test system; these real demand patterns were obtained from the Australian Energy Market Operator database [95]. The generation profiles are computed using (6.11), but the

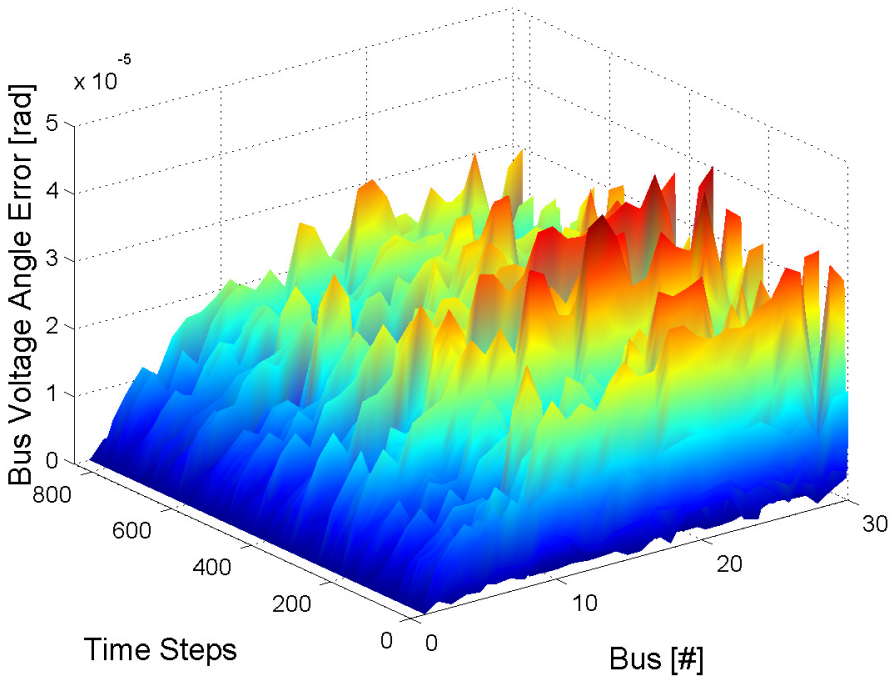

Figure 6.7: Approximation errors of the PCA proposed technique versus the true power flow solution for the IEEE 30-bus test system: bus voltage angle error.

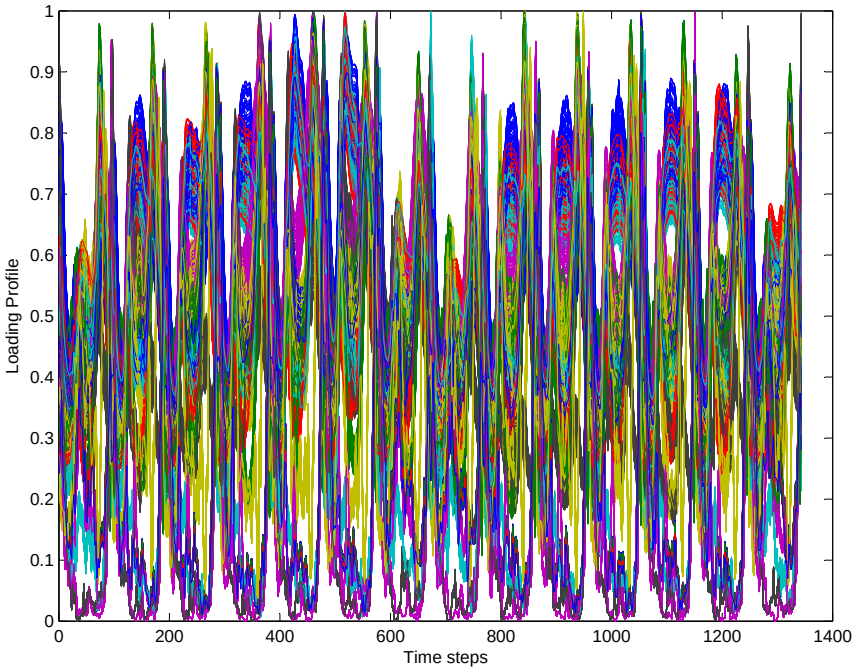

Figure 6.8: Loading profiles used for the power flow analysis of the 2382-bus Polish test system.

dispatch factors are modified with respect to their base values defined by (6.12) perturbing them with a random noise uniformly distributed in the range 0.9-1.1. The bus voltages phasors are then computed and the results were arranged in two sets, namely the knowledge base (first 500 sample points) and the Validation Set (remaining 843 sample points), as shown in Figures 6.9 and 6.10. The knowledge extraction process is then implemented for various numbers of principal components in the interval $N_{PC} = [1, 120]$, obtaining the results summarized in Figure 6.11. Thus, for an approximation error tolerance of 0.05, 40 principal components can be extracted from the knowledge base, corresponding to a compression ratio of 10.98, and the corresponding profiles are depicted in Figure 6.12.

To assess the extrapolation capabilities of the proposed methodology, the PF problem is solved in the principal components domain $\forall K \in [500, 1343]$. The resulting solutions are compared to those obtained by applying an open-source power flow program (Mat-

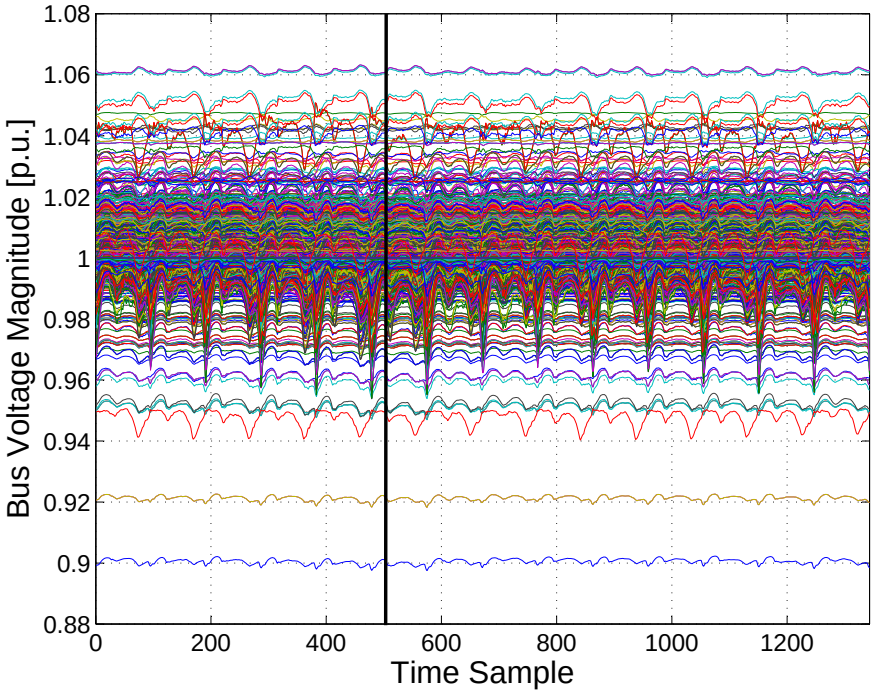

Figure 6.9: Power flow solutions for the IEEE 2382-bus test system: bus voltage magnitudes.

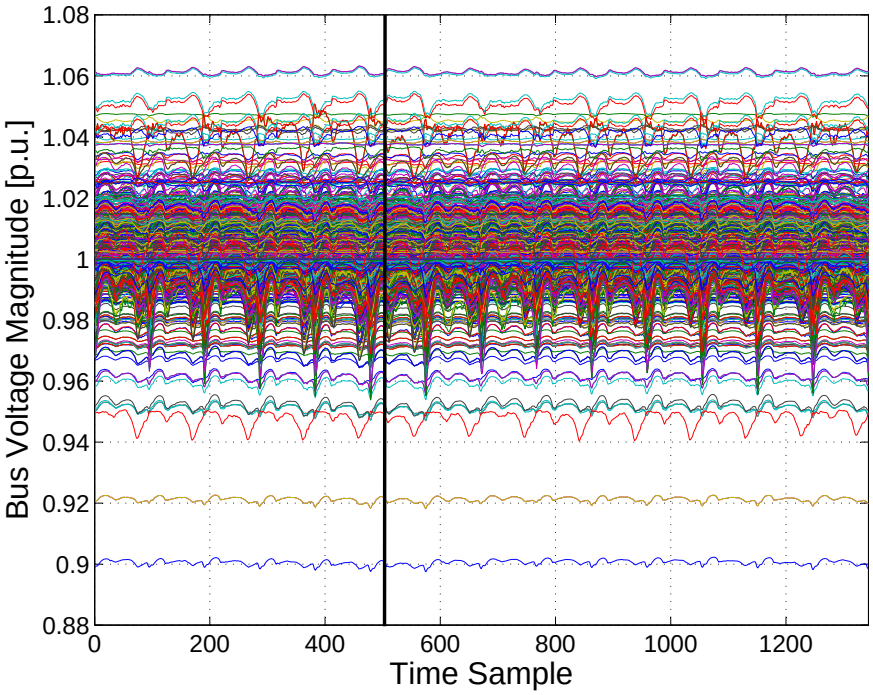

Figure 6.10: Power flow solutions for the IEEE 2382-bus test system: bus voltage angles.

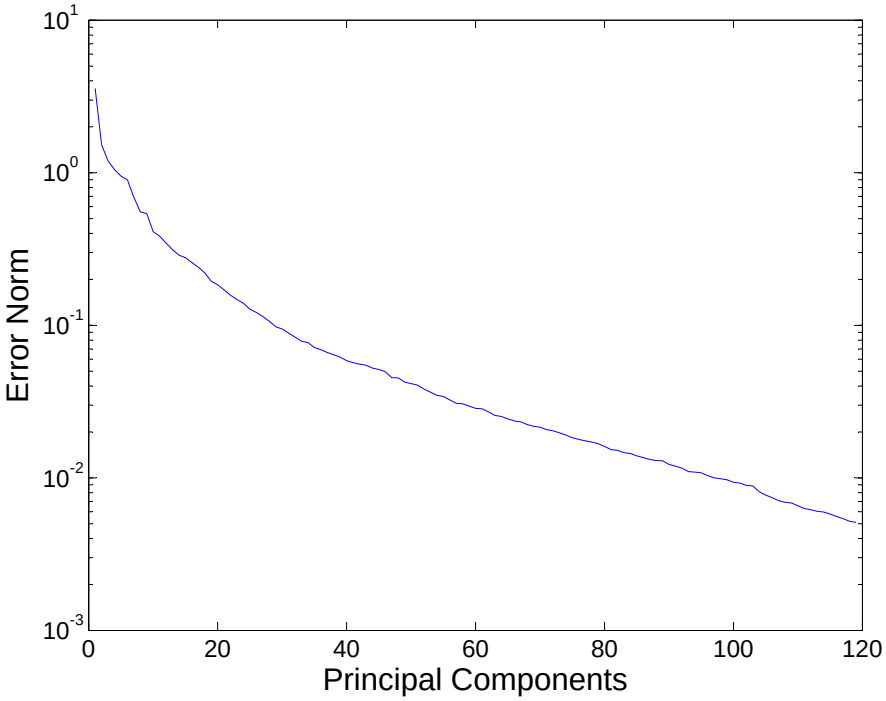

Figure 6.11: Norm of the approximation error, in semi-logarithmic scale, versus the number of principal components for the 2382-bus Polish test system PF.

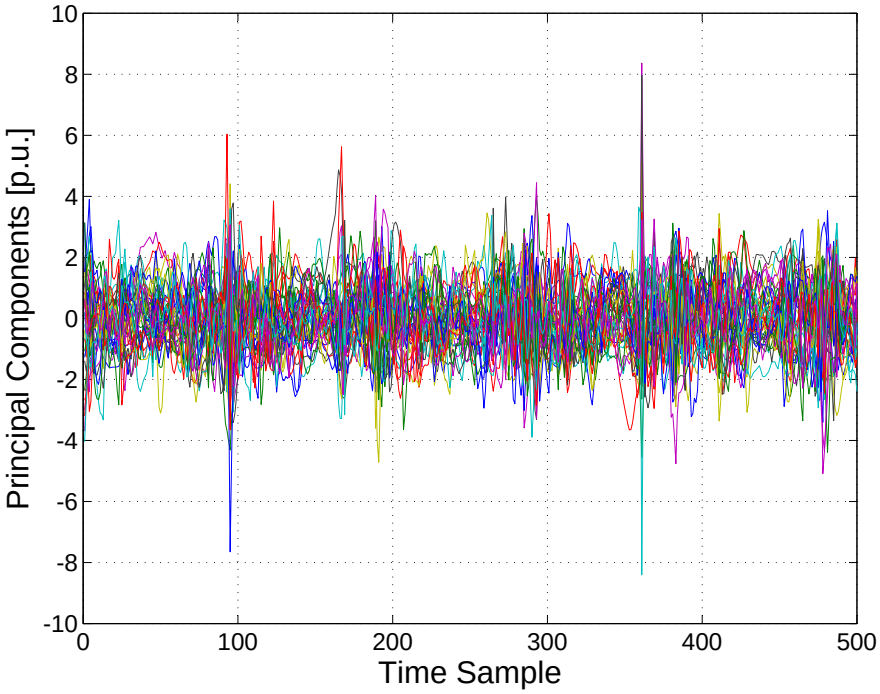

Figure 6.12: Principal components profile for the 2382-bus Polish test system PF.

power 4.11 [96]). To characterize the approximation accuracy for each time sample K, the following index is defined:

$$e(K) = \frac{1}{N} \sum_{i=1}^{N} \|\mathbf{V}_{i,PCA}(K) - \mathbf{V}_{i,NR}(K)\| \quad \forall K \in [500, 1343] \tag{6.14}$$

where $\mathbf{V}_{i,PCA}(K)$ and $\mathbf{V}_{i,NR}(K)$ are the phasors of the i^{th} bus voltage computed with the proposed approach and the traditional solution algorithm, respectively. Furthermore, to assess the computational benefits deriving by the application of the proposed approach, the following complexity reduction factor is defined:

$$C_r(K) = \frac{t_{NR}(K) - t_{PC}(K)}{t_{NR}(K)} * 100 \quad \forall K \in [500, 1343] \tag{6.15}$$

where $t_{NR}(K)$ and $t_{PC}(K)$ are the CPU times required to solve the power flow problem at the K^{th} time sample by the optimized algorithm and by the proposed approach, respectively. Figures 6.13 and 6.14 depict the error and complexity reduction indices obtained from (6.14) and (6.15), respectively. Observe that Figure 6.13 confirms the good accuracy of the solutions computed with the proposed paradigm, and Figure 6.14 shows that the CPU times of the proposed approach, even for non-optimal software routines, are on average 58% faster with respect to those of the traditional solution algorithm. It should be mentioned that both algorithms were tested on the same computer and the same software (Matlab 2013b), and the reactive power generation limits were assumed to be the same in all cases. Furthermore, to solve the power flow problem in the principal components domain, the standard pseudo-inverse operator available in the Matlab suite was used; a more effective pseudo-inverse algorithm may further reduce the computational burden of the proposed method [97].

It is important to note that the approximation accuracy and the CPU time of the proposed algorithm are strictly influenced by the number of principal components assumed for the inverse domain reconstruction (see Figures 6.4 and 6.11). Hence, a proper selection criteria is needed to obtain a suitable tradeoff between solutions accuracy and algorithm complexity. The latter mainly depends on the statistically characteristics of the historical data set adopted for knowledge extraction.

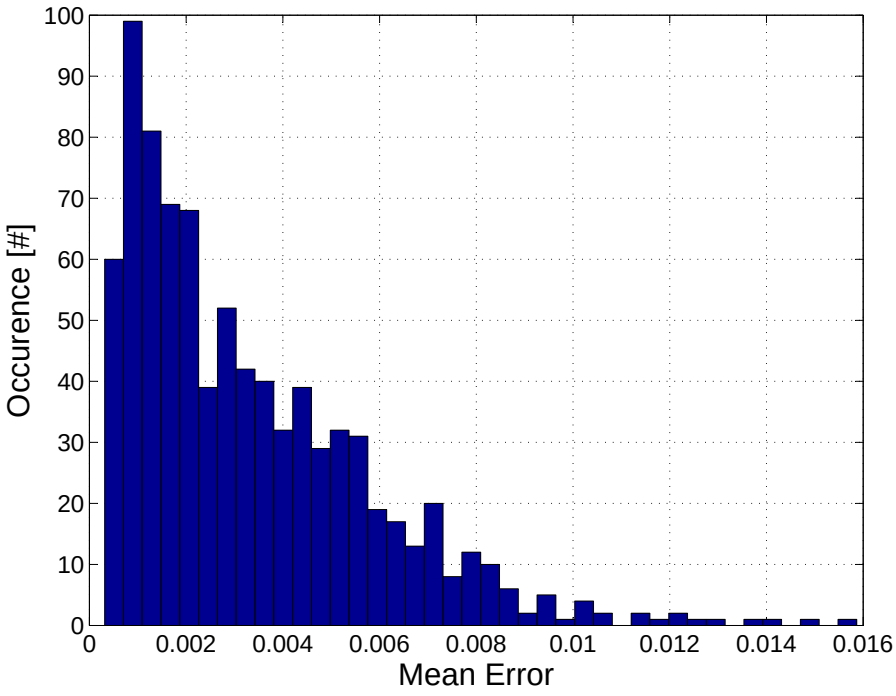

Figure 6.13: Statistical characterization of the approximation accuracy for the 2382-bus Polish test system PF.

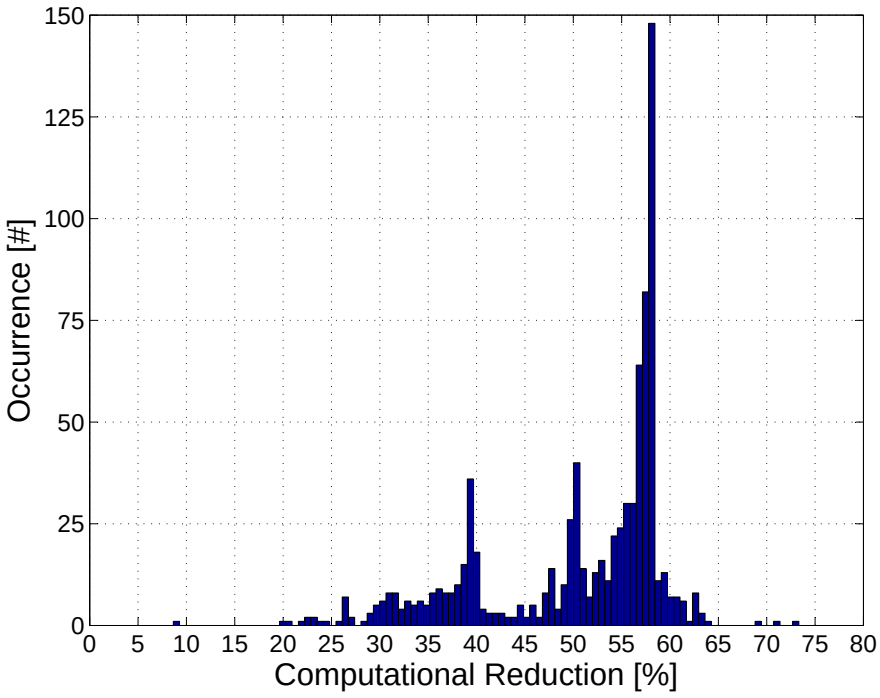

Figure 6.14: Statistical characterization of the complexity reduction factor for the 2382-bus Polish test system PF.

6.3.3 IEEE 118-bus Test System OPF

The proposed technique is also applied to solve OPF problems. Thus, the optimal active power dispatch problem for the IEEE 118-bus test system is studied here. The control variables of the optimization problem in this case are the active power generated by the dispatchable generators, while the dependent variables are the voltage magnitude at the load buses, and the voltage phase angle at all buses except the slack bus. The objective is to minimize the total generation cost satisfying both the equality constraints, described by the power flow equations, and the inequality constraints, described by the limits in the voltage magnitudes at all buses, and the reactive power limits at the PV buses.

The load buses are clustered in 10 different classes characterized by the bi-weekly 15 min profiles depicted in Figure 6.15, using similar load profiles as the ones proposed in [94]. The optimal power flow problem is then solved and the corresponding results are arranged in two sets, namely the knowledge base (first 500 sample points) and the validation set (remaining 843 sample points). The knowledge extraction process is then implemented for various numbers of principal components in the interval $N_{PC} \in [5, 50]$, obtaining the results summarized in Figure 6.16. Thus, for an approximation error tolerance of 10^{-3}, 24 principal components can be extracted from the knowledge base.

To assess the extrapolation capabilities of the proposed methodology, the power flow problem was solved in the principal components domain $\forall K \in [500, 1343]$. The resulting solutions are then compared to those obtained by applying the built-in Matpower optimal power flow program. The corresponding error surfaces are reported in Figures 6.17 and 6.18, where it is possible to observe the high accuracy of the solutions computed by the proposed solution framework. This is also confirmed by analyzing Figures 6.19 and 6.20, which depict the error and complexity reduction indices obtained from (6.14) and (6.15), respectively. Observe that Figure 6.19 confirms the good accuracy of the solutions computed with the proposed paradigm, and Figure 6.20 shows that the CPU times of the proposed approach, even for non-optimal software routines, are on average 77% faster with respect to those of the traditional solution algorithm.

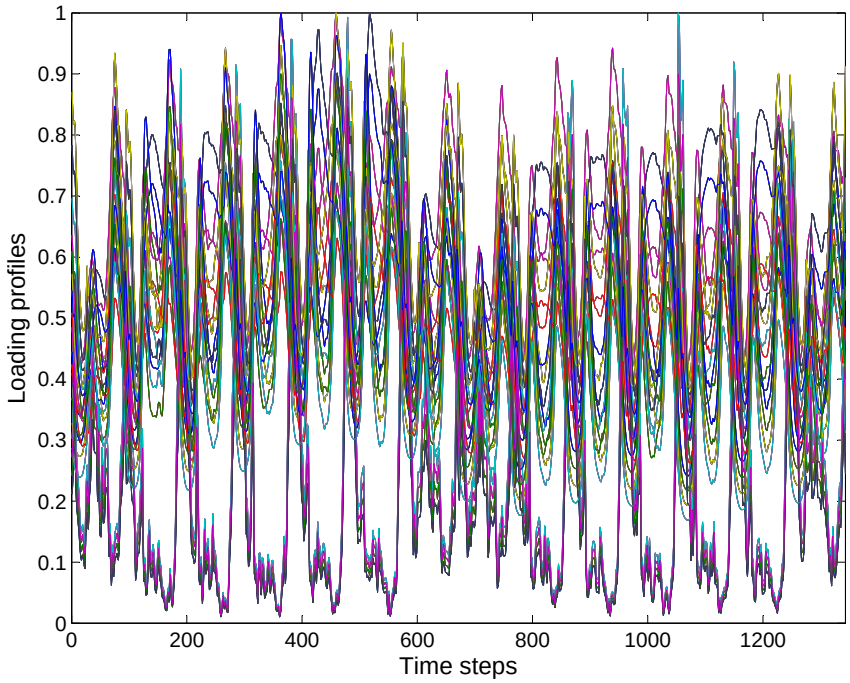

Figure 6.15: Loading profiles adopted for the OPF analysis of the 118-bus IEEE test system.

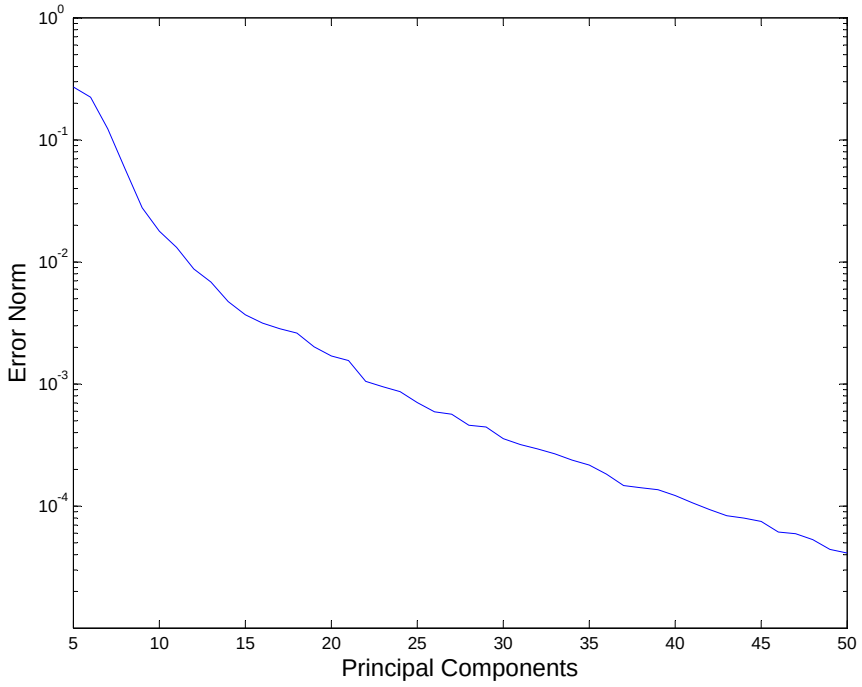

Figure 6.16: Norm of the approximation error, in semi-logarithmic scale, versus the number of principal components for the OPF analysis of the 118-bus IEEE test system.

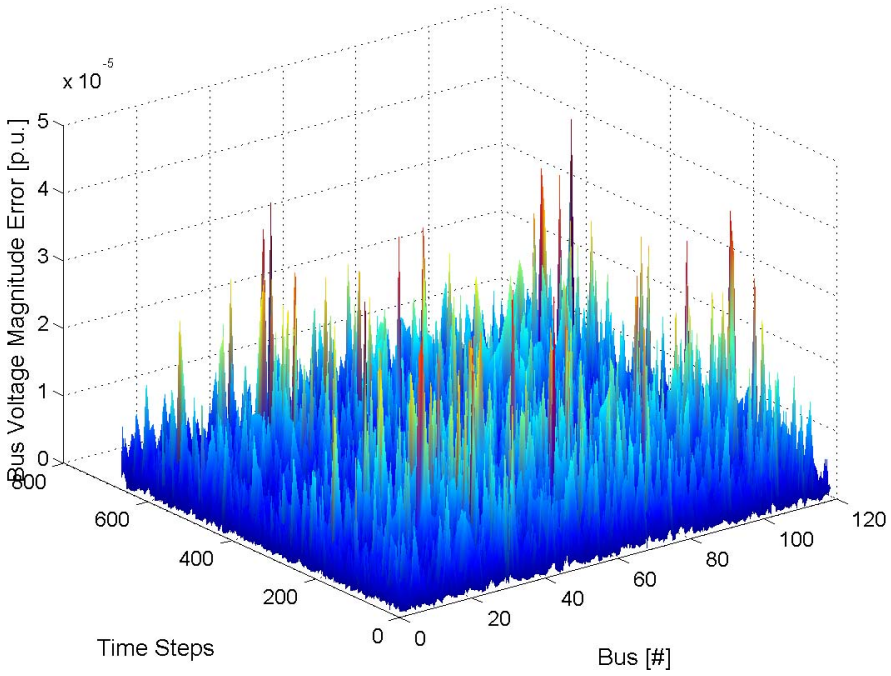

Figure 6.17: Approximation errors of the proposed technique versus the true OPF solution for the IEEE 118-bus test system: bus voltage magnitude error.

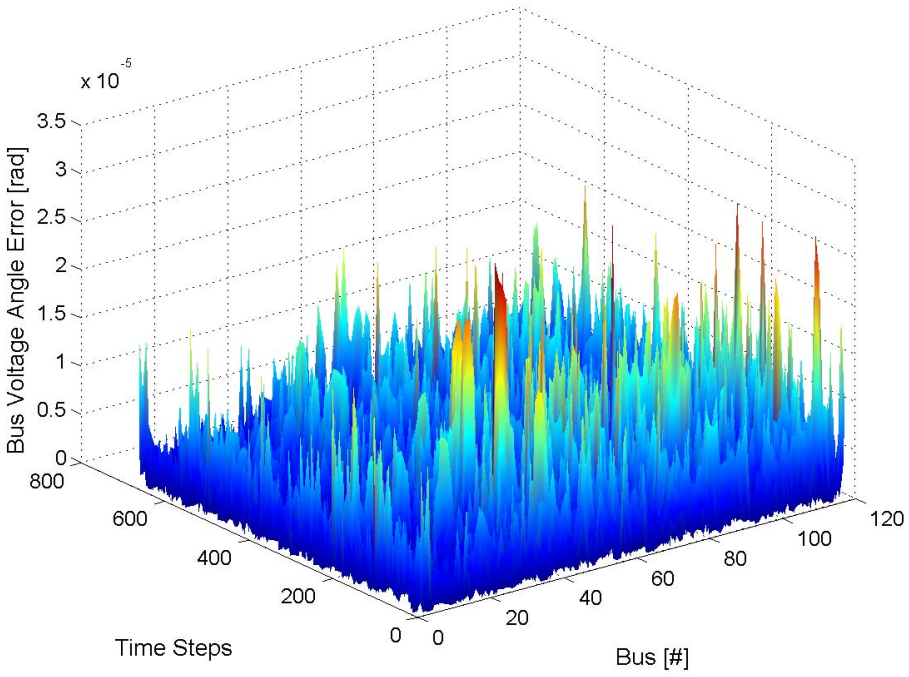

Figure 6.18: Approximation errors of the proposed technique versus the true OPF solution for the IEEE 118-bus test system: bus voltage angle error.

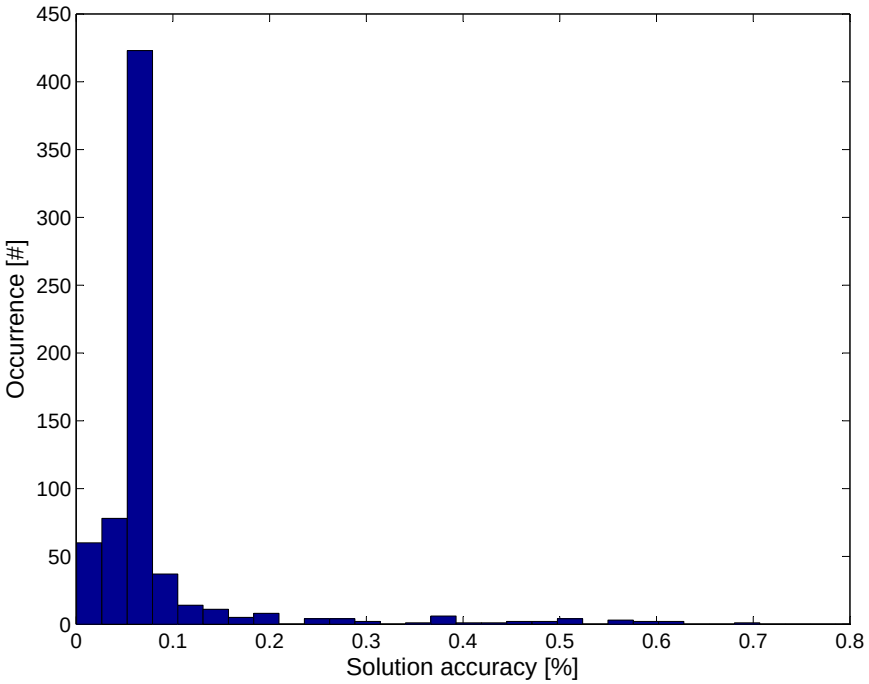

Figure 6.19: Statistical characterization of the approximation accuracy for the OPF analysis of the IEEE 118-bus test system.

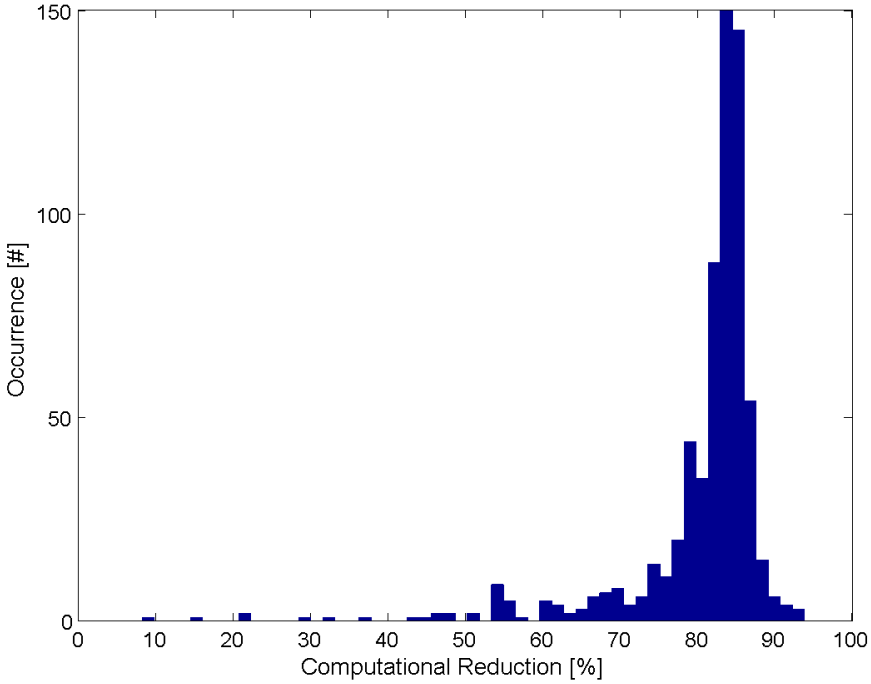

Figure 6.20: Statistical characterization of the complexity reduction factor for the OPF analysis of the IEEE 118-bus test system.

6.3.4 AA Analysis

In order to prove the effectiveness of the proposed PCA framework for identifying the main correlations among historical power system operation data, the load profiles of the PF and the OPF problems discussed in Sections 6.3.1 and 6.3.3 are processed using the methodology presented in Section 6.2.3. This resulted in the injected active and reactive powers being represented, with an approximation error lower than 10^{-3}, by a linear combination of 6 and 15 principal components, respectively. Therefore, for solving the uncertain PF and OPF analyses for these two case studies, the input variables can be properly represented by the following affine forms:

$$\begin{array}{l} \hat{P}_i^{SP} = P_{i,0}^{SP} + \sum_{k=1}^{6} P_{i,k}\varepsilon_k \quad \forall i \in \mathcal{N}_{\mathcal{P}} \\ \hat{Q}_j^{SP} = Q_{j,0}^{SP} + \sum_{k=1}^{6} Q_{j,k}\varepsilon_k \quad \forall j \in \mathcal{N}_{\mathcal{Q}} \end{array} \tag{6.16}$$

for the uncertain PF analysis of the IEEE 30-bus test system, and:

$$\begin{array}{l} \hat{P}_i^{SP} = P_{i,0}^{SP} + \sum_{k=1}^{12} P_{i,k}\varepsilon_k \quad \forall i \in \mathcal{N}_{\mathcal{P}} \\ \hat{Q}_j^{SP} = Q_{j,0}^{SP} + \sum_{k=1}^{12} Q_{j,k}\varepsilon_k \quad \forall j \in \mathcal{N}_{\mathcal{Q}} \end{array} \tag{6.17}$$

for the uncertain OPF analysis of the IEEE 118-bus test system.

The comparison of (6.16)-(6.17) with the affine forms assumed in Chapter 5 to solve uncertain PF and OPF problems, characterized by a number of noise symbols equal to the number of active and reactive power injections, demonstrate the sensible complexity reduction obtained by the application of the proposed PCA-based framework. Thus, the noise symbols are reduced from 53 to 6, and from 128 to 15 for the first and second case studies, respectively.

To check the consistency of these representations, the PF and the OPF problems are solved by applying the method proposed in Chapter 5, by assuming a $\pm 20\%$ (40%) variation of the active and reactive power injections around the corresponding mean values. The obtained results are reported in Figures 6.21-6.24, where Figures 6.21-6.22 depict the bounds of the bus voltage magnitudes and angles obtained for the uncertain PF analysis of the IEEE 30-bus test system, while Figures 6.23-6.24 depict the bounds of the bus voltage magnitudes and angles obtained for the uncertain economic dispatch analysis of the IEEE

118-bus test system. In all these figures, the corresponding bounds computed by a Monte Carlo-based approach are depicted in order to check the accuracy of the obtained solutions, demonstrating that the affine forms obtained using the PCA approach yield adequate results, and allow to represent the data uncertainties with a reduced number of noise symbols, which lead to a sensible reduction of the computational burdens. In particular, compared to the affine forms defined in Chapter 5, an improvement of the convergence times of about 70% and 75% has been observed in solving the two case studies, respectively.

6.4 Summary

In this chapter, a novel framework aimed at identifying potentially regularities of the PF and OPF solutions has been proposed. Based on structural knowledge, a mathematical method projecting the PF and OPF equations to a new domain has been defined, thus reducing the complexity and computational burden of the PF and OPF problem, and a novel method to better identify the noise symbols in AA-based uncertain PF and OPF analyses has been proposed.

The numerical results obtained for small and large scale power system under varius operating scenario demonstrated that the overall complexity of the PF and OPF problem in the transformed domain could be sensibly reduced, especially in the presence of correlated variables. Moreover, the knowledge extracted from operation data sets allows to drastically reduce the number of noise symbols in uncertain PF and OPF analysis, and consequently the computational costs of the proposed AA-based solution methodologies. Finally, it was observed that the approximation accuracy and the computational burdens observed during the experiments were strictly influenced by the number of principal components selected to decompose the power system state variables. Therefore, formal methods aimed at defining a proper tradeoff between the solutions accuracy and the algorithm complexity would be necessary for a comprehensive deployment of the proposed framework. This topic is currently under investigation.

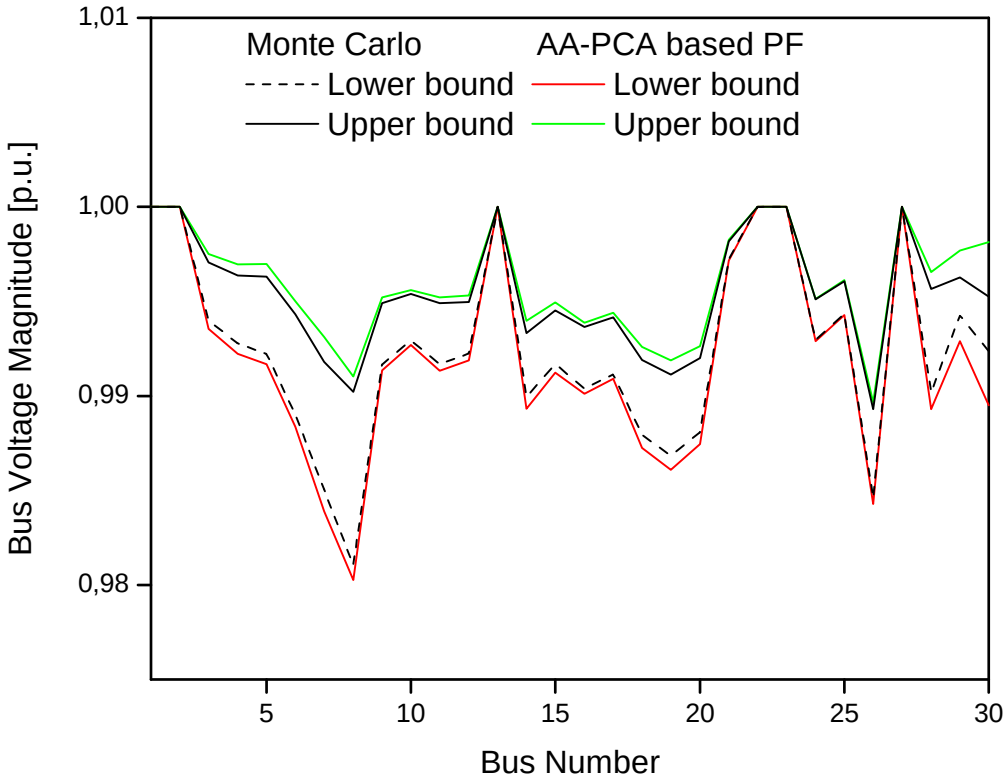

Figure 6.21: Bus voltage magnitude bounds obtained for the IEEE 30-bus test system for the AA-PCA PF method.

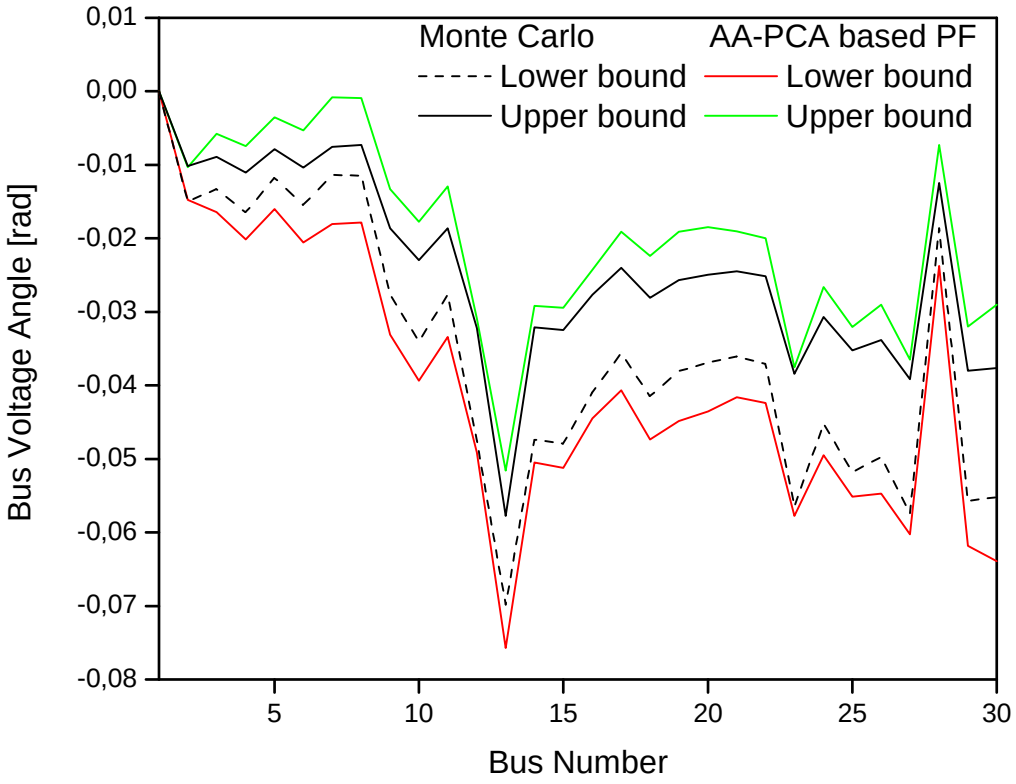

Figure 6.22: Bus voltage angle bounds obtained for the IEEE 30-bus test system for the AA-PCA PF method.

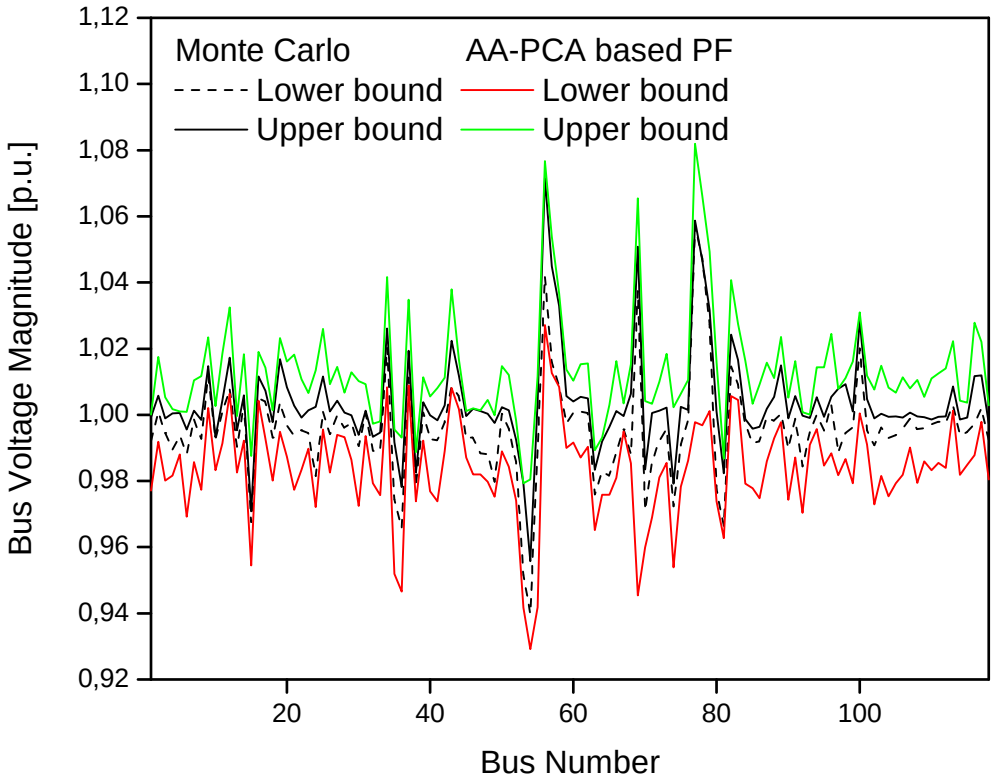

Figure 6.23: Voltage magnitude bounds of the AA-PCA OPF dispatch solutions for the 118-bus test system.

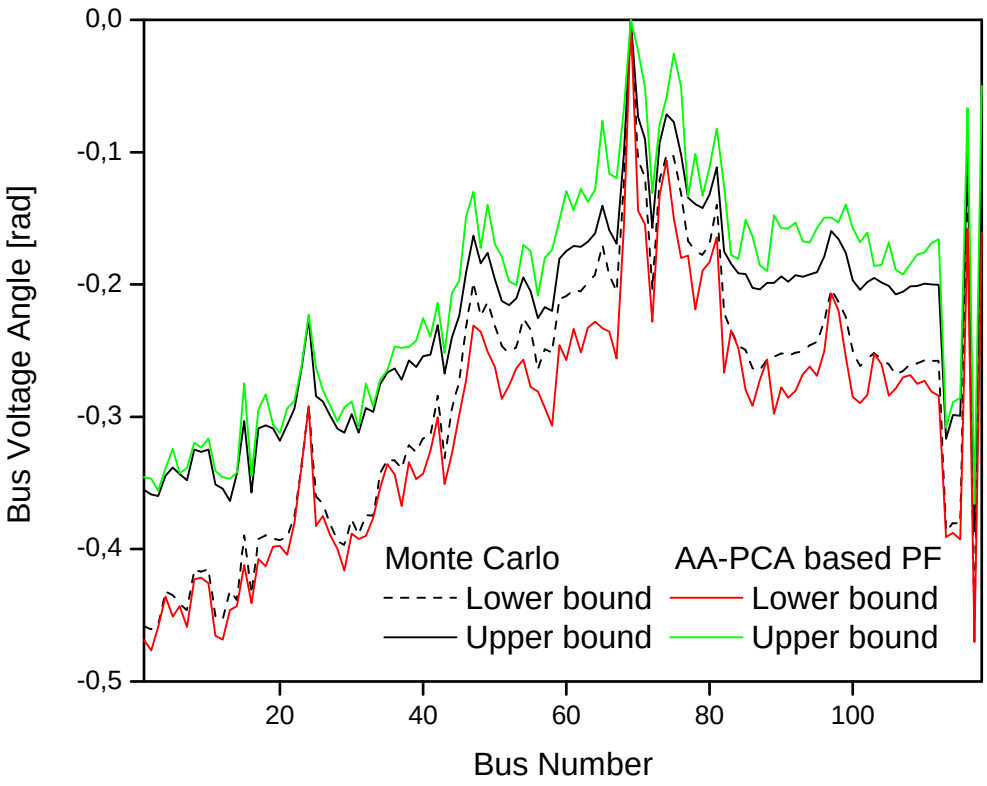

Figure 6.24: Voltage angle bounds of the AA-PCA OPF dispatch solutions for the 118-bus test system.

Chapter 7

Conclusions

7.1 Summary and Conclusions

This thesis proposed the use of AA-based computing paradigms for solving uncertain PF and OPF problems, when no sufficient information is available to identify a probabilistic description of the uncertainty. In particular, after analyzing the more relevant papers published in the scientific literature and introducing the mathematical preliminaries, a methodology for AA-based PF analysis that allows to better handle uncertainty compared to the traditional and widely used IA approaches was described. Based on this AA formalism, the PF solution bounds were readily obtained by means of a domain contraction technique. This paradigm allowed to effectively address the "wrapping effect" and the "dependency problem" of IA, leading to a better characterization of the effects of input data uncertainty in PF solutions, and a more realistic approximation of the solution domain compared to the typical "hyper box" form obtained with IA approaches.

A domain contraction technique based on range arithmetic was then proposed for uncertain OPF analysis. This method allowed to compute the range of OPF solutions associated with input interval uncertainties by solving two determinate problems of the same type, namely, the lower and the upper boundary problems, which were readily solved using state-of-the-art NLP solvers.

To reduce the approximation errors of uncertain PF and OPF analyses by obtaining a better estimation of the solution sets, a novel AA-based computing paradigm was defined. The main idea was to formulate a generic mathematical programming problem under uncertainty by means of equivalent deterministic problems, defining a coherent set of minimization, equality, and inequality operators. Compared to existing AA and Range-Arithmetic-based solution paradigms, this formulation presented greater flexibility, as it allowed to find partial solutions and include multiple equality and inequality constraints, reducing the approximation errors. However, it resulted in higher computational costs, mainly due to the large number of control variables required to solve the "perturbed state" problem. To address this problem, a PCA-based paradigm for knowledge discovery from historical operation data-sets was proposed to lower the cardinality of PF and OPF problems, and to identify the optimal affine forms describing the uncertain parameters in the proposed AA frameworks.

On the basis of the obtained results, it could be argued that a power engineer aiming at using AA-based techniques for solving uncertain PF and OPF problems is confronted with an accuracy/complexity trade-off. On one hand AA techniques based on domain contraction can be used to obtain a rough qualitative insight of the solution in a very short time, comparable to the time required simulations-based methods like Monte Carlo. On the other hand, solution methods based on the definition of formal AA operators can be used to obtain a better description of the uncertainty evolution at the cost of higher simulation times. In both cases, the use of PCA can contribute to sensibly reduce the problem cardinality, and to better identify the affine forms describing the data uncertainty. The results presented in this thesis should help in making the choice between the accuracy and computational costs, based on information about the application of the simulation outputs, and the existing computational resources.

7.2 Contributions

The following are the main thesis contributions:

- Through testing and validation of a methodology for AA-based PF analysis, demon-

strating that it better handles uncertainty compared to the traditional IA-based approaches, based on several realistic test systems.

- Through testing and validation of a novel optimization framework based on range arithmetic for OPF analysis with uncertainty parameters represented as intervals, which allows to compute the bounds of uncertain OPF solutions using state-of-the-art NLP solvers, based on several realistic test systems.

- Proposal of a novel AA-based computing paradigm to drastically reduce the approximation errors of previously proposed AA-based methods for uncertain PF and OPF analyses by obtaining a better estimation of the solution sets.

- Propose and demonstrate a novel PCA-based framework for knowledge extraction from historical power system operation data, which allows to reduce the complexity and computational burden of PF and OPF problems, and to better identify the noise symbols in AA-based uncertain PF and OPF analyses.

Two journal papers are being developed based on the content of Chapters 5 and 6. The main techniques in Chapters 3 and 4 were already published in [44], and [49].

7.3 Future Work

Future directions of the research presented here will be oriented toward:

- Enhancement of the proposed AA-based optimization framework by introducing discrete mathematical operators, which could allow to solve uncertain unit-commitment problems.

- Propose and develop mathematical techniques to identify the optimal number of principal components in PCA-based PF and OPF techniques.

- Propose hybrid computational paradigms for uncertain PF and OPF analysis, in which the data uncertainty can be described by multiple paradigms (e.g. fuzzy numbers, affine forms, intervals) in the context of the Granular Computing Theory.

- Study the use of PCA to improve the efficiency of Monte Carlo simulations for uncertain PF and OPF analyses.

References

[1] G. Verbic and C. Cañizares, "Probabilistic optimal power flow in electricity markets based on a two-point estimate method," *IEEE Transactions on Power Systems*, vol. 21, no. 4, pp. 1883–1893, 2006.

[2] Y. H. Wan and B. K. Parsons, *Factors relevant to utility integration of intermittent renewable technologies*. National Renewable Energy Laboratory, 1993.

[3] P. Chen, Z. Chen, and B. Bak-Jensen, "Probabilistic load flow: A review," in *Proceedings of the 3rd International Conference on Deregulation and Restructuring and Power Technologies, DRPT 2008*, pp. 1586–1591, 2008.

[4] B. Zou and Q. Xiao, "Solving probabilistic optimal power flow problem using quasi Monte Carlo method and ninth-order polynomial normal transformation," *IEEE Transactions on Power Systems*, vol. 29, no. 1, pp. 300–306, 2014.

[5] M. Hajian, W. D. Rosehart, and H. Zareipour, "Probabilistic power flow by Monte Carlo simulation with latin supercube sampling," *IEEE Transactions on Power Systems*, vol. 28, no. 2, pp. 1550–1559, 2013.

[6] C. Su, "Probabilistic load-flow computation using point estimate method," *IEEE Transactions on Power Systems*, vol. 20, no. 4, pp. 1843–1851, 2005.

[7] H. Zhang and P. Li, "Probabilistic analysis for optimal power flow under uncertainty," *IET Generation, Transmission & Distribution*, vol. 4, no. 5, pp. 553–561, 2010.

[8] H. Yu, C. Chung, K. Wong, H. Lee, and J. Zhang, "Probabilistic load flow evaluation with hybrid latin hypercube sampling and Cholesky decomposition," *IEEE Transactions on Power Systems*, vol. 24, no. 2, pp. 661–667, 2009.

[9] H. Mori and W. Jiang, "A new probabilistic load flow method using mcmc in consideration of nodal load correlation," in *Proceedings of the 15th International Conference on Intelligent System Applications to Power Systems*, pp. 1–6, 2009.

[10] H. Yu and W. D. Rosehart, "Probabilistic power flow considering wind speed correlation of wind farms," in *Proceedings of the 17th Power Systems Computation Conference*, pp. 1–7, 2011.

[11] H. Zhang and P. Li, "Probabilistic power flow by Monte Carlo simulation with latin supercube sampling," *IET Generation, Transmission Distribution,*, vol. 4, no. 5, pp. 553–561, 2010.

[12] A. Schellenberg, W. Rosehart, and J. Aguado, "Cumulant-based probabilistic optimal power flow (p-opf) with gaussian and gamma distributions," *IEEE Transactions on Power Systems*, vol. 20, no. 2, pp. 773–781, 2005.

[13] A. S. Meliopoulos, G. J. Cokkinides, and X. Y. Chao, "A new probabilistic power flow analysis method," *IEEE Transactions on Power Systems*, vol. 5, no. 1, pp. 182–190, 1990.

[14] R. Allan, A. da Silva, and R. Burchett, "Evaluation methods and accuracy in probabilistic load flow solutions," *IEEE Transactions on Power Apparatus and Systems*, vol. PAS-100, no. 5, pp. 2539–2546, 1981.

[15] R. Allan and M. Al-Shakarchi, "Probabilistic techniques in ac load-flow analysis," *Proceedings of the Institution of Electrical Engineers*, vol. 124, no. 2, pp. 154–160, 1977.

[16] P. Zhang and S. T. Lee, "Probabilistic load flow computation using the method of combined cumulants and gram-charlier expansion," *IEEE Transactions on Power Systems*, vol. 19, no. 1, pp. 676–682, 2004.

[17] L. Sanabria and T. Dillon, "Stochastic power flow using cumulants and Von Mises functions," *International Journal of Electrical Power & Energy Systems*, vol. 8, no. 1, pp. 47–60, 1986.

[18] H. Zhang and P. Li, "Chance constrained programming for optimal power flow under uncertainty," *IEEE Transactions on Power Systems*, vol. 26, no. 4, pp. 2417–2424, 2011.

[19] A. Dimitrovski and K. Tomsovic, "Boundary load flow solutions," *IEEE Transactions on Power Systems*, vol. 19, no. 1, pp. 348–355, 2004.

[20] F. Alvarado, Y. Hu, and R. Adapa, "Uncertainty in power system modeling and computation," in *Proceedings of the IEEE International Conference on Systems, Man and Cybernetics*, pp. 754–760, 1992.

[21] A. Vaccaro and D. Villacci, "Radial power flow tolerance analysis by interval constraint propagation," *IEEE Transactions on Power Systems*, vol. 24, no. 1, pp. 28–39, 2009.

[22] Z. Wang and F. Alvarado, "Interval arithmetic in power flow analysis," *IEEE Transactions on Power Systems*, vol. 7, no. 3, pp. 1341–1349, 1992.

[23] M. Madrigal, K. Ponnambalam, and V. Quintana, "Probabilistic optimal power flow," in *Proceedings of the IEEE Canadian Conference on Electrical and Computer Engineering*, vol. 1, pp. 385–388, 1998.

[24] X. Li, Y. Li, and S. Zhang, "Analysis of probabilistic optimal power flow taking account of the variation of load power," *IEEE Transactions on Power Systems*, vol. 23, no. 3, pp. 992–999, 2008.

[25] C. L. Su, "Probabilistic load-flow computation using point estimate method," *IEEE Transactions on Power Systems*, vol. 20, no. 4, pp. 1843–1851, 2005.

[26] J. M. Morales and J. Perez-Ruiz, "Point estimate schemes to solve the probabilistic power flow," *IEEE Transactions on Power Systems*, vol. 22, no. 4, pp. 1594–1601, 2007.

[27] G. Verbic, A. Schellenberg, W. Rosehart, and C. A. Cañizares, "Probabilistic optimal power flow applications to electricity markets," in *Proceedings of the International Conference on Probabilistic Methods Applied to Power Systems*, pp. 1–6, 2006.

[28] A. Mohapatra, P. Bijwe, and B. Panigrahi, "Optimal power flow with multiple data uncertainties," *Electric Power Systems Research*, vol. 95, pp. 160–167, 2013.

[29] H. Yu and W. Rosehart, "An optimal power flow algorithm to achieve robust operation considering load and renewable generation uncertainties," *IEEE Transactions on Power Systems*, vol. 27, no. 4, pp. 1808–1817, 2012.

[30] C. Boonchuay, K. Tomsovic, F. Li, and W. Ongsakul, "Robust optimization-based dc optimal power flow for managing wind generation uncertainty," *AIP Conference Proceedings*, vol. 1499, no. 1, 2012.

[31] M. Mohammadi, A. Shayegani, and H. Adaminejad, "A new approach of point estimate method for probabilistic load flow," *International Journal of Electrical Power Energy Systems*, vol. 51, no. 1, pp. 54 – 60, 2013.

[32] L. A. Zadeh, "Fuzzy sets," *Information and Control*, vol. 8, no. 3, pp. 338–353, 1965.

[33] G. Shafer, *A mathematical theory of evidence*, vol. 1. Princeton university press Princeton, 1976.

[34] P. Smets, "Imperfect information: Imprecision and uncertainty," in *Uncertainty Management in Information Systems*, pp. 225–254, Springer, 1997.

[35] P. Bijwe and G. V. Raju, "Fuzzy distribution power flow for weakly meshed systems," *IEEE Transactions on Power Systems*, vol. 21, no. 4, pp. 1645–1652, 2006.

[36] V. Miranda and J. Saraiva, "Fuzzy modelling of power system optimal load flow," in *Proceedings of the Power Industry Computer Application Conference*, pp. 386–392, 1991.

[37] P. Bijwe, M. Hanmandlu, and V. Pande, "Fuzzy power flow solutions with reactive limits and multiple uncertainties," *Electric Power Systems Research*, vol. 76, no. 1, pp. 145–152, 2005.

[38] X. Guan, W. E. Liu, and A. D. Papalexopoulos, "Application of a fuzzy set method in an optimal power flow," *Electric Power Systems Research*, vol. 34, no. 1, pp. 11–18, 1995.

[39] J. Stolfi and L. H. De Figueiredo, "Self-validated numerical methods and applications," in *Proceedings of the Monograph for 21st Brazilian Mathematics Colloquium*, Citeseer, 1997.

[40] R. Moore, *Methods and applications of interval analysis*, vol. 2. SIAM, 1979.

[41] S. Wang, Q. Xu, G. Zhang, and L. Yu, "Modeling of wind speed uncertainty and interval power flow analysis for wind farms," *Automation of Electric Power Systems*, vol. 33, no. 1, pp. 82–86, 2009.

[42] L. Pereira, V. Da Costa, and A. Rosa, "Interval arithmetic in current injection power flow analysis," *International Journal of Electrical Power & Energy Systems*, vol. 43, no. 1, pp. 1106–1113, 2012.

[43] M. Neher, "From interval analysis to taylor models-an overview," *Proceedings of the International Association for Mathematics and Computers in Simulation*, 2005.

[44] A. Vaccaro, C. A. Cañizares, and D. Villacci, "An affine arithmetic-based methodology for reliable power flow analysis in the presence of data uncertainty," *IEEE Transactions on Power Systems*, vol. 25, no. 2, pp. 624–632, 2010.

[45] J. Armengol, L. Travé-Massuyès, J. Vehi, and J. L. de la Rosa, "A survey on interval model simulators and their properties related to fault detection," *Annual Reviews in Control*, vol. 24, pp. 31–39, 2000.

[46] G. Bontempi, A. Vaccaro, and D. Villacci, "Power cables' thermal protection by interval simulation of imprecise dynamical systems," *IEE Proceedings-Generation, Transmission and Distribution*, vol. 151, no. 6, pp. 673–680, 2004.

[47] L. V. Barboza, G. P. Dimuro, and R. H. Reiser, "Towards interval analysis of the load uncertainty in power electric systems," in *Proceedings of the International Conference on Probabilistic Methods Applied to Power Systems*, pp. 538–544, 2004.

[48] F. Alvarado and Z. Wang, *Direct sparse interval hull computations for thin non-M matrices*. 1993.

[49] A. Vaccaro, C. A. Cañizares, and K. Bhattacharya, "A range arithmetic-based optimization model for power flow analysis under interval uncertainty," *IEEE Transactions on Power Systems*, vol. 28, no. 2, pp. 1179–1186, 2013.

[50] M. Pirnia, C. A. Cañizares, K. Bhattacharya, and A. Vaccaro, "An affine arithmetic method to solve the stochastic power flow problem based on a mixed complementarity formulation," *IEEE Transactions on Power Systems*, vol. 29, no. 6, pp. 2775–2783, 2014.

[51] H. Liang, A. K. Tamang, W. Zhuang, and X. Shen, "Stochastic information management in smart grid," *IEEE Communications Tutorials and Surveys*, vol. 16, no. 3, pp. 1746–1770, 2014.

[52] C. Rakpenthai, S. Uatrongjit, and S. Premrudeepreechacharn, "State estimation of power system considering network parameter uncertainty based on parametric interval linear systems," *IEEE Transactions on Power Systems*, vol. 27, no. 1, pp. 305–313, 2012.

[53] M. Pirnia, C. A. Cañizares, K. Bhattacharya, and A. Vaccaro, "A novel affine arithmetic method to solve optimal power flow problems with uncertainties," in *Proceedings of the IEEE Power and Energy Society General Meeting*, pp. 1–7, 2012.

[54] R. Bo, Q. Guo, H. Sun, W. Wu, and B. Zhang, "A non-iterative affine arithmetic methodology for interval power flow analysis of transmission network," *Proceedings of the Chinese Society for Electrical Engineering*, vol. 33, no. 19, pp. 76–83, 2013.

[55] S. Wang, L. Han, and P. Zhang, "Affine arithmetic-based dc power flow for automatic contingency selection with consideration of load and generation uncertainties," *Electric Power Components and Systems*, vol. 42, no. 8, pp. 852–860, 2014.

[56] G. Wei, L. Lizi, D. Tao, M. Xiaoli, and S. Wanxing, "An affine arithmetic-based algorithm for radial distribution system power flow with uncertainties," *International Journal of Electrical Power Energy Systems*, vol. 58, no. 0, pp. 242 – 245, 2014.

[57] T. Ding, H. Z. Cui, W. Gu, and Q. L. Wan, "An uncertainty power flow algorithm based on interval and affine arithmetic," *Automation of Electric Power Systems*, vol. 36, no. 13, pp. 51–55, 2012.

[58] M. Pirnia, C. A. Cañizares, and K. Bhattacharya, "Revisiting the power flow problem based on a mixed complementarity formulation approach," *IET Generation, Transmission & Distribution*, vol. 7, no. 11, pp. 1194–1201, 2013.

[59] R. R. Shoults and D. Sun, "Optimal power flow based upon pq decomposition," *IEEE Transactions on Power Apparatus and Systems*, no. 2, pp. 397–405, 1982.

[60] J. A. Momoh, "A generalized quadratic-based model for optimal power flow," in *Proceedings of the IEEE International Conference on Systems, Man and Cybernetics*, pp. 261–271, 1989.

[61] R. Burchett, H. Happ, and K. Wirgau, "Large scale optimal power flow," *IEEE Transactions on Power Apparatus and Systems*, no. 10, pp. 3722–3732, 1982.

[62] K. Pandya and S. Joshi, "A survey of optimal power flow methods," *Journal of Theoretical & Applied Information Technology*, vol. 4, no. 5, 2008.

[63] D. I. Sun, B. Ashley, B. Brewer, A. Hughes, and W. F. Tinney, "Optimal power flow by newton approach," *IEEE Transactions on Power Apparatus and Systems*, no. 10, pp. 2864–2880, 1984.

[64] J. A. Momoh and J. Zhu, "Improved interior point method for opf problems," *IEEE Transactions on Power Systems*, vol. 14, no. 3, pp. 1114–1120, 1999.

[65] G. Tognola and R. Bacher, "Unlimited point algorithm for opf problems," *IEEE Transactions on Power Systems*, vol. 14, no. 3, pp. 1046–1054, 1999.

[66] L. V. Kolev, "A method for outer interval solution of linear parametric systems," *Reliable Computing*, vol. 10, no. 3, pp. 227–239, 2004.

[67] I. Skalna, "A method for outer interval solution of parametrized systems of linear interval equations," *Reliable Computing*, vol. 12, no. 2, pp. 107–120, 2006.

[68] C. Jiang, X. Han, and G. Liu, "A sequential nonlinear interval number programming method for uncertain structures," *Computer Methods in Applied Mechanics and Engineering*, vol. 197, no. 49, pp. 4250–4265, 2008.

[69] C. Jiang, X. Han, G. Liu, and G. Liu, "A nonlinear interval number programming method for uncertain optimization problems," *European Journal of Operational Research*, vol. 188, no. 1, pp. 1–13, 2008.

[70] H. Ishibuchi and H. Tanaka, "Multiobjective programming in optimization of the interval objective function," *European Journal of Operational Research*, vol. 48, no. 2, pp. 219–225, 1990.

[71] A. Bonarini and G. Bontempi, "A qualitative simulation approach for fuzzy dynamical models," *ACM transactions on Modeling and Computer Simulation*, vol. 4, no. 4, pp. 285–313, 1994.

[72] L. H. De Figueiredo and J. Stolfi, "Affine arithmetic: concepts and applications," *Numerical Algorithms*, vol. 37, no. 1-4, pp. 147–158, 2004.

[73] N. S. Nedialkov, V. Kreinovich, and S. A. Starks, "Interval arithmetic, affine arithmetic, taylor series methods: why, what next?," *Numerical Algorithms*, vol. 37, no. 1, p. 325336, 2004.

[74] A. Neumaier, "Taylor formsuse and limits," *Reliable Computing*, vol. 9, no. 1, pp. 43–79, 2003.

[75] F. Song, Z. Guo, and D. Mei, "Feature selection using principal component analysis," in *Proceedings of the International Conference on System Science, Engineering Design and Manufacturing Informatization*, vol. 1, pp. 27–30, 2010.

[76] R. Bo and F. Li, "Power flow studies using principal component analysis," in *Proceedings of the 40th North American Power Symposium*, pp. 1–6, 2008.

[77] P. R. Peres-Neto, D. A. Jackson, and K. M. Somers, "How many principal components? stopping rules for determining the number of non-trivial axes revisited," *Computational Statistics Data Analysis*, vol. 49, no. 1, pp. 974–997, 2005.

[78] D. J. Burke and M. J. O'Malley, "A study of principal component analysis applied to spatially distributed wind power," *IEEE Transactions on Power Systems*, vol. 26, no. 4, pp. 2084–2092, 2011.

[79] J. Yin, I. Gorton, and S. Poorva, "Toward real time data analysis for smart grids," in *Proceedings of the SC Companion: High Performance Computing, Networking, Storage and Analysis*, pp. 827–832, 2012.

[80] S. Das and P. N. Rao, "Principal component analysis based compression scheme for power system steady state operational data," in *Proceedings of the IEEE PES Innovative Smart Grid Technologies-India*, pp. 95–100, 2011.

[81] D. Grabowski, M. Olbrich, and E. Barke, "Analog circuit simulation using range arithmetics," in *Proceedings of the Asia and South Pacific Design Automation Conference*, pp. 762–767, 2008.

[82] E. D. Dolan and J. J. Moré, "Benchmarking optimization software with performance profiles," *Mathematical programming*, vol. 91, no. 2, pp. 201–213, 2002.

[83] L. Kolev and I. Nenov, "A combined interval method for global solution of nonlinear systems," in *Proceedings of the XXIII International Conference on Fundamentals of Electronics and Circuit Theory*, pp. 365–368, 2000.

[84] L. Kolev, "A general interval method for global nonlinear dc analysis," in *Proceedings of the European Conference on Circuit theory and design*, vol. 97, pp. 1460–1462, 1997.

[85] R. D. Christie, "Power systems test case archive," in *available on line at http://www.ee.washington.edu/research/pstca*.

[86] A. Saric and A. Stankovic, "Ellipsoidal approximation to uncertainty propagation in boundary power flow," in *Proceedings of the IEEE PES Power Systems Conference and Exposition*, pp. 1722–1727, 2006.

[87] V. Levin, "Nonlinear optimization under interval uncertainty," *Cybernetics and Systems Analysis*, vol. 35, no. 2, pp. 297–306, 1999.

[88] M. Hladík, "Optimal value bounds in nonlinear programming with interval data," *Top*, vol. 19, no. 1, pp. 93–106, 2011.

[89] A. Lemke, L. Hedrich, and E. Barke, "Analog circuit sizing based on formal methods using affine arithmetic," in *Proceedings of the IEEE/ACM international conference on Computer-aided design*, pp. 486–489, 2002.

[90] V. Levin, "Comparison of interval numbers and optimization of interval-parameter systems," *Automation and Remote Control*, vol. 65, no. 4, pp. 625–633, 2004.

[91] A. Gomez-Exposito, A. J. Conejo, and C. A. Cañizares, *Electric Energy Systems: Analysis and Operation*. CRC Press, 2009.

[92] V. Loia and A. Vaccaro, "Decentralized economic dispatch in smart grids by self-organizing dynamic agents," *IEEE Transactions on Systems, Man, and Cybernetics: Systems*, vol. 44, no. 4, pp. 397–408, 2014.

[93] X. Liu, W.-S. Luk, Y. Song, P. Tang, and X. Zeng, "Robust analog circuit sizing using ellipsoid method and affine arithmetic," in *Proceedings of the 2007 Asia and South Pacific Design Automation Conference*, pp. 203–208, 2007.

[94] A. Mutanen, M. Ruska, S. Repo, and P. Järventausta, "Customer classification and load profiling method for distribution systems," *IEEE Transactions on Power Delivery*, vol. 26, no. 1, pp. 1755–1763, 2011.

[95] A. E. M. Operator, "Energy market data,"

[96] R. Zimmerman, C. , Murillo-Sanchez, and R. Thomas, "Matpower: Steady-state operations, planning, and analysis tools for power systems research and education," *IEEE Transactions on Power Systems*, vol. 26, no. 1, pp. 12–19, 2011.

[97] P. Horata, S. Chiewchanwattana, and K. Sunat, "A comparative study of pseudo-inverse computing for the extreme learning machine classifier," in *Proceedings of the 3rd International Conference on Data Mining and Intelligent Information Technology Applications*, pp. 40–45, 2011.